Bernardos Bau, A.; Piacenza, E.; Sancenón Galarza, F.; Hamidi, M.; Maleki, A.; Turner, R.; Martínez-Máñez, R. (06-2). Mesoporous Silica-Based Materials with Bactericidal Properties. Small. 15(24):1-34. https://doi.org/10.1002/smll.201900669

DOI: 10.1002/ ((please add manuscript number))
Article type: Review

Mesoporous Silica-Based Materials with Bactericidal Properties

*Andrea Bernardos, Elena Piacenza, Félix Sancenón, Hamidi Mehrdad, Aziz Maleki,**

Raymond J. Turner and Ramón Martínez-Máñez**

Dr. A. Bernardos, Dr. F. Sancenón, Prof. R. Martínez-Máñez
Instituto Interuniversitario de Investigación de Reconocimiento Molecular y Desarrollo Tecnológico (IDM), Universitat Politècnica de València, Universitat de València. Camí de Vera s/n, 46022, València, Spain. CIBER de Bioingeniería, Biomateriales y Nanomedicina (CIBER-BBN), Spain. Unidad Mixta UPV-CIPF de Investigación en Mecanismos de Enfermedades y Nanomedicina, València, Universitat Politècnica de València, Centro de Investigación Príncipe Felipe, València, Spain.
Dr. F. Sancenón, Prof. R. Martínez-Máñez
Departamento de Química, Universitat Politècnica de València, Camí de Vera s/n, 46022, València, Spain. Unidad Mixta de Investigación en Nanomedicina y Sensores. Universitat Politècnica de València, Instituto de Investigación Sanitaria La Fe, Valencia, Spain.
E-mail: *rmaez@qim.upv.es*

E. Piazenca, Prof. R. J. Turner
Faculty of Science, Department of Biological Sciences, University of Calgary, Calgary, AB, Canada.
E-mail: *turnerr@ucalgary.ca*

Prof. H. Mehrdad, Dr. A. Maleki
Zanjan Pharmaceutical Nanotechnology Research Center (ZPNRC), Zanjan University of Medical Sciences, Zanjan, Iran.
E-mail: *amchem2010@gmail.com*

Keywords: nanoparticles, mesoporous silica materials, antibiotics, controllable drug delivery systems

Bacterial infections are the main cause of chronic infections and even mortality. In fact, due to extensive use of antibiotics and, then, emergence of antibiotic resistance, treatment of such infections by conventional antibiotics has become a major concern worldwide. One of the promising strategies to treat infection diseases is the use of nanomaterials. Among them, mesoporous silica materials (MSMs) have attracted burgeoning attention due to high surface area, tunable pore/particle size, and easy surface functionalization. This review discusses how one can exploit capacities of the MSMs to design and fabricate multifunctional/controllable drug delivery systems (DDSs) to combat bacterial infections. At first, it describes emergency

of bacterial and biofilm resistance towards conventional antimicrobials and then discusses how nanoparticles exert their toxic effects upon pathogenic cells. Next, it introduces the main aspects of MSMs (e.g. physico-chemical properties, multifunctionality and biosafety) which one should consider in the design of MSM-based DDSs against bacterial infections. Finally, a comprehensive analysis of all the papers published dealing with the use of MSMs for delivery of antibacterial chemicals (antimicrobial agents functionalized/adsorbed on mesoporous silica (MS), MS-loaded with antimicrobial agents, gated MS-loaded with antimicrobial agents, MS with metal-based nanoparticles and MS- loaded with metal ions) is provided.

1. Introduction

Antimicrobials are compounds able to locally kill bacterial cells (i.e., bactericidal agents), inhibit or slow down their growth (bacteriostatic compounds).[1] Among the various substances acting as antimicrobial agents, we find pure natural products (e.g., aminoglycosides), chemically modified natural substances, which include most of the antibiotics used today (e.g., beta-lactams and cephalosporins),[2] or completely synthetic compounds.[3] Although the antimicrobials available up to date are chemically diverse, pathogenic microorganisms are able to develop resistance mechanisms against them, leading to their loss of efficacy when used in clinical settings.[4] The emergence of bacterial resistance to antimicrobials has mainly arisen from their extensive misuse in both agriculture and human health services,[5] leading to: (i) inheritable evolutionary processes or (ii) horizontal gene transfer phenomena between different pathogenic microorganisms.[1],[6] To date, the number of reports on the antimicrobial resistance (AMR) of pathogen microorganisms is exponentially growing, as highlighted by the World Organization for Animal Health, the Food and Agriculture Organization, and the World Health Organization, which indicated AMR as a serious threat towards human and animal health, and, subsequently, an economic and social concern as well.[7,8] Indeed, the acquisition of resistance mechanisms in pathogen bacteria

towards the conventional antimicrobials led to the generation of the so-called “superbugs” that are not affected by the antibacterial treatments available these days, causing the spread of infections that increase the severity of illness and subsequent human death rates.[9]

A crucial factor contributing to the spread of AMR among microorganisms is their ability and preference to create, in most of the natural settings, multicellular aggregates that live closely associated to interfaces or surfaces.[10–12] Although such microbial systems were already observed in 1600’s,[13], was not until 1978 these complex communities were defined as biofilms, and they are now recognized as the primary form of bacterial life compared to the “free-swimming” planktonic cells.[10,11] Biofilms are generated through a staged process in which both planktonic cells and those adhering to a surface are present.[13,14] Upon attachment, bacterial cells start to produce the so-called Extracellular Polymeric Substance (EPS) or matrix, which is also indicated as the ‘slime’ layer on a surface, and contains a high amount of water, polysaccharides, proteins, extracellular-DNA (e-DNA) and lipids.[13,14] The presence of EPS ensures the protection of bacterial cells from several external stresses, such as desiccation, oxidation, UV radiation [15]. Moreover, the thickness and the chemistry of the EPS matrix constitutes a barrier for biocides, antibiotics and metallic ions, limiting their penetration inside the biofilm itself and, therefore, avoiding their direct interaction with bacterial cells.[4]

During the life cycle of bacterial biofilms, several intra- and inter -cellular signaling processes occurs (e.g., quorum sensing), which can result in enhancing of AMR in these communities. [16] Additionally, the presence within biofilms of bacterial cells in different physiological states can lead to the development of AMR phenomena.[13] Indeed, the diverse physiology of the so-called “persister cells”, which are dormant and non-dividing cells,[17,18] confers them the ability to survive the presence of several antimicrobials, as they are not effective against metabolically inactive cells as targets.[19] A similar dormant and non-growing state has been described for other subpopulations of bacterial cells, which are defined as morphology or

phase variants, as internal signalling by cyclic-di-GMP gives them a different phenotype compared to the parental ones.[20–22] Thus, their different phenotype results in their less susceptibility towards antibiotics, leading to the ability of these phenotypic variants to survive even at high concentrations of antibiotics.[23,24]

Considering the structural and physiological complexity of biofilms, those formed by pathogen bacteria are able to populate settings in which sterility is of fundamental importance for human health (e.g., food processing facilities, dental hygiene equipment, catheters, orthopedic implants).[13],[25] As a result, microorganisms living as complex communities are responsible for 85% of human bacterial infections in the Western world.[26] Although high resistance towards antibiotics is typical of pathogenic biofilms and is well documented, pathogenic infections in the form of biofilms are still treated with these antimicrobial compounds [4]. Moreover, since antibiotics are typically from 100 to 1000 times less efficient in the case of biofilms,[27] to obtain significant antimicrobial effect against these infections, it is necessary to administer higher antibiotic dosage than those established for planktonic cells. However, host organisms are often not capable of tolerating these high levels of antimicrobials, leading to either (i) detrimental side effects or (ii) the use of lower dosage, resulting in inefficient treatment.[4] In this scenario, the development of new and alternative antimicrobial compounds with long-term efficiency in preventing the reoccurrence of both planktonic and biofilm infections is recognized as an immediate and fundamental need in agriculture, livestock, as well as in the human biomedical field.

1.1. Nanoparticles as new effective antimicrobial agents

The exponential development of nanotechnology we have witnessed in the last 30 years has guaranteed the possibility to tune chemical-physical features of antimicrobial compounds at the nanoscale (1-100 nm) in order to generate new and effective formulations.[28] Thus,

nanomaterials are considered to date novel therapeutic agents and the most promising alternative to the conventional antimicrobials.[29]

Nanomaterials exhibit unique features as compared to their bulk counterpart, mostly reliant on their dimensions (1nm = 10^{-9} m)[29]. Indeed, when synthetic compounds are scaled down to approach the atomic level, new mechanical, chemical, electrical, optical and magnetic properties arise, making them suitably manipulated for different applications.[30] Particularly, nanostructures are featured by a high surface-to-volume ratio,[1] which determines a surface area much larger as compared to their size, enhancing the contact of these nanomaterials with the microorganisms.[29] Thus, the increased possibility of interaction between nanosized formulations and pathogenic cells leads to the activation of a broad range of antimicrobial mechanisms,[29] therefore improving the antimicrobial efficacy of these nanomaterials. Further, the antimicrobial activity of nanostructures can be influenced by other chemical-physical parameters, such as shape, chemical modification or coating, and the generation of mixed population of different nanocomposites.[31]

Although a great variety of nanomaterials with different morphology have been developed, nanoparticles (NPs) are those most investigated for medical and antimicrobial purposes, mainly as a consequence of their regular structure, which better allows a prediction of their interaction with both eukaryotic and prokaryotic cells. In this context, NPs have found important applications in biomedicine (e.g., drug delivery, imaging, sensing, coating for artificial implants),[32] as they shared the size range with biological molecules involved in the major processes occurring within the cells.[29]

A general and broad classification of NPs is based on their composition, allowing to distinguish between organic and inorganic nanomaterials.[29] Indeed, organic NPs contain antimicrobial polymers (quaternary ammonium compounds,[33] quaternary cation polyelectrolytes,[34] polysiloxanes,[35] triclosan,[36] chitosan,[37]) antimicrobial peptides (e.g., poly-ε-lysine[38]) or antibiotics,[4] which are usually released upon interaction with pathogenic

cells, exerting an enhanced antimicrobial effect.[4] Nevertheless, since a common feature of organic NPs is their poor stability in various conditions (temperature ranges, pH and ionic conditions, solubility), their design for antimicrobial purposes tends to be more challenging.[4] Therefore, inorganic formulations are now considered the preferential choice as new NP antimicrobials. Particularly, NPs made of metals, metal oxides and metalloids have received increasing interest as metals have intrinsic antimicrobial properties.[29],[39] Indeed, metal compounds containing silver or copper have been used since ancient times to treat burns or chronic wounds, and to make water potable.[29],[40]. More recently, metal-based NPs, such as silver (Ag),[41] gold (Au),[42] titanium oxide (TiO^2),[43] copper oxide (CuO)[44] and zinc oxide (ZnO) NPs,[45] and mesoporous silica (MS) have been greatly investigated for their antimicrobial efficacy.

2. Mesoporous silica nanostructures

Since their inception in the early 1990,[46,47] mesoporous silica (MS) structures (*e.g.*,SBA-, MCM-, KIT, HMS, FDU and MSU-family) have attracted a lot of attention in fundamental science and technology due to high surface area (800-1000 $m^2 g^{-1}$), tunable pore size (2-5 nm) and particle dimensions (typically <200 nm), controllable morphology (e.g., rod, spherical, platelet, and ellipsoid), high mechanical/thermal stability, easy large-scale preparation (even at kilogram scale) and their selective functionalization on both interior and exterior surfaces.[48–52] Besides the appealing properties, high biocompatibility and good biodegradability of the porous structures allow one to design and fabricate powerful delivery systems for different applications.[49,50],[53,54] Synthesis of MS is rather feasible and it is based on sol-gel chemistry, which involves two main steps: hydrolysis and condensation of silica (organo silica) precursors around a template generated via supramolecular self-assembly of surfactants in aqueous solution, followed by the elimination of the template by using calcination or solvent extraction.[47],[55] Similar to other NPs, interaction of MS NPs with

biological systems and their biological behavior (e.g., cytotoxicity, biocompatibility, biodegradability and tissue compatibility) depend heavily on physico-chemical properties (PCPs) of the NPs (e.g., shape, pore/particle size and surface properties).[53],[56,57] Therefore, the tuning of the PCPs acquires significant thought to achieve an appropriate biological performance (**Figure 1**).

Traditional synthesis employing small molecule surfactants such as *cetyl* trimethylammonium bromide (CTAB) as structure directing agent (SDA) produced MS with pore diameter less than ~ 5 nm, limiting their application in accommodating large guest (cargo) molecules. Such concerns has led to the development of synthesis through pore-extended MS for drug delivery systems. In general, the pore sizes of MS can be tuned through the use of tetra-alkylammonium salts featured by different alkyl chain lengths and pluronic (or non-pluronic) surfactants with diverse molecular weights. Along with pore and particle size, particle shape and topology of MS should be considered to determine their interaction with biological systems.[56]

The high surface area and the high amounts of silanol groups on MS surface make possible to prepare hybrid organic-inorganic nanomaterials through surface functionalization, allowing to better control their loading capacity, cargo release rate, cellular uptake efficiency, etc.[57] The functionalization of MS generally occurs through three pathways: 1) grafting method, 2) co-condensation method, and 3) direct incorporation of organic units into the silica wall to obtain periodic mesoporous organosilicas (PMOs) or mesoporous organosilica nanoparticles (MONs) (Figure 1).

As mentioned in the above sections, internal/external surface of MS can be functionalized by diverse agents (**Sheme 1**), resulting in great opportunities to design and construct antibacterial structures for instance due to the attachment of well-known bactericides, by including the bactericides in the pores for a sustained cargo release or via the incorporation in the MS structure of nanoparticles known for their antimicrobial activity. Moreover, although MS NPs

are feasible structures to generate effective DDSs, it is imperative to control the pore opening, which in turn is responsible for the cargo releasing.[58,59] Thus, once the mesopores are loaded with a cargo, the pore outlets of the MS can be blocked by diverse organic or inorganic "molecular gates" to prevent undesired premature leakage. Moreover, the pore-blockers should respond to appropriate external or internal triggers to close or open the well-defined pores, causing on-demand intelligent cargo delivery.[49],[60–62] Various porekeepers[63] including polymers (e.g., polymer poly(2-vinylpyridine) (PVP),[64] Poly(N-succinimidyl acrylate),[65] poly(2-dimethylaminoethyl methacrylate),[66] poly(acrylic acid) (PAA) brush[67]), host–guest assemblies (e.g. CDs,[68,69] Cucurbit[7]uril,[70] Pillararenes[71]), inorganic nanomaterials (e.g., Au NPs,[72] quantum dots,[73,74] Ag NPs,[75] cerium oxide NPs,[76] manganese oxide NPs,[77] and reduced graphene[78]), biomacromolecules (e.g., peptides,[79–81], nucleic acids,[82–84] saccharides,[85–88] and proteins [89–92]) have been employed under certain internal or external stimuli, such as pH,[64,65] temperature,[79] light,[78],[83],[93] redox potential,[91],[94] ultrasound,[95] small molecules,[96],[97],[98] biomolecules,[90],[99] and or a combination of these stimuli[67],[76] to achieve controllable DDSs based on mesoporous silica nanoparticles (MSNs).[100-113]

An important feature of multifunctional MS to consider for the design delivery systems is their possibility to selectively deliver antimicrobians to prevent unwanted side effects to healthy cells caused by non-targeted release. In order to achieve this goal, passive or active targeting, or combination of them is required.[49,59,62,114] In cancer therapy, passive targeting relies on the enhanced permeability and retention (EPR) effect of tumors, an effect of their unique physiology and metabolic rates. Existing evidences showed that EPR effect not only present in tumors, but also exist in bacterial infections.[115,116] Indeed, it has been shown that diffusion of therapeutic-NPs into biofilm was highly depended on PCPs of NPs (e.g., size[117,118] and surface charge[119–121]), demonstrating EPR effect in biofilm drug delivery. However, to the best of knowledge, the effect of PCPs of MS on biofilm drug delivery has not

been systematically investigated. Moreover, in order to overcome the associated limitations of passive targeting approach, active targeting as an effective/complementary way can be considered. This is usually achieved by decorating external surface of the NPs with targeting ligands. In drug delivery to bacteria/biofilms, however, targeted-MSNs have been scarcely used as drug carrier.[87,88,122,123] As an example the disaccharide trehalose has been used as targeting ligand TL for targeted drug delivery to mycobacteria (*vide infra*). Moreover, one of the biggest challenges when using antimicrobials is AMR. Due to high surface area, tunable surface charge/pore size of MS and the possibility of creating hierarchical structures and gated supports, the mesoporous structures can be considered as an excellent candidates for codelivery antimicrobials to circumvent AMR. In general, AMR can occur through different processes in microorganisms, such as increasing bacterial efflux pumps, decreasing the drug uptake, expression of specific gene inactivating antibiotic drugs, alteration of drug targeting sites, reducing antibiotic effectiveness, and biofilm formation.[124] One of the efficient ways to combat AMR is packaging of multiple antibacterial drugs within the same NP. This all-in-one systems can overcome AMR mechanisms, because it is unlikely possible that bacterial cells can develop multiple simultaneous resistance mechanisms to counteract the multiple simultaneous gene mutations induced by the integrated systems. However, there are relatively few examples of codelivery of by MSN-based carriers to overcome AMR.

Moreover, MSNs hold great potential in order to integrate therapeutic and diagnostic functions (such as imaging contrasting agents) within a single system to create unique structures.[125,126] In this context, various nanocomposites (e.g. MSN-magnetic NPs,[126] MSN-quantum dots, MSN-silver NPs,[127] MSN-gold nanoparticles,[128] and MSN- upconversion NPS[129,130]) designed/fabricated for different applications that can be also used in the treatment of bacterial infection. It should be emphasized that the core of the MS can serve not only as imaging tool but also acts as therapeutic function. For example the magnetic, gold, silver, and upconversion NPs could be employed as hyperthermia, photothermal, antibacterial,

and photodynamic agents.[125] Beside the therapeutic capability of core, the mesoporous silica shell can act as excellent reservoirs to load/controlled release drugs, thus demonstrating application of the sandwich-structured nanomaterials as promising platform for synergistic therapy.

For any nanoparticle, which will be employed as therapeutic carrier/agent, it is essential to assess its interaction with the body (cells, tissues and organs) to avoid adverse effects. Encouragingly, many studies have been showing that MSNs are non-toxic and biocompatible if they are prepared with appropriate structural/compositional features and used with appropriate dosages. However, given that size, shape, pore diameter, surface properties, composition, and concentration features can all contribute to this aspect of MS NPs, it is hard to state generalities regarding the biocompatibility of the silica-based carriers to describe their adsorption, distribution, metabolism and excretion (ADME) properties.[53,57] In order to achieve acceptable therapeutic results and mitigate side effects of MS NPs in nanomedicine applications, biodistribution of MS NPs to healthy tissues should be reduced as much as possible while targeting in infecting bacterial cells. Similar to other ADME properties, biodistribution of MS NPs is highly depend on their PCPs.[53,56]

Silica-based NPs is hydrolytically unstable and is gradually converted to silicic acid or polysilicic acid which are nontoxic and can safely be excreted/absorbed by the human body.[131,132] Moreover, today it is possible to design highly biodegradable MS NPs.[132] Recent studies showed that organic doping biodegradable bonds (such as disulfides[133] or tetrasulfides[134]) or inorganic doping metal ions (such as iron,[135] calcium,[136] and manganese[137]) inside the silica framework could control degradation kinetics of MS NPs. Surface modification can also alter degradation rate of MS NPs.[138,139] For instance, there are examples showing that PEGylation can reduce degradation kinetic MS NPs,[140,141] whereas extended pore size MS exhibited faster degradation.[142] Apart from the mentioned PCPs, surfactant removal method can also have significant impact on biodegradation of MS NPs [143].

Similar to other biosafety parameters discussed above, excretion MS NPs is highly depend on their PCPs.[53,132]

This review intends to be a comprehensive analysis of all reports published until the first months of 2019 using MS for antibacterial applications. **Chart 1** shows the chemical structures of the cargos loaded into the MS supports used in the preparation of antibacterial materials. **Table 1** contain a summary of MS-based antibiotics against diverse microorganisms. The review is arranged around the different use of the antimicrobials and the form they are used in combination with MS and is divided in five sections: (i) antimicrobial agents functionalized/adsorbed on MS, (ii) MS loaded with antimicrobial agents, (iii) gated MS loaded with antimicrobial agents, (iv) MS with metal-based NPs and (v) MS loaded with metal ions. This review concludes with a section that discusses future perspectives.

3. MS in antibacterial applications

3.1. Antimicrobial agents functionalized/adsorbed on MS

This section describe MS that are functionalized with antimicrobial molecules or MS containing adsorbed antimicrobial molecules in which the bactericidal effect is not due to the delivery of the cargo but to the interaction of the functionalized/adsorbed molecules with bacteria or the generation of toxic species for instance by adsorbed/functionalized molecules with antibacterial photodynamic activity. Reported examples are based in the use of MCM-41 type mesoporous silica nanoparticles, although also some examples using SBA have been reported. In most cases the antibacterial efficacy of the prepared materials are significantly higher than that of free antimicrobials due to an effective raising of the local concentration of the antimicrobial due to its anchoring or adsorption on the MS.

Several examples are based in the functionalization of MS with small molecules such as vancomycin, essential oils, fatty acids, etc. For instance, vancomycin decorated MS NPs was

prepared by Wang et al. and used for the recognition of gram + bacteria in the presence of macrophages and also for the inhibition of bacterial growth.[146] For this purpose, the nanoparticles were functionalized with aminopropyl moieties and vancomycin was covalently grafted through an amidation reaction using EDC/NHS. Moreover, the solid was covalently functionalized with fluorescein isothicyanate. Confocal laser scanning microscopy studies showed that prepared nanoparticles were able to selectively recognize gram + bacteria (*S. aureus*) in the presence of gram – counterparts (*E. coli*). This selective recognition was ascribed to the fact that vancomycin, grafted on the outer surface of the NPs, form a five-point hydrogen bonding interaction with the terminal D-Ala-D-Ala moieties of the β-1,4-linked-*N*-acetylglucosamine and *N*-acetylmuramic acid peptide on the *S. aureus* membrane. On the other hand, the prepared nanoparticles presented a marked inhibition of *S. aureus* growth with a minimum inhibitory concentration of 200 μg mL^{-1}. Scanning electron microscopy studies showed that cell walls of *S. aureus* started to collapse after 12 h of nanoparticles administration, which led to cell death. Finally, the antibacterial activity of the NPs was also tested *in vivo* in a mice model with remarkable results; a remarkable decrease of bacteria in *S. aureus* infected tissues.

The essential oil components carvacrol, eugenol, thymol and vanillin were covalently anchored onto three different MS supports (fumed silica, amorphous silica and MCM-41) and the antibacterial properties of the prepared materials tested against *E. coli* and *L. Innocua.*[147] For the covalent immobilization of carvacrol, eugenol and thymol onto the inorganic siliceous supports, the aromatic compounds were functionalized with aldehyde groups using well-known formylation protocols. Then, in a second step, the aldehyde-containing derivatives were reacted with (3-aminopropyl)triethoxysilane. In the case of vanillin, direct reaction with (3-aminopropyl)triethoxysilane yielded the final silane compound. The four silane derivatives were directly grafted onto the MS supports. The prepared materials presented enhanced antimicrobial activity against *E. coli* and *L. innocua* when compared with the free essential oil

components. The antimicrobial activity was influenced by both the grafted essential oil component and by the inorganic support. Besides, nanoparticles functionalized with thymol and vanillin were used to eliminate *L. innocua* incorporated into pasteurized milk demonstrating their effectiveness in reducing bacterial content in a real food system.

Delgado and co-workers prepared MCM-41 MS NPs functionalized with lysine and studied the adhesion of *S. aureus* and *E. coli* onto the functionalized scaffold.[148] In afirst step the authors functionalized the surface of the MS NPs with cyanuric chloride, which was then reacted with a lysine-Cu(II)-lysine complex. This reaction yielded the final system grafted with lysine amino acid in its zwitterionic form. Confocal microscopy studies showed that *E. coli* and *S. aureus* were unable to form biofilms onto the lysine-modified nanoparticles as the zwitterionic moieties onto the surface of the nanoparticles decreased the attachment of both bacteria.

Several examples of SBA-15 functionalized in the surface with different groups showing antibacterial activity were reported by Pędziwiatr-Werbicka et al that used silylated natural fatty acids (**1**-**6**, derivatives of undecenoic and oleic acids, see **Figure 2**) to functionalize the external surface of SBA-15 particles by grafting and for the synthesis of PMOs.[149] The different prepared materials presented several degrees of bacterial inhibition growth (in the 10-50% range) depending on the functionalization and the bacteria (*S. aureus, E. coli, S. epidermis, P. vulgaris* and *P. aeruginosa*). The most active solids was a SBA-15 support functionalized with the fatty acid derivative **3** and a PMO synthesized using **6**. Addition of both materials to the selected gram – bacteria induced moderate reduction growths in the 20-40% range.

El Kadib and co-workers prepared SBA-15 simply functionalized with amino, thiol and carboxylic acid moieties and tested their antibacterial properties.[150] Bare SBA-15 was unable to inhibit the growth of gram + (*S. aureus* and *S. epidermis*) and gram – (*E. coli*) bacteria. The

best results were obtained with SBA-15 functionalized with amino and thiol groups, yet were only able to reduce the growth of *S. epidermis* by 18-20%.

Lysozyme-adsorbed MS NPs as efficient *in vitro* and *in vivo* antibacterial agent was developed by Li and Wang.[151] The material showed high antibacterial effect over 24 h against *E. coli*. The lysozyme corona provided multivalent interaction between the support and bacterial walls and consequently raised the local concentration of lysozyme, which promoted hydrolysis of peptidoglycans and increased membrane perturbation. The minimal inhibition concentration (MIC) of the lysozyme-adsorbed MS (75 μg mL^{-1}) was fivefold lower than that of free lysozyme *in vitro* (400 μg mL^{-1}). Furthermore, the antimicrobial efficacy was also evaluated *in vivo* by using an intestine-infected mouse model. Experimental results indicated that the number of bacteria surviving in the colon was three orders of magnitude lower than in the untreated group. Moreover, the support demonstrated low cytotoxicity and negligible hemolytic side effects.

Several examples reported the use of MS coated with *N*-halanine-based polymers. In fact, antimicrobial *N*-halamine polymers have been extensively studied in the last decade thanks to their effectiveness toward a broad spectrum of microorganism.[152] Zou and co-workers prepared MS NPs coated with poly(1-allylhydantoin-*co*-methyl methacrylate) using radical polymerization. Subsequent chlorination with hypochlorous acid yielded the final *N*-halamine decorated NPs.[153] Time killing assays carried out with the prepared nanoparticles indicated that were able to inactivate bacterial growth in a remarkable fashion; 95 and 98% of reduction for *E. coli* and *S. aureus* after 10 min, respectively.

In a similar line Ren and co-workers covalently anchored the poly (5,5-dimethyl-3-(3'-triethoxysilylpropyl)-hydantoin) polymer to SBA-15 microparticles and in a second step chlorinated the polymer with sodium hypochlorite to generate *N*-halamine groups.[154] The final material showed excellent antibacterial activity against *S. aureus* and *E. coli*, inactivating both bacterial strains in 1 min. The same authors also prepared SBA-^{15} microparticles covered

with another *N*-halamine polymer.[155] In this case the external surface of the mesoporous support was functionalized with 3-(trimethoxysilyl)propyl methacrylate and then polymerized with acryloyl ester of 3-(3'-hydroxypropyl)-5,5-dimethylhydantoin. Finally, clorination with sodium hypochlorite yielded the final *N*-halamine-functionalized material. The prepared microparticles were able to inactivate *S. aureus* and *E. coli* in ca. 5 min by the direct transfer of oxidative chlorine atoms to the microbial cell walls, which induced the rupture of receptors in cells and inhibited enzymatic and metabolic processes. The same authors also used the mesoporous materials on the modification of cotton.[156] Soaking in household bleach, the coated cotton showed good antimicrobial efficacy against *S. aureus* and *E. coli*. The chlorinated samples were completely inactivate 100% *S. aureus* within 10 min, and 99.99% *E. coli* within30 min.

Some other reported examples are based in mesoporous particles coated with other polymers containing antimicrobial carbazole or imidazole heterocycles. Sharma and co-workers prepared several vinyl carbazole–SBA-15 nanocomposites for antibacterial activity studies.[157] Carbazole derivatives have been reported to show antibacterial and anti-yeast activities.[158] In this case, the authors loaded SBA-15 mesoporous silica with different quantities of styrene and vinyl carbazole monomers and with fixed amounts of divinyl benzene (cross-linker) and α,α'-azoisobutyronitrile (radical initiator). Using this method, several SBA-15 particles with a carbazole-containing co-polymer were prepared. The antibacterial behavior of the prepared systems was tested against *S. aureus*, *S. mutans*, *E. coli* and *S. typhi*. All nanocomposites were able to inhibit bacterial growth being the lower MIC (350, 200, 320 and 640 μg mL^{-1} for *S. aureus*, *S. mutans*, *E. coli* and *S. typhi* respectively) for the material containing the higher amount of the vinyl carbazole monomer. The antimicrobial activity of the particles was attributed to the disruption of bacteria membrane probably induced by the carbazole heterocycle.

The same authors used a similar strategy to prepare vinyl imidazole–SBA-15 NPs and tested their antibacterial activity against *S. aureus*, *S. mutans*, *E. coli* and *S. Typhi*.[159] This is in line with the extensive work done on heterocycles, especially the imidazole ring, to obtain derivatives with potential antibacterial properties.[160] The final nanocomposites were prepared using an identical procedure to that described above but using a vinyl imidazole monomer instead of vinyl carbazole. Again, all the nanocomposites prepared showed antibacterial activity being the most active that with the higher vinyl imidazole content (MIC in the 320-500 μg mL^{-1} range). The antibacterial activity of the nanocomposites was ascribed to electrostatic (between the positively charged imidazole and the negatively charged bacterial membranes) and hydrophobic interactions (between the alkyl chain of vinyl imidazole and the cytoplasmic membrane of bacteria) that induced an agglomeration of the NPs on bacterial membranes resulting in its disruption.

Another approach in this section is the functionalization or adsorption onto mesoporous silica supports of molecules and nanoparticles able to display antibacterial photodynamic activity. Examples using Rose Bengal, protoporphyrin IX, etc have been reported. Polarz and co-workers developed sunlight-triggered PMOs functionalized with thiols.[161] In one type of the materials, Rose Bengal (RB), as an efficient reactive oxygen species (ROS) producer, was covalently bound to the thiol-PMO. In the second type of materials, nitric oxide (NO·) was functionalized on the thiol-PM, transforming the thiol groups into S-nitrosothiol functionalities. Besides, the oxidation power of RB-thiol-PMO alone and in combination with NO-thiol-PMO using sunlight as a trigger was evaluated. The simultaneous release from NO-thiol-PMO of nitric oxide (NO·) in combination with ROS leaded to the emergence of the highly reactive peroxynitrite molecules ($ONOO^-$) with significantly enhanced biocidal activity. The high antibacterial efficiency of dual action nanoparticles was demonstrated using disinfection assays with the pathogenic bacterium *P. aeruginosa*.

Antibacterial photodynamic activity of the photosensitizer methylene blue-loaded amino-functionalized (AM-MS) or mannose-functionalized (M-MS) MS NPs were developed by Nonell and co-workers (**Figure 3**).[162] Antimicrobial assays were developed against *E. coli* and *P. aeruginosa*. The studies showed that methylene blue adsorbed on the NPs was capable of efficiently inactivating *E. coli* and *P. aeruginosa* upon exposure to red light. The antibacterial photodynamic activity was similar to that of free methylene blue but, in the case of *E. coli*, the NPs clearly reduced the dark toxicity of methylene blue while preserving its photoinactivation activity. In the case of *P. aeruginosa*, M-MS showed higher antibacterial activity than observed when using AM-MS.

Nonell, Latterini and co-workers prepared different silica-protoporphyrin IX (PpIX) derivatives as antimicrobial agents.[163] The systems - compact silica nanoparticles (CSNP), mesoporous silica nanoparticles (MPSAm), stellate mesoporous silica nanoparticles (MPSSt) and larger pore mesoporous silica nanoparticles (MPSLP) – functionalized with PpIX were synthesized to evaluate the morphology-dependence of the nanomaterials in the singlet oxygen production and their bacterial efficiency against *S. aureus*. The studies showed that singlet oxygen production was higher in the sample with the greatest pore volume (i.e PpIX-MPSLP). Moreover, photoinduced antimicrobial tests of PpIX-doped silica nanoparticles for 15 minutes, confirmed the antimicrobial effect of the PpIX-CSNP, PpIX-MPSSt and PpIX-MPSLP. However, PpIX-MPSAm did not develop any photo-induced antibacterial activities.

3.2. MS loaded with antimicrobial agents

In this section, examples of MS able to deliver an antimicrobial molecule are described. Most reported examples use classical MS derivatives loaded with well-known small molecules acting as antimicrobials such as caprylic acid, tetracycline, isoniazid, amoxicillin, and curcumin. Iron oxide-MS and more advanced composites for certain antimicrobial

applications have also been reported (*vide infra*). Moreover, MS loaded with antimicrobials but also containing AgNPs are described in section "MS with metal-based NPs".

For instance, MCM-41 type MS NPs loaded with caprylic acid were prepared by Marcos et al., and their antibacterial activity against *E. coli, S. enterica, S. aureus* and *L. monocytogenes* was studied.[164] The prepared nanoparticles showed a total inhibition of bacterial growth at concentration of released caprylic acid in the 18.5-20 mM range. Transmission electron microscopy images revealed that the released caprylic acid disrupted the bacterial membrane with subsequent leakage of cytoplasmic content and cell death.

Di Pasqua and co-workers prepared two different sized tetracycline-containing MS particles (41 ± 4 nm and 406 ± 55 nm) for the treatment of *E. Coli.*[165] A burst release was observed in both formulations and the drug was released by after 5 h, although most tetracycline was released over the first hour. Antimicrobial tests showed similar inhibition of *E. coli* growth within 4 h after treatment, using free tetracycline, tetracycline loaded in the small MS and tetracycline loaded in the large MS. However, after 4 h and up to 24 h, both tetracycline-loaded MS exhibited greater inhibition on bacteria growth than free tetracycline. MS NPs loaded with tetracycline were also prepared by Sujitha and co-workers and its antibacterial activity against *S. aureus* and *E. coli* was tested.[166] The prepared tetracycline loaded NPs were able to inhibit the growth of *S. aureus* and *E.coli* in inhibition zone assays being more effective for the gram negative bacteria.

Yan and co-workers prepared amine-functionalized hollow MS NPs with efficient antibacterial (and anticancer) effects.[167] The nanoparticles loaded with isoniazid (INH) (an ant-tuberculosis agent) exhibited excellent killing efficiency against *Mycobacteria* (*M. smegmatis* strain mc^2 651). The material in PBS at pH 6.6 reached a drug release of ~60% after 72 h. Colony counting antimicrobial tests were used to evaluate the antibacterial effect of free INH and INH-loaded hollow MS against *M. smegmatis* mc^2 651 over 72 h. Free INH-treated *Mycobacteria* were completely inhibited at the concentration of 1280 μg mL^{-1}, while

INH-loaded MS treated *Mycobacteria* were completely inhibited at the concentration of 640 and 320 μg mL^{-1}, for 24 and 72 h incubation respectively. This enhanced antibacterial activity was attributed to increased intrabacterial accumulation of INH delivered from the hollow MS and partly by the strong interactions between the MS and bacteria.

Yan, Ramström and co-workers also prepared INH-loaded MS NPs in this case additionally functionalized with α,α-trehalose through azide-mediated surface photoligation for the selective targeting of *M. smegmatis* mc^2 651.[168] The nanomaterial showed increased ability to kill bacteria, displaying the advantageous target function of trehalose to facilitate the localized release of INH, with a complete growth inhibition within 3−4 mg mL^{-1}. Indeed, trehalose exists as both free form in the cytosol of mycobacteria and as glycolipids in the cell wall,[169] constituting a great target molecule for this bacterial genus. The targeted MS-based delivery system showed an eightfold improvement in the antibacterial activity towards mycobacteria as compared to the free drug, demonstrating the ability of the targeting ligand to selectively target these bacterial cells.

Alhabardi prepared MS NPs loaded with amoxicillin and erythromycin and tested its antibacterial behavior against *S. aureus* and *E. Coli.*[170] Both nanoparticles were able to inhibit the growth of *S. aureus*. However, only erythromycin-loaded nanoparticles effectively inhibited *E. coli* growth. The authors suggested that the inability of amoxicillin-loaded NPs to kill the gram negative *E. coli* was due to the small amount of drug released from the MS.

Film-, platelet-, sphere-, and rod-like MS NPs synthesized by varying the mole ratio of cationic surfactant templates, cetyltrimethylammonium bromide (CTAB) and tetrabutylammonium iodide (TBAI), were developed by Yan and co-workers.[171] The release profiles of CTAB and TBAI from differently shaped materials were determined by suspending equal quantities of each material in PBS (pH 7.4) over 48 h. Colony counting antimicrobial test was used to evaluate MS behavior against *M. smegmatis* strain mc^2 651. Film-like MS showed higher and faster antibacterial activity than other particle shapes against

M. smegmatis, and completely inhibited the formation of colonies at a concentration as low as 25 μg mL^{-1} after 48 h treatment.

In addition to the use of small molecules as antimicrobials Yu and co-workers prepared small- and large-pore dendritic MS NPs loaded with the antimicrobial enzyme lysozyme.[172] MS with a smaller pore size showed a burst release of 100% of the lysozyme within 2 h, which was attributed to the surface adsorption of lysozyme. In contrast, MS with a large pore size exhibited sustained release patterns with about 67% of lysozyme released within 48 h. Besides, lysozyme loaded into MS with a large pore size showed significantly better antibacterial activity (MIC value of 500 μg mL^{-1}) compared to the NPs with a smaller pore size. The optimized MS loaded with lysozyme exhibited total inhibition towards *E. coli* throughout five days.

Thompson and co-workers developed effective delivery of allyl isothiocyanate (AIT) and cinnamaldehyde (CNAD) by using MS NPs for treating biofilms.[173] The release of both AIT and CNAD from MS, showed a high initial rate over the first hour due to the steep concentration gradient established from within and outside the pores in the external solution or due to release of compounds adsorbed on the external surface of the NPs. Subsequently, there was a slight and gradual decrease in concentration in the solution from 1 to 24 h for both compounds due to their highly volatility. Besides, AIT and CNAD demonstrated increase antimicrobial activity against *E. coli* when packaged into MS NPs than in free forms. IC_{50} for CNAD-loaded MS NPs was around 2 μg mL^{-1}, while IC_{50} for AIT-loaded MS NPs was 1 μg mL^{-1}. The authors also found that the biocide-loaded NPs showed activity against *P. aeruginosa* biofilms that have inherent resistance to antimicrobial agents.

Chakravortty, Raichur and co-workers developed MS nanocarriers functionalized with arginine and loaded with an antibiotic for targeting and treatment of intracellular *Salmonella*.[174] The arginine based nanocarrier system was developed using a layer-by-layer coating approach (**Figure 4**). First, the negatively charged MS NPs were coated with the

cationic polymer protamine and subsequently with the negatively charged pectin polyelectrolyte to form a shell of oppositely charged polyelectrolyte layers. The polyelectrolyte-coated MS was decorated with L-arginine (to target intracellular *Salmonela*) by conjugation with the exterior pectin layer. Ciprofloxacin, a fluoroquinolone antibiotic, was additionally entrapped in the pores of the NPs. Ciprofloxacin was gradually released over a period of 24 h from the NPs in PBS at neutral pH. *In vitro* antibacterial activity of ciprofloxacin-loaded MS was compared with free ciprofloxacin on *S. typhimurium;* the ciprofloxacin-loaded MS exhibited two-fold higher antibacterial activity. The increased antibacterial activity of ciprofloxacin-loaded MS was in line with the co-localization of the NPs with the intravacuolar *Salmonella* and localized delivery of the antibiotic. Besides, *in vivo* bacterial burden and morbidity studies in BALB/c mice exhibited nearly ten-fold lower *Salmonella* burden in infected organs such as spleen, liver and mesenteric lymph nodes. Similar survival rates were observed at a lower dosage of ciprofloxacin-loaded MS than when using free ciprofloxacin.

Different MS NPs having various particle morphologies, including spheres, ellipsoids, rods, and tubes, for controlled release of antibacterial ionic liquids (i.e 1-tetradecyl-3-methylimidazolium bromide (C_{14}MIMBr), 1-hexadecyl-3-methylimidazolium bromide (C_{16}MIMBr), 1-octadecyl-3-methylimidazolium bromide (C_{18}MIMBr), and 1-tetradecyloxymethyl-3-methylimidazolium chloride (C_{14}OCMIMCl)) were described by Lin and co-workers.[175] Delivery of the ionic liquids from MS was governed by the particle and pore morphology. Besides, antibacterial activities against *E. coli* of ellipsoids C_{16}MIMBr-MS and tubes C_{14}OCMIMCl-MS, measured over 48 h showed higher activity for the former. The mechanism of the antibacterial activity of ellipsoids C_{16}MIMBr-MS was attributed to the electrostatic interaction of phosphate groups on the microbial cell wall and the cationic methylimidazolium head group of the ionic liquid. The pronounced difference in antibacterial activity was attributed to the different release profiles and pore morphologies, ellipsoids

C_{16}MIMBr-MS has hexagonal array of ordered pores that all line up parallel allowing faster release, while tubes C_{14}OCMIM-MS has a disordered pore arrangement.

Portolés, Vallet-Regí and co-workers developed different mesoporous microparticles loaded with levofloxacin using different drug-loading methods, i.e. impregnation (IP) and surfactant-assisted drug loading, also denoted as one-pot (OP).[176] Surfactant-free (calcined) and surfactant-templated (non-calcined) MS were used for IP and OP starting materials, respectively. Flow cytometry studies showed that IP and OP MS did not exert any cytotoxic effect on osteoblasts, however, OP induced on fibroblasts a significant proliferation delay with morphological alterations and intracellular calcium content but without cell lysis or apoptosis. Moreover, both IP and OP MS loaded with levofloxacin, exhibited similar drug release profiles. Release studies showed an initial fast delivery followed by a sustained release during 13 days. For antibacterial activity studies, IP and OP MS loaded with levofloxacin were incubated with *E. coli*. Bactericidal effectiveness was observed for 14 days for the material loaded by IP and for 5 days for the material loaded by OP.

MS particles loaded with PA-824 (a hydrophobic bactericidal agent) and moxifloxacin were prepared and their effect in macrophages infected with *M. tuberculosis* tested.[177] For this purpose, Raw 264.7 macrophages were infected with *M. tuberculosis* and then were incubated with the loaded MS particles for 5 days. Both loaded particles were able to induce a reduction in *M. tuberculosis* population. Encapsulated PA-824 reached the highest antibacterial activity at a concentration of 3.33 μg mL^{-1}. On the other hand, the highest antibacterial activity for encapsulated moxifloxacin is 1.11 μg mL^{-1}. Besides, EC_{50} values were 1.03 and 0.88 μg mL^{-1} for the particles loaded with PA-824 and moxifloxacin, respectively.

Tailored silica nanoparticles functionalized with (3-aminopropyl)triethoxysilane (APTES) and loaded with curcumin were prepared by Cardoso and co-workers.[178] The bactericidal properties of these materials were tested against *E. coli* showing higher effect when the silica was functionalized with APTES and loaded with curcumin than their bare silica counterparts

(silica functionalized with APTES but without curcumin or silica loaded with curcumin without APTES). The bactericidal activity of the materials was evaluated by counting the number of colonies formed on *E. coli* Agar plates. The antibacterial effect of silica nanoparticles functionalized with APTES and loaded with curcumin was justified due to (i) the electrostatic attraction between the positively charged of the amino groups and the negatively charged bacteria membrane, and (ii) the curcumin drug effectively loaded into the mesoporous silica.

Raichur and co-workers used MS NPs loaded with ciprofloxacin and coated with a lipid bilayer of 1,2-dipalmytoil-*sn*-glycero-phosphocholine, for the elimination of *S. Typhimurium*.[179] Lipid-coated nanoparticles showed a moderate ciprofloxacin release at neutral pH (30% after 30 min) whereas at pH 2.5 a more marked release of the drug was observed (probably due to an increase in its solubility at acidic pH). Besides, MTT viability assays carried out in RAW 264.7 cells indicated that the system was not toxic. The NPs (at 50 $\mu g\ mL^{-1}$ concentration) effectively killed *S. typhimurium* in RAW 264.7 and HeLa cells infected with the bacteria. Also, lipid coated nanoparticles were used for the treatment of mice infected with *S. typhimurium* with remarkable results. For this purpose, *S. typhimurium* was administered orally to mice and then treated with nanoparticles (10 $mg\ kg^{-1}$ given orally twice a day for three days). The treated mice were able to survive till 15 days post infection.

Xiao and co-workers prepared a multifunctional nanoplatform based on MS NPs for imaging guided chemo/photodynamic synergetic therapy (**Figure 5**).[180] In a first step, carbon dots (C-dots) were prepared and then embedded in MS NPs (MS@C-dots). Then, Rose Bengal (RB, a photosensitizer) was adsorbed onto the MS@C-dots to form MS@C-dots/RB nanoparticles, in which C-dots served as a fluorescence probe to achieve cell fluorescence imaging and RB generated singlet oxygen to perform photodynamic therapy (PDT). A remarkable chemo/photodynamic synergistic anti-tumor effect was achieved with MS@C-dots/RB nanoparticles loaded with doxorubicin (Dox) under green light irradiation. Moreover,

MS@C-dots/RB nanoparticles showed a significant bacterial inhibitory effect against *E. coli*. Photographs of *E. coli* colonies grown on agar plates showed bacterial inhibition with increasing concentrations of MSN@C-dots/RB. 100 mg mL^{-1} of particles inhibited *E. coli* growth over 12 h under green light irradiation. Besides, a significant bacterial inhibitory effect against *E. coli* was also achieved using MSNs@C-dots/RB nanoparticles loaded with ampicillin without light irradiation due to ampicillin delivery.

Anirudhan and co-workers prepared MS NPs loaded with amoxicillin and thiamine hydrochloride and coated with chitosan.[181] In a first step, mesoporous silica nanoparticles containing cyanopropyl moieties were prepared using the co-condensation method. Then, the cyano moieties were oxidized to carboxylic acids by treatment with sulfuric acid. The pores of the carboxylic acid-functionalized NPs were loaded with thiamine hydrochloride. Afterward, chitosan was grafted onto the external surface of the nanoparticles by the formation of amide linkages using EDC. Then, the chitosan layer was modified with a polymer formed by free radical graft copolymerization using methacrylic acid, itaconic acid and ethylene glycol dimethacrylate as crosslinker agent. Finally, amoxicillin was adsorbed onto the structure of the final nanoparticles. Inhibitory zone assays carried out with the prepared nanoparticles and *E. coli* and *S. aureus* bacteria showed only moderate *E. coli* growth inhibition (MIC of 50 μg mL^{-1}) as consequence of amoxicillin release.

Apart of the examples described above, SBA-15 supports (functionalized and un-functionalised on the surface) have also been used for loading different antimicrobials that were delivered by simple diffusion from the mesopores. Malmsten and co-workers prepared bare and mercaptopropyl-functionalized SBA-15 MS monoliths whose pores were loaded with chlorhexidine or with the antimicrobial peptide LL-37 (LLGDFFRKSKEKIGKEFKRIVQRIKDFLRNLVPRTES).[182] The four prepared materials released, in a sustainable form, chlorhexidine and LL-37 (maximum release achieved after 200 h). Moreover, thiol functionalized monoliths released smaller amounts of cargo due to

their hydrophobic internal surface, when compared to the un-functionalized material. The four prepared materials were able to kill *E. coli* and *S. aureus* at concentrations of 1.0×10^4 and 2.0×10^5. However, when higher concentrations of bacteria were used (1.0×10^6), only materials loaded with chlorhexidine were efficient. The authors ascribed this fact to the incomplete release of LL-37 peptide from the monoliths.

Vallet-Regí and co-workers prepared SBA-15 disks loaded with vancomycin, rifampicin and with a combination of the two drugs and studied the antimicrobial features of the materials against biofilms of *S. aureus* and *S. Epidermidis*.[183] After 6 h of incubation, the three materials were able to induce reduction in the biofilms density for both bacteria. However, the observed reduction was more marked for *S. epidermidis* than for *S. aureus*. At longer times (24 h) the materials loaded with vancomycin and with both drugs showed a marked antimicrobial activity for *S. aureus* and *S. epidermidis*.

Hua and co-workers prepared a silica nanocomposite loaded with human bone morphogenic protein-2 (rhBMP-2) and tested against *E. coli* and *S. Aureus*.[184] In a first step, mesoporous SBA-15 NPs were prepared using Pluronic P123 as structure directing agent. Then, the NPs, zein (a water insoluble storage protein found in corn), and hydroxypropyltrimethyl ammonium chloride chitosan were mixed and transformed onto a nanocomposite using a solvent casting-particulate leaching procedure. Finally, rhBMP-2 was loaded upon dropwise addition onto the nanocomposites. The prepared system showed a long-term antibacterial activity against *E. coli* and *S. aureus* with marked inhibitions from day 1 to day 28. This antibacterial activity was ascribed to the sustainable release of rhBMP-2 protein from the scaffold. Besides, the prepared scaffolds are biocompatible and induced early osteogenic differentiation *in vitro* and ectopic ossification *in vivo*.

Vallet-Regí and co-workers used a co-condensation route to functionalize SBA-15 with primary and secondary amine groups.[185] The tests against *S. aureus* demonstrated that the amine functionalized SBA-15 was capable of inhibiting 99.9% of the bacterial adhesion

compared to pure SBA-15 (both materials in the form of disk-shaped pieces of 6 mm diameter and 1 mm height prepared by compacting fractions of 20 mg of the dried powders). Loading and release assays using cephalexin as a model antibiotic proved that amine-functionalized SBA-15 can release the cargo over long time periods (more than 15 days) compared to pure SBA-15. Agar disk-diffusion tests with *S. aureus* were also performed. Cephalexin-free samples did not provoke inhibition zones during the test, which accounts for their lack of bactericidal effect. In contrast, well-defined inhibition zones were observed in the assays with the cephalexin-loaded materials.

Grumezescu and co-workers prepared MS of ca. 200 nm diameter loaded with eucalyptus, orange and cinnamon essential oils[186] and the antimicrobial properties of the nanoparticles were tested against *S. aureus*, *E. coli* and *C. albicans*. The most efficient NPs against *S. aureus* were those loaded with orange essential oil (MIC of 0.37 μg mL^{-1}) whereas those containing cinnamon were the most efficient for *E.coli* (MIC of 2.5 μg mL^{-1}). In addition, the highest activity toward the yeast *C. albicans* was observed for the NPs loaded with eucalyptus essential oil (MIC of 0.18 μg mL^{-1}). Besides, NPs loaded with the three essential oils showed a marked inhibitory effect toward the formation of *S. aureus* and *E. coli* biofilms. NPs loaded with orange essential oil showed the highest inhibitory effect in *C. albicans* biofilms. The authors also tested the biocompatibility of the prepared NPs using the MTT assay with L929 cells. The three nanoparticles showed good biocompatibility at low concentrations (10 μg mL^{-1}).

Shchukin and co-workers loaded MCM-48 NPs (400 nm diameter), with the biocide parmetol S15, and additionally functionalized the external surface with the bactericidal derivatives dimethyloctadecyl[3-(triethoxysilyl)propyl]ammonium chloride and dimethyltetradecyl[3-(triethoxysilyl)propyl]ammonium chloride.[187] Unloaded materials were able to reduce bacterial population of *E. coli* (77-89%) and *S. aureus* (78-94%), being that functionalized

with octadecyl groups more effective due to the presence of longer alkyl chains that penetrated easily in the bacteria membrane. Besides, the nanoparticles loaded with parmetol S15 presented 100% reduction after 3 h for both *E. coli* and *S. aureus*.

Some MS particles combined with magnetic nanoparticles have also been reported for the efficient capture and elimination of bacteria. For instance, magnetic Janus nanorods for the efficient capture, separation and elimination of bacteria were prepared by Dong and co-workers.[188] These Janus nanodevices consisted of a Fe_3O_4 head (nanoparticles of 100 nm diameter) and a mesoporous silica rod (200 nm length) with the surfactant CTAB in the inner of the pores and aminopropyl moieties grafted onto the external surface. The prepared Janus nanorods could capture and separate *E. coli* and *S. aureus* by using an external magnet. The capture was a direct consequence of electrostatic interactions between the positively charged silica nanorod and the negatively charged surface of the bacteria. The efficiency of the capture process reached 90.1 and 85.4% for *E. coli* and *S. aureus* respectively. Besides, using a concentration of nanorods of 50 μg mL^{-1} the measured antibacterial efficiencies for *E. coli* and *S. aureus* were 95.9 and 73.6% respectively. The use of 100 μg mL^{-1} of Janus nanorods inhibited completely bacterial growth.

Fang and co-workers also prepared Fe_3O_4 magnetic NPs coated with a MS shell containing CTAB in the pores.[189] When the concentration of the prepared nanoparticles was set at 50 μg mL^{-1}, remarkable inhibition growths for *E. coli* (98%) and *B. subtilis* (97%) were observed after 24 h of incubation. Besides, the authors showed that magnetic nanoparticles could be efficiently used for bacteria capture and separation by using a magnet.

Faivre, Sitti and Sánchez prepared magnetotactic bacteria powered biohybrids targeting *E. coli* biofilms.[190] The nonpathogenic magnetotactic bacteria *Magnetosopirrillum gryphiswalense* (MSR-1) was adhered inside ciprofloxacin-loaded MS microtubes, to build controllable microswimmers for ciprofloxacin delivery to target *E. coli* biofilm. Applying an

external magnetic guidance the biohybrids were directed and pushed into matured *E. coli* biofilms, showing high antibacterial efficacy due to effective ciprofloxacin delivery. The solubility of ciprofloxacin in aqueous solutions is pH dependent, and in this context ciprofloxacin release was triggered by the acidic microenvironment at pH 5.8 of the biofilm. At pH 7.4, almost no ciprofloxacin was released from the tubes over 24 h.

Examples above are based in the use of MS that allowed a targeted or untargeted delivery of a certain bactericidal. Moreover, more advanced systems in which MS are incorporated in films, hydrogels, fabrics, and bone implants have also been prepared. Thus, Shen and co-workers prepared titanium films coated with an antibacterial MS layer, which could be used as implant material.[191] The pores of the MS coating were loaded with heparin and vancomycin. When the prepared films were dipped onto a PBS solution, vancomycin and heparin were simultaneously released reaching a maximum value of 400 and 700 μg of drugs per cm^2 of film respectively (after 30 days). The prepared films presented high levels of viability with rat osteoblasts. Besides, the prepared films were able to inhibit the growth and adhesion of *S. aureus* and *E. coli* due to the release of the entrapped heparin and vancomycin. In a closely related approach, the same authors prepared silicone films functionalized with aminopropyl moieties and adsorbed, through electrostatic interactions, MS NPs loaded with agarose and heparin.[192] The prepared materials were able to release heparin when introduced into a PBS solution (40% of delivery after 1 day). The films presented remarkable antifouling properties against red blood cells, platelets, fibrinogen and bacteria (*E. coli* and *S. aureus*). The inhibition of bacterial adhesion was ascribed to the improved surface hydrophilicity imparted by the agarose loading.

Xu, Cai and co-workers coated titanium disks with MS NPs using an electrophoretic-enhanced micro-arc oxidation procedures. The MS NPs were loaded with the antiseptic agent octenidine dyhidrochloride.[193] A marked reduction in bacterial adhesion (*E. coli* and *S. aureus*) was observed using the loaded disks. In contrast, bacteria adhesion was observed

when the MS-coated disks without any cargo were used. The authors ascribed the reduction in bacterial adhesion to the release of octenidine dyhidrochloride. This compound was inserted into the bacteria walls, through electrostatic interactions, breaking down the integrity of bacteria.

Huang and co-workers prepared hydroxyapatite-MS materials loaded with epigallocatechin-3-gallate for the therapeutic elimination of *Streptococcus mutants* biofilms.[194] UV-visible measurements indicated that epigallocatechin-3-gallate was released from the material in a sustainable fashion over 96 h. Besides, MTT viability assays carried out with the nanocomposite showed non-toxicity for human dental pulp stem cells. Dentin tubules were filled with the prepared bio-nanocomposite and a marked *S. mutans* biofilms inhibition was observed due to the release of epigallocatechin-3-gallate.

He and co-workers developed an organic–inorganic hybrid hemostatic material by incorporating curcumin-loaded MS NPs into polyvinyl pyrrolidone (PVP) nanofiber mats by electrospinning.[195] *In vitro* cytotoxic studies demonstrated that the hybrid nanofiber mats had no obvious toxic effect on the growth of murine L929 fibrosarcoma cells. Moreover, the hybrid nanofiber mats exhibited enhanced *in vitro* antibacterial effect against methicillin-resistant *S. aureus* due to the delivery of the loaded curcumin. Furthermore, an *in vivo* liver injury model for hemostasis studies revealed that the hybrid nanofiber mats rapidly transform into hydrogel when in contact with blood, and activate the clotting system to stop wound bleeding. This provides an example of nanofiber-based hemostatic materials with good biocompatibility and high antibacterial activity.

MS SBA-15 particles have also been used for the preparation of more complex composites of potential applications by its incorporation in fabrics and in dental composites. Thus, SBA-15 NPs, functionalized with 3-aminopropyl moieties and loaded with betamethasone sodium phosphate, were grafted onto a cotton fabric surface using chitosan and polysiloxane.[196] The SBA-15 loaded-NPs were covalently grafted onto the modified cotton fabric surface through

an addition reaction of the silanol moieties of the MS with the epoxide groups of the polysiloxane. The growth of *E. coli* and *S. aureus* strains was remarkably reduced in the cotton fabric samples containing the loaded SBA-15 particles (99.9 and 99.4% reduction for *E. coli* and *S. aureus* respectively). In addition, Xu and co-workers developed an antibacterial dental composite against *S. mutans* and *Lactobacillus casei* containing chlorhexidine encapsulated in SBA-15.[197] For the preparation of the composite, in a first step, the pores of the SBA-15 were loaded with chlorhexidine. Then, the loaded nanoparticles were mixed with bisphenol A glycidyl methacrylate, hexanediol dimethacrylate, ethoxylated bisphenol A dimethacrylate, urethane dimethacrylate and a photo-initiator (camphorquinone: phenyl bis(2,4,6-trimethyl benzoyl)phosphine oxide: ethyl 4-dimethylaminobenzoate). Irradiation with a visible light yielded the final composite. Upon immersion of the prepared nanocomposite in water at 37 ºC a sustainable release of chlorhexidine over a long time period was observed. The antibacterial efficacy of the composite was evaluated using two methods: planktonic bacterial growth and biofilm tests. Both assays showed strong inhibition against S. *mutans and L. casei* by the SBA-15-containing composite.

In a system for applications in bone-implant technology, Grumezescu and co-workers used matrix assisted pulsed laser evaporation to deposit thin coatings of MS NPs loaded with the antibiotic Zinforo (ceftarolinum fosmil) at the bone-implant interface.[198] Microbiological analyses performed on Zinforo-loaded films against *E. coli* demonstrated a decrease of the microbial adherence and colonization of the surface for 72 h. Moreover, *in vitro* MTT assays showed no-cytotoxicity of the Zinforo-loaded thin coatings against endothelial EAhy926 cells over 72 h. Besides, *in vivo* assays were carried out with mice intraperitoneally inoculated in the groin area with the Zinforo-loaded MS nanoparticles, providing the excellent biodistribution and biocompatibility. At 7 and 14 days after inoculation mice were killed and the different tissues fixed in paraffin. The subsequent histological evaluation showed than Zinforo-loaded MS nanoparticles were found only into the red pulp of the spleen.

Santamaría and co-workers prepared hollow porous medical grade stainless steel pin implants filled with MCM-48 microparticles for linezolid release.[199] In a first step, MCM-48 microparticles were prepared and their pores loaded with linezolid. Then, the linezolid-loaded microparticles were packed inside of a porous stainless steel pin. This nanodevice was able to release, for 6 days, the loaded linezolid upon its immersion in simulated body fluid at 37 ºC. Besides, the prepared stainless steel pin was able to reduce *S. aureus* growth up to 3 orders of magnitude after 48 h when compared with a similar nanodevice packed with empty MCM-48 microparticles.

Behrens and co-workers prepared MS coatings for the release of ciprofloxacin from implants to prevent bacterial infection.[200] The authors prepared three different MS coated supports. For this purpose, and in a first step, a glass substrate was coated with a MS layer. Then, the silica layer was functionalized with mercaptopropyl units and, afterward, the thiol groups were oxidized to sulfonic acids using hydrogen peroxide. The pores were finally loaded with ciprofloxacin (material A). Moreover, the pores of the loaded substrate were capped by dip-coating using bis(trimethoxysilyl)hexane, yielding material B. Finally, for the preparation of material C, the capping layer was further treated with dioctyltetramethyldisilazane. The three materials, when submerged in PBS, where able to release the entrapped drug at a constant rate during several days (12, 30 and 63 for materials A, B and C respectively). Besides, the three materials released a similar amount of ciprofloxacin (ca. 2 μg cm^{-2}). The authors found that the three prepared materials were able to inhibit the growth of *P. aeruginosa* for up to ten days being the uncapped glass the most effective.

Vallet-Regí and co-workers developed multifunctional pH sensitive 3D scaffolds for treatment and prevention of bone infection.[201] The hierarchical meso-macroporous 3D scaffolds consisted of a mesostructured SiO_2–CaO–P_2O_5 glass wall with embedded hydroxyapatite nanoparticles, whose mesopores were loaded with levofloxacin. These 3D platforms exhibited controlled and pH-dependent levofloxacin release, over 4 h, at

physiological pH (7.4), which notably increased at pH 6.7 and 5.5. This was attributed to the different interaction between levofloxacin species and the silica matrix. 3D scaffolds were able to inhibit the *S. aureus* growth over 15 days and to destroy the bacterial biofilm. Furthermore, *in vitro* co-culture studies showed no cytotoxic effects of the scaffold on MC3T3-E1 cells, a murine calvaria-derived pre-osteoblastic cell line. Besides, the scaffold showed biocompatibility on human osteosarcoma Saos-2 cell line.

Jin and co-workers loaded the pores of MS nanoparticles with chlorhexidine and studied the antibacterial activity of the loaded material against several biofilms.[202] The prepared chlorhexidine-loaded nanoparticles were able to release the entrapped antibiotic in a sustainable fashion for 72 h reaching the maximum delivery after 6 h. The prepared nanoparticles showed a marked antibacterial effect and were able to inhibit bacterial biofilms of *S. mutans*, *S. sobrinus*, *F. nucleatum*, *A. actinomycetemcomitans* and *E. faecalis* with MICs of 100, 200, 100, 100 and 200 μg mL^{-1}, respectively. Besides, nanoparticles were also able to inhibit growth of mixed biofilms. At this respect, for biofilms of *S. mutans*, *F. nucleatum* and *P. gingivalis* the MIC after 24 h was 12.5 μg mL^{-1} whereas for *S. sobrinus*, *F. nucleatum* and *P. gingivalis* MIC was 25 μg mL^{-1} after the same time period. Finally, for a biofilm of 4 bacteria (*S. mutans*, *F. nucleatum*, *A. actinomycetemcomitans* and *P. gingivalis*) the measured MIC was 25 μg mL^{-1} after 24 h.

MS nanoparticles loaded with gentamicin were deposited onto thin films and its antibacterial performance was tested against *S. aureus* biofilms.[203] For the preparation of the final thin films, quartz slides were coated with polyelectrolyte layers of polyehtyleneimine and polystyrene sulfonate-polyallylamine. Then, gentamicin-loaded MS nanoparticles were deposited onto the polyelectrolyte layers and finally a protective outer nafion layer was applied. Inhibition zone experiments, carried out with the prepared thin films and *S. aureus* and *S. pneumoniae*, showed marked antibacterial effects due to the sustained gentamicin release from the nanodevices. The observed effects are maintained even after 103 days.

Besides, the prepared films were able to inhibit the growth of *S. aureus* biofilms and negligible bacterial attachment onto the external surface of the films was observed by confocal laser scanning microscopy measurements after 2 months.

3.3. Gated MS loaded with antimicrobial agents

As explained above gated MS are nanodevices which are able to release an entrapped cargo at will upon application of selected external stimuli. Gated MS have been used for the controlled released of drugs in nanomedice applications,[102] as new sensory materials[113] and, very recently, in abiotic communication processes,[107] however gated MS in bactericidal applications have been scarcely used. Examples of gated MS able to release an entrapped antimicrobial in the presence of bacteria, pH changes, enzymes, certain chemical species, temperature and light have been described.

Some examples of antimicrobial gated MS were able to release its entrapped cargo in the presence of bacteria by simple detachment of the capping molecules upon interaction with the bacterial wall. Following this approach Martínez-Máñez and co-workers enhanced the efficacy and broadening of antibacterial action of drugs.[204] The nanodevice was based in MS NPs loaded with vancomycin (MS-Van). Then, the external surface of the loaded support was functionalized with *N*-[(3-trimethoxysilyl) propyl]ethylendiamine triacetic acid trisodium salt and capped, through electrostatic interactions, with the cationic polymer ε-poly-L-lysine (ε-PL). MS-Van was used as antimicrobial agent against *E. coli, Salmonella typhi* and *Erwinia carotovora.* Moreover, using a similar procedure, MS nanoparticles loaded with rhodamine B and capped with ε-PL were prepared (MS-Rho) and *in vitro* dye-release studies were carried out (see **Figure 6**). Dye delivery from MS-Rho was studied in the presence and absence of *E.coli*. In the absence of *E. coli* negligible dye release was observed, indicating that the NPs were tightly capped. In contrast, in the presence of bacteria the uncapping of the pores was clearly observed, attributed to the adhesion of the positively charged ε-PL of the MS-Rho

with the negatively charged bacterial wall, which resulted in cargo delivery. Moreover, the effect on bacterial cell integrity by clonogenic cell-viability assays was carried out with bare MS nanoparticles, free vancomycin, free ε-PL, free ε-PL/vancomycin, MS-Rho and MS-Van. A remarkable enhancement of the toxicity of ε-PL and vancomycin in MS-Van was found against *E. coli*. For instance, MS-Van exhibited a noteworthy six-fold decrease in MIC (2.89 μg ε-PL mL^{-1}) when compared to that of MS-Rho (16.7 mg ε-PL/mL). Furthermore, antimicrobial activity of the solid MS-Van against *E. coli* 405, *Salmonella typhi* and *Erwinia carotovora* was also carried out. The obtained results indicated a strong inhibition of bacterial growth and a large synergistic effect (due to the release of both ε-PL and vancomycin) when this nanoformulation was used.

Using a similar approach, Velikova and co-workers prepared different gated MS NPs loaded with histidine kinase autophosphorylation inhibitors (HKAIs). Pores of the loaded support were again functionalized with *N*-[(3-trimethoxysilyl) propyl]ethylendiamine triacetic acid trisodium salt and capped with ε-PL.[205] Antimicrobial tests using the prepared nanoparticles against *E. coli* and *Serratia marcescens* showed higher activity that free HKAIs. As before, the mechanism of action of the particles was attributed to the interaction of the positively charged capped-MS with the negatively charged *E. coli* bacterial cell wall, and displacement of the capping ε-PL, which resulted in release of the loaded HKAIs and subsequent inhibition of bacteria growth. Moreover, cytotoxic assays showed no adverse effects of the particles on mammalian cells or on the immune function of macrophages, and showed no signs of toxicity to zebrafish larvae *in vivo*.

Colloidal gold nanoclusters spiked silica fillers in mixed matrix coatings for detection and inhibition of healthcare-associated infections were prepared by Khashab and co-workers.[206] The authors developed an antibacterial polymer coating containing gold nanoclusters-lysozyme (AuNC@Lys) capping kanamycin (Kana)-loaded aminated MS nanoparticles,

applied on a medical device for safer X-ray dental imaging. The electrostatic self-assembly of negatively charged and fluorescent AuNCs onto positively charged aminated MS provided a bacteria responsive system. Upon encountering bacteria, AuNC@Lys detached from the MS NPs surface due to the interaction of lysozyme with the bacterial cell wall, and the release of the entrapped Kana antibacterial occurred. This mixed-matrix coating was able to detect bacteria growth on a common radiographic dental imaging device (photostimulable phosphor plate) by evaluating the variation and eventually disappearance of the red fluorescence surface of AuNC@Lys under UV light. Besides, the controlled release of Kana from the coating by *E. coli* was studied over 3 h. Decreased of the viability of E. coli by 50% in only 50 min, and by about 80% in 170 min was observed. The system was also very effective toward the Gram+ *Bacillus safensis* (*B. safensis).*

Other stimulus used to uncap antibacterial nanodevices is pH changes. For instance, Qu and co-workers prepared a "sense-and-treat" hydrogel, which contained MS NPs, for detection and elimination of bacteria.[207] For this purpose, MS NPs were loaded with vancomycin and the external surface functionalized with fluorescein isothiocyanate (FITC). Afterwards, the pH-sensitive polymer poly(*N*-isopropyl acrylamide-*co*-acrylic acid) was copolymerized with a rhodamine B derivative functionalized with an acrylamide moiety (RhBAM). The obtained copolymer was then grafted onto the MS scaffold as a "gatekeeper" to control drug release (see **Figure 7**). In this context, FITC and RhBAM made up a ratiometric fluorescence probe. The nanoparticles had a strong emission at 518 nm in basic or neutral pH, whereas the emission was reduced at acidic pH, because of the pH-sensitive properties of FITC. Moreover, the RhBAM moiety existed in the spirolactam form at basic pH and exhibited no fluorescence, whereas at acidic pH it was transformed into the "open" form and emitted a strong fluorescence at 575 nm. According to the aforementioned principles, the protons produced by bacteria caused a fluorescence change of the pH sensitive hydrogel and also triggered vancomycin release to simultaneously inhibit bacterial growth. Furthermore, vancomycin

release studies from the MS NPs without RhBAM were compared with vancomycin release studies from the MS NPs with RhBAM at different pH over 12 h. Release studies showed higher vancomycin release at acidic pH from the MS NPs with RhBAM. In contrast, for the MS NPs without RhBAM, drug release showed similar profiles at different pHs. Furthermore, the presence of *E. coli* was evaluated using MS-hydrogel (280 μg mL^{-1}), showing high antimicrobial activity over 36 h.

Li and co-workers used Fe(III)-carbenicillin (a β-lactam antibiotic) metal organic framework (carMOF) as capping unit for the development of a nanodevice with enhanced penetration and highly efficient inhibition of methicillin-resistant *S. aureus* (MRSA).[208] MS NPs were loaded with sulbactam (sul-MS), a β-lactamase inhibitor, and then the external surface coated with carMOF (carMOF-sul-MS, **Figure 8**). Drug release (carbenicillin and sulbactam) from carMOF-sul-MS was carried out at pH 7.4 and pH 5.0 over 96 h. A higher cargo release was observed at pH 5.0, which was consistent with the dissolution of the carMOF in an acidic environment. The carMOF-sul-MS nanodevice was able to inhibit MRSA growth at acidic pH due to the delivery of carbecillin (from the degraded carMOF) and sulbactam (loaded in the pores of sul-MS). Moreover, the final material showed non-toxicity against RAW 264.7 cells over 48 h. Besides, *in vivo* studies showed decreased MRSA infection in the skin of mice treated with carMOF-sul-MS.

Physical stimuli (such as temperature) have also been used as external triggers to induce antimicrobial release. Using this approach, nanoparticles containing a Fe_3O_4 core and a MS layer, capped with the thermoresponsive poly(*N*-isopropylacrylamide) (PNIPAM) and loaded with a dye or the antibacterial enzyme lysozyme were prepared by Martínez-Máñez and co-workers (see **Figure 9**).[209] Both capped-core-shell nanoparticles showed no cargo release at 25 ºC, whereas abrupt payload delivery was observed at 37 ºC, due to pore opening as the PNIPAM polymer was in the collapsed form at this temperature. Moreover, antibacterial test

were carried out at different temperatures against *Bacillus cereus* and *Micrococcus luteus*. The results demonstrated that the nanoparticles were not toxic for bacteria at a concentration of 0.50 mg mL^{-1} at 25 ºC, whereas delivery of lysozyme at 37 ºC resulted in a remarkable reduction of bacteria growth after 24 h, demonstrating that the PNIPAM gates played an important role in modulating the release of the lysozyme.

Capped MS able to release an entrapped cargo in the presence of certain (bio)molecules, excreted by bacteria or externally added, have also been described. At this respect, Gao and co-workers developed layer-by-layer (LBL) self-assembled bio-hybrid nanomaterials for efficient antibacterial applications.[210] For this purpose, MS NPs were loaded with the antibiotic amoxicillin and then functionalized with carboxylates onto the external surface of the support. Then, positively charged lysozyme was adsorbed onto the external surface of the loaded support (through electrostatic interactions) and these nanoparticles were consecutively coated with hyaluronic acid (HA) and 1,2-ethanediamine-modified polyglycerol methacrylate (PGMA) (see **Figure 10**). The final systems was designed to release the encapsulated antibiotic in the presence of hyaluronidase, an enzyme produced by *S. aureus*. The authors found that the release of loaded amoxicilin was accelerated with the addition of hyaluronidase, compared with the control without the enzyme. The antibacterial effect was measured with amoxiclin-resistant *E. coli* and *S. aureus* with varied concentrations of the NPs. The final nanodevice showed better antibacterial effect than that of lysozyme or amoxiciline after 16 h. MIC values toward amoxicilin-resistant *E. coli* and *S. aureus* were, respectively, 62 μg mL^{-1} and 47 μg mL^{-1}, which was much lower than that of free lysozyme (500 μg mL^{-1}). The authors suggested that the presence of cationic polymers in the NPs provided multivalent interactions between the NPs and the bacterial membrane. The antibacterial activity of the NPs was also evaluated *in vivo*, using a mouse wound model infected with *S. aureus*. Epidermal drug delivery with a single dose of lysozyme and amoxiciline significantly reduced the number of

bacteria to a bacteriostatic rate of 67.4%, compared to the negative controls, while the application of the NPs inhibited completely the bacteria, with a bacteriostatic rate of 99.9%. The same authors also prepared a multifunctional material, using the layer-by-layer self-assembly method, for bacterial detection and inhibition.[211] For the preparation of the material, MS were loaded with amoxicillin. Then, the external surface of the nanoparticles was coated with 1,2-ethanediamine-modified polyglycerol methacrylate and cucurbit[7]uril (CB7) was attached onto the polymeric layer by forming inclusion complexes with the 1,2-ethanediamine moieties. Finally, tetraphenylethylene tetracarboxylate was adsorbed, through electrostatic interactions, onto the polymeric layer. The prepared nanoparticles were unable to release the entrapped amoxicillin when suspended in water at neutral pH. However, in the presence of adamantaneamine a marked delivery of the drug was observed. This release was a consequence of the formation of a supramolecular inclusion complex between adamantaneamine and CB7, which disrupted the assembly, releasing the polymer and tetraphenylethylene tetracarboxylate. PBS suspensions of the multifunctional nanoparticles were emissive due to the aggregation of tetraphenylethylene tetracarboxylate onto the polymeric layer. This emissive feature of the nanoparticles was used to detect *E. coli* and *S. aureus* because adsorption of both bacteria onto the positively charged polymeric layer induced the displacement of tetraphenylethylene tetracarboxylate, which was reflected in a marked emission decrease. The prepared nanoparticles presented moderate bacterial killing ability with minimum inhibitory concentrations of > 1000 μg mL^{-1} for both *E. coli* and *S. aureus*, whereas in the presence of adamantaneamine the values were lower (125 and 250 μg mL^{-1} for *S. aureus* and *E. coli* respectively). SEM measurements indicated that treatment of *E. coli* and *S. aureus* with the nanoparticles and adamantaneamine induced marked changes in the bacteria membrane morphology.

Zink and co-workers prepared MS NPs loaded with moxifloxacin and capped with a redox-sensitive disulfide snap-tops.[212] MS were functionalized with (3-mercaptopropyl)

trimethoxysilane and with adamantanethiol forming a disulfide bond. Then, the solid was loaded with moxifloxacin and capped by adding β-CD that formed inclusion complex with the grafted adamantanethiol. In reducing environments (e.g., after addition of glutathione or after uptake by macrophages), the disulfide bond is cleaved and cargo delivery was observed. Furthermore, similar nanoparticles were also loaded with Hoechst fluorescent dye. The authors found that the cargo was released intracellularly, staining the nuclei of macrophages due to the presence of glutathione in cells. The nanoparticles were able to eliminate *Francisella tularensis* in macrophages. In particular, treatment with the moxifloxacin-loaded MS (6.25–400 ng mL^{-1}) or moxifloxacin (1–64 ng mL^{-1}) reduced bacterial CFU in macrophages in a dose dependent manner. In a mouse model of lethal pneumonic tularemia, moxifloxacin-loaded MS prevented weight loss, illness and death, markedly reduced the burden of *F. tularensis* in the lung, liver, and spleen, and were significantly more efficacious than an equivalent amount of the free drug.

Vallet-Regí and co-workers prepared "nanoantibiotics" using MS nanoparticles loaded with levofloxacin and with their external surface decorated with polycationic dendrimers.[213] Poly(propylene imine) G3 dendrimer was reacted with (3-isocyanatopropyl) triethoxysilane and the external surface of levofloxacin-loaded MS nanoparticles was decorated with the trialkoxysilane derivatized dendrimer. PBS suspensions of the prepared nanoparticles at pH 7.4 showed a marked and sustainable levofloxacin release which follows a first order kinetics (100% drug release after 72 h). Confocal microscopy studies, carried out with *E.coli*, showed a complete internalization of the nanodevice and its localization in the cytosol of the bacteria. This internalization is a consequence of the positive charge of the external surface of the nanodevice that was attracted by the negatively charged bacteria membrane. This binding induced slightly changes in membrane permeability allowing nanodevice internalization. After 48 h of incubation, the prepared nanodevices were able to reduce ca. 99% the number of

CFUs for *E. coli*. Besides, dendrimer-functionalised nanoparticles, at 5 μg mL^{-1} concentration, induced a marked disruption of *E. coli* biofilms.

3.4. MS with metal-based NPs

At present, silver nanoparticles (AgNPs) are considered the best alternative to antibiotics, as these nanomaterials exert great toxic effects against a wide range of AMR pathogenic organisms without the addition of other compounds.[214–217] AgNPs are already used as biomedical additives in bandages, catheters, and in medical garrisons for treating wounds and burns.[29] Similarly, metal oxide NPs showed to be effective in killing a variety of bacterial pathogens responsible for hospital-acquired infections, even if a higher concentration of this formulation was required as compared to AgNPs to obtain the desired antimicrobial activity.[218,219]

The mechanisms by which metal-based NPs exert their toxic effects upon pathogenic cells constitute still a black hole of this research field, as several structural parameters of NPs (e.g., composition, surface modification, intrinsic physical properties) can influence their antimicrobial activity.[1] Moreover, the intrinsic biodiversity of the existing pathogenic microorganisms in their genetic arrangement, cell wall structure, and metabolic pathways strongly contributes to increase the complexity in determining the mechanisms of action of metal-based NPs.[4] Nevertheless, since NPs can directly act against pathogenic cells by contact with the target cell membrane, most of the AMR mechanisms already established for antibiotics are inefficient,[1],[4] suggesting that NPs should lead to a low level of resistance arising within pathogens.

One of the antimicrobial effect of metal-based NPs towards pathogens is triggered by the electrostatic binding of these nanomaterials to the cellular membranes, causing their modification and/or disruption through metal ion release or the physical structure of the NPs themselves.[4] Indeed, the NP-cell membrane interaction can substantially alter the membrane

integrity by changing its potential and depolarization, therefore causing a transport imbalance and an impairment of the respiratory chain, which can in turn lead to cell lysis or cell death.[220] In this regard, the antimicrobial efficacy of AgNPs seems to rely on the strong affinity between Ag and sulfur (S), nitrogen (N) and even phosphorous (P), which are key biochemical elements of the cell.[29] Thus, AgNPs directly interact with S-containing proteins of the cellular membrane, affecting the functionality of these macromolecules and, therefore, the permeability of the membrane, causing a loss of cell viability.[221] Moreover, it has been shown that Ag(I) ions released by a high amount of administered AgNPs can interact with P present in DNA molecules, leading to an inactivation of the DNA replication and /or repair machinery.[222]

Further, AgNPs,[223–226] which is caused by respiratory chain disruption or by the physical-chemical properties of the NPs themselves.[227] As a consequence of the oxidative stress response, Reactive Oxygen Species (ROS) are produced within pathogenic cells,[228] leading to severe macromolecular damages (e.g., lipid peroxidation, alteration and inhibitions of proteins or enzymes, DNA mutations or RNA damage)[4] or, at high ROS concentration, cellular death.[225],[229]

Although metal-based NPs have shown promising efficacy in inhibiting the growth of AMR pathogenic microorganisms, several bacterial strains result to be naturally adapted to specific toxins or ions contained in NPs.[1] Indeed, one of the resistance mechanism mostly diffuse in AMR bacterial cells is their ability to change the structure and the composition of their cell walls in order to become resistant towards antibiotics.[230] Similarly, an increase in the amount of saturated fatty acids present in bacterial cell membranes can lead to an increased membrane fluidity, conferring to these bacterial cells a high degree of protection from oxidative stress caused by metal-based NPs,[231] while the peculiar physical properties of the peptidoglycan layer of some Gram-negative bacteria can mediate an efflux mechanism of metal-based NPs.[232,233] Another factor influencing the resistance of bacterial cells towards metal-based

NPs is the rate of cell growth. Indeed, slow-growing bacterial strains are more resistant towards these nanocompounds, as one of their features is the greater expression of stress-response genes compared to fast-growing species.[1] Finally, metal oxide NPs (e.g., CuO or ZnO NPs) can be very inefficient as an antimicrobial when administered to bacterial strains that are able to produce EPS under stress conditions, as these NPs if adsorbed on the bacterial cell surface, can be degraded by specific enzymes.[1]

Most of the examples described in this section contain AgNPs although some examples containing Au, ZnO, TiO_2, CuO and CdS NPs in MS have also been reported. We will first summarize examples containing Ag NPs, whereas at the end of the section examples using MS with other metal-based NPs are described. In the synthesis of MS containing AgNPs, in most cases Ag(I) ions are added to the MS and then reduced to AgNPs using different reducing agents. At this respect, Jiang and co-workers prepared MCM-41 MS NPs functionalized with AgNPs and tested their antibacterial activity against *E. coli* and *S. Aureus.*[234] The authors prepared the silica nanoparticles by the co-condensation method using *N*-(aminoethyl)-amino-propyl trimethoxysilane and tetraethylorthosilicate. Then, silver nitrate was added and the Ag(I) ions coordinated with the nitrogen atoms of the grafted amino-propyl moieties. Finally, Ag(I) ions were reduced to AgNPs using formalin. The AgNPs obtained were well dispersed around the MCM-41 framework and the prepared nanocomposite had good biocompatibility. The growth of bacteria was completely inhibited using concentrations of nanoparticles of 80 and 320 μg mL^{-1} *E. coli* and *S. aureus* respectively. Besides, the antibacterial activity of the prepared nanoparticles was preserved for 30 days. Scanning laser confocal microscopy measurements showed the adsorption of the prepared nanoparticles onto the bacterial wall. The authors suggested that sustainable release of Ag(I) ion from the adhered nanocoposites was most likely the responsible of bacterial death.

Fu and co-workers prepared MS NPs functionalized with AgNPs and tested their antibacterial behavior against *E. coli* and *S. Aureus.*[235] The final material was prepared from MS particles of ca. 130 nm that were coated with a mesoporous shell containing aminopropyl moieties. Silver nitrate was added to a MS suspension and the mixture was treated with ultrasounds for 2 h. This ultrasonic treatment reduced Ag(I) to AgNPs. The prepared AgNPs-containing MS support presented a marked bacterial growth inhibition with MIC of 0.156 and 0.313 mg mL^{-1} for *S. aureus* and *E. coli* respectively.

Long and co-workers prepared MS nanoparticles decorated with well dispersed AgNPs using a co-condensation procedure and *N*-(aminoethyl)-amino-propyl trimethoxysilane (as coupling agent) and silver nitrate (as Ag source). Once prepared, the nanoparticles were deposited onto nanofibrous membranes prepared from poly-ε-caprolactone by using a electrospinning device.[236] The authors found that nanofibrous membranes were able to inhibit the growth of *E. coli* and *S. aureus* after 12 h of contact. Besides, these antibacterial membranes were able to reduce inflammatory response and accelerate wound healing in Wistar rats.

Hollow MS NPs have also been used as reservoir for depositing AgNPs.[237] For the preparation of the mesoporous scaffold the authors used poly(styrene-*co*-methyl methacrylate-*co*-methacrylic acid) as hollow-structure template and CTAB as mesostructured directing agent. The AgNPs were deposited onto the surface of the hollow MS nanoparticles by the *n*-butylamine-induced reduction of silver nitrate. Inhibition zone tests indicated that the prepared hollow nanoparticles were able to inhibit the growth of *S. aureus* and *E. coli* strains.

Hollow MS microspheres loaded with AgNPs were also prepared by Yang, Shen and co-workers.[238] The dosage of $AgNO_3$, polyvinylpyrrolidone, tetraethoxysilane and ammonia was investigated to explore the variation in the morphology of the prepared materials. Results showed that high AgNPs loading and large pore size increased the Ag(I) ion release rate.

Tang and co-workers prepared hierarchically wrinkled MS NPs loaded with AgNPs and tested their antibacterial behavior against *E. coli* and *S. Aureus.*[239] In a first step, the mesoporous

scaffold was functionalized with mercaptopropyl moieties. Then, the thiol groups were oxidized to sulfonic acid using hydrogen peroxide. Afterward, Ag(I) ions are loaded, through electrostatic interactions with the sulfonate moieties, and finally AgNPs were obtained upon addition of sodium borohydride. The prepared material presented remarkable antibacterial effects. At this respect, MIC of 73.10 and 36.55 μg mL^{-1} for *S. aureus* and *E. coli* were determined. On the other hand, minimal bactericidal concentrations were set at 97.10 and 48.55 μg mL^{-1} for *S. aureus* and *E. coli* respectively.

Chen and co-workers prepared SBA-15 MS microparticles decorated with AgNPs.[240] The authors adsorbed dopamine onto the surface of the mesoporous scaffold by electrostatic interactions and then silver nitrate was added to coordinate Ag(I) ions with de catechol subunit of the dopamine. The suspension at pH 8.5 was heated at 80ºC for 12 h in order to reduce Ag(I) ions forming AgNPs. The prepared nanocomposite was able to completely inhibit bacterial growth after 12 h for *E. coli* and after 36 h for *S. aureus*.

Zink and co-workers prepared AgNPs (less than 20 nm in diameter) coated with a MS shell and studied its antimicrobial behavior against *E. coli* and *B. Anthracis.*[241] The authors observed that nanoparticles at concentration of 100 μg mL^{-1} inhibited completely the formation of colonies for *B. anthracis*. However, the NPs had no effect on *E. coli* growth. The authors prepared another set of nanoparticles by coating the external MS shell with PEI polymer (through electrostatic interactions). These PEI-coated nanoparticles, at 100 μg mL^{-1}, were able to induce growth inhibition of both strains due to the fact that positively charged NPs surface interacted more efficiently with the negatively charged bacteria.

Liu and co-workers prepared AgNPs (10 nm of diameter) also coated with a MS shell (50 nm of diameter after the coating process) and tested its antimicrobial behavior against *V. Natriegens.*[242] The prepared nanoparticles were able to inhibit *V. natriegens* growth at 10 μg mL^{-1} concentration. Besides, the same authors embedded these nanoparticles in an

organosiloxane polymer that was then deposited in aluminum films.[243,244] The prepared films successfully inhibited the formation of bacterial films of *V. natriegens*.

Yang, Shen and co-workers proposed a method to fabricate mesoporous silica microcapsules with AgNPs loaded onto the interior walls of the MS shell, which gave a sustained-release of Ag(I) ions, and displayed high antibacterial durability.[245] AgNPs-MS microcapsules was fabricated via a two-step process: (i) Ag(I) ions were adsorbed on the surface of monodisperse sulfonated polystyrene beads via electrostatic interaction, and then reduced and protected by polyvinylpyrrolidone to obtain sulfonated polystyrene-Ag composite spheres; (ii) then silica precursor colloids were assembled on the sulfonated polystyrene-Ag composite spheres via hydrogen bond forces to form a silica shell. The prepared composite slowly release Ag(I) ions from 6 h to 10 days. The antibacterial activity against *E. coli* reached up to 99.8% and maintained a high level over two months.

The same authors also prepared an antibacterial film fabricated by loading MS microcapsules containing AgNPs on a fluoro-silicone resin film (**Figure 11**). Moreover, the surface of the prepared material was hydrophobically modified by a controlled dosage of fluoro-silicone resin solution, to obtain a completely hydrophobic surface and to increase film thickness.[246] A prolonged release of Ag(I) from the prepared composite was achieved over 10 days. The films exhibited an excellent antibacterial activity due to (i) the formation of a lotus-leaf-like hierarchical micro-nanoscale structured surface, resulting in enhanced hydrophobicity and (ii) release of Ag^+ ions from the mesopore channels.

Pandey and Ramontja prepared MS microparticles with embedded alginate-coated AgNPs and studied its effect in gram positive and gram negative bacteria.[247] In a first step, the authors prepared the alginate-coated AgNPs and used this solution to prepare the MS. Using this procedure AgNPs were well dispersed onto the MS matrix. Values of MIC for gram positive bacteria (*S. aureus, S. epidermis, B. cereus, B. subtilis, E. faecalis*) ranged from 80 to 250 μg mL^{-1} whereas for gram negative (*E. coacae, E. coli, K. oxytoca, K. pneumonia, P. mirabilis, P.*

vulgaris, *P. aeruginosa*, *E. aerogenes*) ranged from 55 to 125 μg mL^{-1}. The authors suggested that the microparticles adhered to the bacterial membrane and altered its integrity, thus facilitating the bactericidal effect of the AgNPs.

Yusufu, Cao and co-workers developed a multifunctional bioactive material that stimulated osteogenesis and promoted the vascularization of bone marrow stem cells (BMSC) and their resistance to bacterial infection.[248] The material consisted of silver nanocrystals coated with a MS shell and loaded with the peptide platelet-derived growth factor BB (PDGF-BB) - a growth factor that regulates cell growth and division. The aims of the study were to evaluate (i) the released of silicon to stimulate osteogenic differentiation of BMSC, (ii) to evaluate the BMSC angiostimulation capacity of PDGF-BB, and (iii) the silver ion bactericidal effect of the AgNPs on bone modeling and remodeling. After biodegration of the material inside the BMSC, Si ions stimulated osteogenic differentiation of BMSC by activating the alkaline phosphatase (ALP) activity of bone-related genes and increasing protein (OCN, RUNX2 and OPN) expression. Furthermore, the 70±80 % of the loaded PDGF-BB was released during the first 10 days and stimulated the angiogenic differentiation of BMSC. Besides, Ag(I) ions were released from the interior of the shell, showing suitable release over 14 days. The antibacterial activity of Ag(I) from the MS support was evaluated by the OD600 bacterial growth curve against *E. coli*, *S. aureus*, *P. aeruginosa*, *Bacteroides fragilis*, *Candida sporogenes* over 24 h. The results showed high antibacterial activity on *E. coli*, *P. aeruginosa*, *Bacteroides fragilis* and *Candida sporogenes*, however, the prepared material exhibited poor bactericidal effects against *S. aureus*.

Qiu, Zhang and co-workers proposed a strategy for the preparation of flexible MS fibres containing AgNPs as effective wound dressing.[249] Additionally, the mesopores served as hosts for the accommodation of ibuprofen (IBU). The loading capacity of IBU reached up to 18 wt%, and its release was relatively fast; more than 85% of the drug was released within 12 h. The condensed core of the SiO_2 nanofiber not only endowed the sample with a high

flexibility, but also allowed slow release of silver overall having a sustained antibiotic effect. Besides, antibiotic ability of the fibers with different doping concentrations of AgNPs was tested against *E. coli*. The results showed a sustained antibiotic effect over 48 h.

Ghosh and co-workers prepared Ag/AgCl-MS NPs against *E. Coli*.[250] The materials were based on SBA-15 containing Ag or AgCl nanoparticles by using two methods: (i) the impregnation method (for Ag nanoparticles) and (ii) the 'one pot' method (in which SBA-15 and AgCl nanoparticles were formed at the same time). Antibacterial activity of Ag/AgCl-MSNs was investigated against *E. coli* using a conventional plate-count methodology at 24 h. All materials showed high antibacterial activity even when the percentage of loaded Ag in the nanocomposites was as low as 10 wt%.

MS NPs loaded with CdTe quantum dots and coated with AgNPs were also used as antibacterial materials.[251] The pores of the mesoporous nanoparticles were loaded with mercaptopropionic acid-coated CdTe QDs and the external surface functionalized with *N*-(aminoethyl)-aminopropyl trimethoxysilane. Finally, Ag(I) ions were coordinated with the *N*-(aminoethyl)-aminopropyl moieties and then transformed onto AgNPs using the silver-mirror reaction. The prepared nanoparticles were able to kill colonies of *E. coli* and *S. aureus*.

The examples shown above have in common the use of MS containing AgNPs. Moreover, there are additional examples in which MS-AgNPs support are additionally loaded with other antimicrobials to prepare dual-effect highly efficient bactericidal agents. For instance, Santamaría and co-workers developed SBA-15 loaded with peracetic acid and AgNPs.[252] The system showed a strong bactericidal effect on antibiotic-resistant biofilms of *S. aureus*, considerably larger than that expected from the summation of the independent effects of both antimicrobials. Peracetic acid enhanced the bactericidal effect of Ag(I) by hindering biofilm formation and by promoting Ag(I) production by oxidation/dissolution of the AgNPs. The protective environment of the mesopores together with a strong peracetic acid adsorption allowed maintaining the biocidal activity for a prolonged period of time.

Janus silver MS NPs were used by Dong and co-workers to kill *E. coli* and *S. Aureus*.[253] The Janus nanoparticles consisted of AgNPs linked to a mesoporous phase that contained cetyltrimethylammonium bromide (CTAB) inside the pores and aminopropyl moieties grafted in the outer surface. PBS suspensions of the prepared Janus nanoparticles were able to release CTAB and Ag(I) ions in a sustainable fashion and, as a consequence, killing *E. coli* (IC_{50} = 10 μg mL^{-1}) and *S. Aureus* (IC_{50} = 20 μg mL^{-1}). The low IC_{50} obtained was ascribed to a synergic effect between the CTAB (which induced a marked loss of bacterial membrane integrity) and Ag(I) ions (which are more efficiently internalized).

Zhou and co-workers prepared MS NPs decorated with AgNPs and loaded with chlorhexidine.[254] In a first step the authors prepared, following a co-condensation method, MS NPs functionalized with aminopropyl moieties. Then, AgNPs were formed onto the mesoporous scaffold by ultrasonication-assisted method using the $[Ag(NH_3)_2]^+$ complex. Moreover, the amino groups of the mesoporous scaffold were reacted with succinic anhydride and, finally, the pores were loaded with chlorhexidine. The prepared nanoparticles were able to release chlorhexidine and Ag(I) ions at acidic pH (5.0) whereas less pronounced delivery was observed at neutral pH. Besides, *E.coli* and *S. aureus* growth was markedly inhibited in the presence of the prepared NPs. MIC of 12.5 and 25 μg mL^{-1} for *E. coli* and *S. aureus* were found. The obtained bactericidal outcome was ascribed to a synergic effect due to the simultaneous release of chlorhexidine and Ag(I) ion.

Chehimi and co-workers functionalized SBA-15 with APTES and polypyrrole was adsorbed under ultrasonication. Afterwards AgNPs were prepared inside the pores and the antibacterial activity of the systems against *E. coli* was studied.[255] The material showed a strong bacteriostatic effect for concentrations in the 200-300 μg mL^{-1} range. The antibacterial performances of the hybrid particles are ascribed to the efficient functionalization of SBA-15,

which ensures the robustness of the nanocomposites, and the antibacterial effect of the polypyrrole and AgNPs.

Guo, Gu and co-workers developed silver core-shell MS NPs loaded with levofloxacin (Ag-MSNs-Lev) as a synergistic antibacterial agent for the treatment of drug-resistant infections.[256] Drug release profile of levofloxacin from Ag-MSNs-Lev or from MSNs-Lev was measured at pH 7.4 and a marked and sustainable release of the entrapped drug was observed (reaching 95.9 and 83.8% of the loaded levofloxacin for MSNs-Lev and Ag-MSNs-Lev respectively and after 96 h). Antimicrobial assays were developed by counting the number of CFU after cultured the bacteria *E. coli* and *K. pneumoniae* 39 in the presence of the nanoplatform for 24 h at 37 ºC. Ag-MSNs-Lev exhibited superior antibacterial activity when compared to Lev-loaded MSNs and silver embedded MSNs. Ag-MSNs-Lev was evaluated also in *in vivo* acute peritonitis mouse model. Peritoneal cavity of the mice was infected with *E. coli* GN102 and treated with Ag-MSNs-Lev. The results showed a reduction of the infection by nearly three orders of magnitude. Moreover, the aberrant pathological of spleen and peritoneum disappeared after treatment with Ag-MSNs-Lev. The NPs rendered no obvious toxic side effects to mice during the tested time.

Levofloxacin/silver co-loaded electrospun fibrous membranes were prepared by Cui, Huang and co-workers and their *in vivo* and *in vitro* antibacterial effect tested.[257] In a first step, the authors prepared AgNPs coated with a MS layer and loaded the pores with levofloxacin. Then, in a second step, the nanoparticles were incorporated onto electrospun nanofibers of poly-L-lactide yielding the final nanocoposite (**Figure 12**). The composite showed an antibacterial effect against methicillin-resistant *S. aureus* (MRSA) at low doses of levofloxacin and Ag over 8 weeks (28 mg mL^{-1} levofloxacin and 12 mg mL^{-1} Ag). Besides, *in vivo* studies in rats infected with MRSA were carried out. Treatment with the fibers significantly inhibited *S. aureus* growth and infection over 8 weeks through the combined effect of low dosage of the antibacterials.

Some examples combine MS with AgNPs and copper derivatives. Lee and co-workers prepared Cu(II) impregnated MS nanoparticles loaded with curcumin and containing immobilized AgNPs), which showed excellent photodynamic inactivation against *E. coli* due to the synergistic effects of silver, Cu(II) and curcumin.[258] The bactericidal effect of the nanoparticles against *E. coli* in the presence of light (to activate curcumin photosensitizer and produce ROS) was higher when compared with the use of curcumin or AgNPs alone. In particular, the system resulted in ~90% eradication of the bacterial cells, which accounts to an enhancement in bacterial destruction around 5 log and 4 log in comparison to free curcumin and Cu-AgNPs, respectively. This observed enhancement is ascribed to the overproduction of ROS from AgNPs and curcumin.

Beyond AgNPs, AuNPs, ZnO, TiO_2 and CuO NPs have also been recently used as antimicrobial agents. ZnO NPs have been employed in creams, lotions and skin coatings for dermatological applications,[219] while TiO_2 NPs are currently present in cosmetic products, sterile filter, food industries, and for waste water treatment.[29],[259] Particularly, TiO_2 nanoformulation have shown bactericidal activity also towards pathogenic biofilms, suggesting their possible use as alternative to antibiotics in the treatment of severe infections caused by the generation of mature pathogenic biofilms.[260–262] CuO NPs and AuNPs can exert their toxic effect upon pathogenic cells by (i) binding to DNA molecules and, therefore, inhibiting their uncoiling and their transcription,[223] or (ii) interacting with amine and carboxylic groups (Cu), or S (Au) present in the cellular membranes, which causes the release of cell components in the extracellular environment.[1] AuNPs are less efficient than the other metal-based NPs.[263] Indeed, these Au-based nanomaterials have enhanced antimicrobial properties when photothermally functionalized,[264] when they are bound to antibiotics (e.g., ampicillin or vancomycin),[265,266] or when they are added to amino-substituted pyrimidines or citrate.[267] Ion release has been indicated as one of the main mechanism of toxicity exerted by ZnO NPs, whose Zn^{2+} ions can interact and damage the cellular membrane, leading to cell

lysis.[268] The toxicity of metal oxide NPs, such as CuO or ZnO NPs is also mediated by their ability to activate variations in the extracellular environments nearby pathogenic microorganisms, therefore leading to the production of ROS along with an increase solubility of the NPs themselves.[269] The generation of ROS can also be caused by TiO_2 NPs irradiated with UV light (usually at $\lambda < 385$ nm), causing the photocatalytic production of a strong oxidizing power, which in turn results in a cascade of cellular processes,[270] such as lipid peroxidation, inhibition of essential enzymes and induction of Nitrogen Reactive Species (NRS), and, finally, cell death.[1],[4],[271,272]

Despite these interesting features of AuNPs and nanoparticles of ZnO, TiO_2 and CuO, there are very few examples of MS incorporating these metal-based antimicrobials. For instance, Rosal and co-workers prepared SBA-15 mesoporous particles functionalized by aminopropyl moieties and decorated with CuO or with AgNPs. The prepared particles were incorporated onto polyethersulfone ultrafiltration membranes.[273] Both types of membranes were able to inhibit the growth of *E. coli* and *S. aureus* being most effective that containing AgNPs. Besides, bacterial adhesion on the prepared membranes was very low. The observed antibacterial effect was related with the release of Ag(I) and Cu(II) from the membranes. Mosquera and co-workers prepared MS-based nanocomposites, containing CuO as bioactive component for application on building stone.[274] The synthetized CuO/SiO_2 nanocomposite acted as a multifunctional (biocide and consolidant) coating, increased mechanical resistance and decreased microbial growth on a typical building limestone. Antibacterial effect of CuO/SiO_2 nanocomposites on building stone was tested with *E. coli* and the yeast *Saccharomyces cerevisiae*. The coatings inhibited the growth of bacteria and yeast up to an 85% and 77%, respectively. The CuO/SiO_2 support released Cu^{2+} ions, which played an important role in the biocide effect.

Qu and co-workers prepared bi-functionalized MS-supported AuNPs for antibacterial applications.[275] For the preparation of the final material, MS NPs with aminopropyl moieties

in the internal surface of the pores and with carboxyl groups on the outer surface were prepared. Then, reduction of $HAuCl_4$ with $NaBH_4$ in the presence of the bi-functionalized silica nanoparticles yielded AuNPs that were fixed onto the mesoporous scaffold. The prepared nanoparticles efficiently inhibited the growth of *E. coli* and *S. aureus* as a consequence of ROS generation induced by AuNPs. Scanning electron microscopy studies showed that bacterial surface became rough and wrinkled after the treatment with the NPs. The authors ascribed these changes to oxidation of the membrane by the ROS generated by the nanoparticles. Besides, the prepared material was also able to destroy *B. subtilis* biofilms. Mijowska and co-workers prepared MS NPs functionalized by TiO_2 using the titania precursor titanium(IV) butoxide as a photoactive antibacterial agent.[276] The antibacterial effects of the TiO_2-containing MS on *E. coli* after 24 h was evaluated by CFU. The assay showed strong enhancement upon visible and ultraviolet light irradiation compared with commercial TiO_2. In darkness, the nanostructure revealed low antibacterial activity. Furthermore, the non-cytotoxicity of the TiO_2-containing MS was confirmed with WST1 assay and LDH assay over 24 h on fibroblast cells L929. Mijowska and co-workers also prepared MS nanotubes modified with TiO_2 as antibacterial agent.[277] The material showed a strong enhancement of the antibacterial activity under visible and ultraviolet irradiation on *E. coli* at 24 h. Besides, cell viability using LDH assay over 24 h confirmed the non-toxicity of the nanotubes in mouse fibroblast L929 cells.

A carboxymethyl cellulose hydrogel containing MCM-41 MS NPs decorated with ZnO and loaded with tetracycline was prepared by Namazi et al.[278] The MS NPs were introduced into an aqueous solution of zinc nitrate, and after filtration, heated at 400ºC for 3 h to generate ZnO. Then, the mesoporous NPs decorated with ZnO were loaded with tetracycline and incorporated onto a carboxymethyl cellulose hydrogel. Marked inhibition growth of *E. coli* and *S. aureus* was observed when using the prepared hydrogels mainly due to the tetracycline release and to the antibacterial properties of ZnO.

Qian and co-workers developed MS nanospheres functionalized with CdS nanocrystals for enhanced photocatalytic and excellent antibacterial activities.[279] The authors prepared uniform SiO_2/CdS mesoporous nanospheres with an average diameter of 300 nm decorated with ca. 5 nm CdS nanocrystals. The antibacterial activity of the mesoporous SiO_2/CdS nanospheres was evaluated against *E. coli*. The material was able to kill 70% of the *E. coli* in 24 h at concentrations as low as 50 μg L^{-1}. The mechanism was ascribed to the presence of CdS nanoparticles that showed enhanced photon absorption and activated oxygen species generation efficiency under visible light irradiation.

Polarz and co-workers prepared periodic mesoporous silica (PMOs) nanoparticles using 1,5-bistri(isopropoxysilyl)-benzene-3-sulfonyl chloride and 1,5-bistri(isopropoxysilyl)-benzene-3-thiol as sol-gel precursors and studied their biocidal activity.[280] The prepared PMOs contained thiol and sulfonyl moieties (in different amounts) in the walls of the pores for further immobilization of Ag nanoparticles. The prepared PMOs were able to inhibit *P. aeruginosa* growth with MIC in the 0.5-0.25 mg mL^{-1} range due to the sustained release of Ag^+ ions. Besides, confocal laser scanning microscopy studies showed that glass slides coated with the prepared PMOs inhibited the growth of *P. aeruginosa* bacterial films and negligible number of alive bacterial were found onto the surface of the films.

3.5. MS loaded with metal ions

This section highlights examples in which MS are loaded with bactericidal metal cations (MS with metal-based NPs are described in the section above). Most of the reported examples are loaded with Ag(I), although there are also some examples of MS loaded with copper derivatives, Ni(II), Ga(III) and Bi(III). In most cases the metals form complexes with different appended ligands and are used as low soluble salts or are adsorbed on MS surfaces. In all cases bactericidal activity is a consequence of the delivery of the corresponding metal cation to the medium from the MS support. This section was splitted into two subsections taking into

account if the antibacterial activity arises simple adsorbed ions or from supported or adsorbed metal complexes.

3.5.1. Containing adsorbed ions

Calcium-doped MS spheres loaded with Ag(I) ions were prepared ant its antibacterial activity tested.[281] The prepared spheres were able to efficiently reduce *E. coli* (5.5$\log_{10}$ after 2 h) and *S. aureus* (4$\log_{10}$ after 4 h) bacterial population. The antibacterial activity of the spheres was ascribed to the sustainable release of Ag(I) ions. Besides, the authors demonstrated that the prepared spheres promoted blood clotting, activated the intrinsic pathway of coagulation cascade and induced platelet adherence achieving an effective homeostasis in animal models. Hong, Yuan, Liu and co-workers also developed amino-functionalized calcium-doped MS containing silver ions.[282] A material without amino moieties in which Ag(I) ions were simply adsorbed on the MS was also prepared. Antimicrobial tests against *E. coli* showed that, at the same silver ion loading, the Ag(I)-containing amino-functionalized MS displayed longer and more efficient (2.5 times lower MIC) antibacterial activity for 24 h compared to the non-amino-functionalized MS. Further studies demonstrated that the excellent and sustained antibacterial efficiency of Ag(I)-containing amino-functionalized MS is attributed to complexation of Ag(I) with the amino groups, the strong interaction of the positively-charged nanoparticle's surface with the negatively charged bacteria and the strong inhibition effect of Ag(I).

MS NPs with different aspect ratios (1 (spherical), 2 (small rods) and 4 (larger rods)) were prepared using well known procedures by Rosenholm and co-workers.[283] Once the inorganic scaffold was prepared the authors adsorbed, through simple electrostatic interactions, Ag(I) ions onto the external surface. Finally, the nanoparticles were coated with chitosan biopolymer. The antibacterial activity of the prepared nanoparticles was tested against *E. coli*, *V. cholerae* and *S. aureus*. The three prepared nanoparticles showed good antibacterial activity against the three tested strains. The highest antimicrobial behavior was obtained using

the nanoparticles with aspect ratio of 4 which were able to induce a 100% killing of *E. coli*. The MIC of this material for the three bacterial strains was 200 μg mL^{-1}. SEM images of the bacteria treated with the nanoparticles showed a marked elongation with severe membrane damage resulting in intracellular protein leakage. Besides, the authors developed a more effective treatment against *V. cholerae* by combining the nanoparticles with aspect ratio 4 with kanamycin.

Kwon and co-workers developed an antibacterial material based on silver chloride nanoparticles inside the pores of SBA-15.[284] The resulting support was processed with polypropylene to form a polymer composite. The antibacterial activity of Ag(I)-containing SBA-15 alone and incorporated in the polypropylene polymer was tested against *E. coli* for 24 h. Both materials showed a high antibacterial activity.

In addition to the silver examples, Towler et al reported the use of mesoporous bioactive glasses containing different amounts of Ga(III) ion as antimicrobial materials.[285] The authors prepared the glasses by using P123 as structure directing agent, tetraethyl orthosilicate, triethyl phosphate, calcium nitrate and gallium nitrate (in 1, 2 and 3 mol%). The three Ga(III)-doped bioactive glasses showed marked antibacterial activity against *E. coli* and *S. aureus*. The best antibacterial activity was observed for the mesoporous glass containing the higher amount of Ga(III). The observed antibacterial effect was ascribed to a sustainable Ga(III) release and the efficacy was enhanced with time. Besides, the prepared mesoporous glasses displayed a more significant antibacterial activity against *S. aureus* than against *E. coli*. This different effect was related with the characteristics of the cell walls of the two bacteria. *S. aureus* is surrounded by a peptidoglycan layer with a loosely packed network structure that allowed Ga(III) to pass through the wall and reach the interior. On the other hand, *E. coli* has a thicker peptidoglycan wall which difficult Ga(III) internalization. Ga(III) has a similar size than Fe(III) and could compete with the later in several biochemical processes with subsequent disruption or inhibition of reactions such as DNA and protein synthesis.

Mesoporous silica materials such as KIT-6 (Korea Advanced Institute of Science and Technology-6)-encapsulated bismuth oxychloride (BiOCl) were prepared under hydrothermal conditions by Chen, Wu, Wei and co-workers.[286] The composite materials xBiOCl/KIT-6 (molar ratio Bi−Si x = 6, 8, and 10) were labeled as 6Bi−Si, 8Bi−Si, and 10Bi−Si. The antibacterial activities of BiOCl−KIT-6 composites were explored against *S. aureus* and *E. faecalis*, and *E. coli* and *P. aeruginosa* over 24 h, showing no activity against gran - bacteria. However, the antibacterial effect of BiOCl−KIT-6 composites against *S. aureus* and *E. faecalis* was pronounced. 6Bi−Si composite had the maximized antibacterial activity against *S. aureus*, and the inhibition rate was up to 96.6% much higher than 10Bi−Si (77.7%), 8Bi−Si (91.5%), BiOCl (78.3%), and KIT-6 (52.5%), which is attributed to the mesoporous KIT-6 support the antibiotic effect of BiOCl. The MICs of 6Bi−Si toward *S. aureus* and *E. faecalis* were 32 and 40 μg mL^{-1}, respectively.

3.5.2. Containing supported or adsorbed metal complexes

Ghosh and Vandana prepared MS flakes that where functionalized, using a grafting procedure, with aminopropyl moieties. Then, the primary amines were reacted with formaldehyde in order to decorate the inorganic support with -NH-CH_2-OH groups. Finally, Ag(I) was complexed with the -NH-CH_2-OH moieties yielding the final support.[287] Experiments carried out by the authors showed a complete inhibition growth using 70 and 110 μg mL^{-1} of the particles for *E. coli* and *S. aureus*, respectively.

Other MS NPs which released Ag(I) were also prepared by Lee and co-workers.[288] The nanoparticles were first functionalized with butylaldehyde and then, indole-3-acetic acid hydrazide was grafted through the formation of imine bonds with the previously anchored aldehyde. Finally, Ag(I) was complexed with the indole-3-acetic acid moieties by adding silver nitrate to an aqueous suspension of the NPs. The prepared nanoparticles were able to release marked amounts of Ag(I) at acidic pH as a consequence of the hydrolysis of the imine

bonds, whereas at neutral pH only a moderate delivery was observed (ca. 25% of the ion). The NPs completely inhibited the growth of *E. coli* and *S. aureus* when using at 120 μg mL^{-1} concentration. Besides, NPs were also able to inhibit the formation of biofilms of *E. coli*, *B. subtilis*, *S. aureus* and *S. epidermis* at doses as low as 30 μg mL^{-1}. The observed bacterial death was ascribed to the Ag(I)-induced ROS generation which resulted in bacterial cell membrane damage. Besides, the prepared nanoparticles showed a good antibacterial activity *in vivo* in C57BL/6 mouse with an intraperitoneal *E. coli* infection.

Chen and co-workers prepared SBA-15 microparticles functionalized with ethylenediaminetretraacetic acid (EDTA) which was able to coordinate high valence silver ions.[289] SBA-15 microparticles functionalized with aminopropyl moieties were obtained by the co-condensation method and then, the amino groups were functionalized with EDTA using thionyl chlroride to activate the carboxylate groups. Finally, addition of silver nitrate induced the formation of Ag(II)-EDTA and Ag(III)-EDTA complexes. The prepared microparticles were able to inhibit *E. coli* and *S. aureus* growth with IC_{50} values of 30 μg mL^{-1} for both bacteria. Besides, inhibition zone assays indicated that microparticles could be stored for 210 days without any remarkable loss in its antibacterial properties.

Apart of the examples using Ag complexes some authors have also used AgCl as source of silver. Song and co-workers prepared thiol-functionalized MS particles loaded with silver chloride and dispersed in coatings against *Candida albicans* and *S. mutans* on a denture base.[290] Molar fractions of thiol in the silica precursors were 10% and 20%. The antibacterial activity of the hybrid coatings was evaluated by film contact method measuring the reduction rate of the microorganisms. The materials with a 10% thiol molar fraction and loaded with silver chloride showed higher antibacterial activity than the materials with a 20% thiol molar ratio.

Rostamnia, Karimi and co-workers growth silver chloride nanoparticles within the pore channels of SBA-15 functionalized with SO_3H groups as a system with antibacterial properties against *E. Coli*.[291] The growth of AgCl NPs within the pore channels of the SBA-15 MS was achieved by sequential dipping steps in alternating baths of KCl and $AgNO_3$ under ultrasound irradiation at pH 9. The solid gave a remarkable antibacterial activity against *E. coli* when compared with the same support without Ag(I) ions.

Compared with silver, less examples using the bactericidal effect of copper cations have been reported in MS. Laskowski and co-workers two different SBA-15 materials containing (i) copper ions bonded inside the pores via propylphosphonate units (SBA-prop-POO_2Cu) forming copper-containing groups in concentrations of 10% and 5%, or (ii) free CuO.[292] The materials were used to study the antibacterial effect on *E. coli*. The obtained results showed that the sample with a lower concentration of active copper-containing groups had stronger antimicrobial properties than the one with the higher concentration at 24 h. The MS containing CuO support had no antimicrobial properties.

Páez, Gómez-Ruiz and co-workers prepared MS NPs containing a maleamato ligand (MS NP-maleamic) which was used to coordinate copper(II) ions (MS NP-maleamic-Cu) and explored their potential application as antibacterial agents against *E. coli* and *S. aureus* (see **Figure 13**).[293] The results showed a low activity of MS NP-maleamic and MS NP-maleamic-Cu against *S. aureus*, while a good activity against *E. coli* was found. The material MS NP-maleamic-Cu (MIC of 4.1 μg mL^{-1}) was more active than MS NP-maleamic (MIC of 10.4 μg mL^{-1}) against *E. coli*.

Sedaghat and co-workers prepared MS NPs functionalized with 3-aminopropyltriethoxysilane which was reacted with 2-hydroxy-3-methoxybenzaldehyde to obtain a Schiff base.[294] The latter material was then treated with Cu(II) and Ni(II) separately to obtain copper and nickel complexes anchored on the mesoporous support. The nanocomposites were investigated for antibacterial activity against gram + (*B. subtilis* and *S. aureus*) and gram - (*E. coli* and *P.*

aeruginosa) bacteria. The results of the growth curve of treated bacteria showed that MS nanoparticles having the Ni(II) complex had bactericidal effect against *S. aureus* while the MS NP and MS NP functionalized with the Cu(II) complex displayed only inhibitory effect and caused growth retardation of this bacterium. All three solids (i.e. MS NP and those containing the Ni or Cu complexes) were bacteriostatic against *E. coli* and caused reduction of bacterial growth. All compounds were found to be good carriers for gentamicin and both, being the MS NP containing the Cu and Ni complexes effective against gram + and gram - bacteria.

4. Conclusion

We have herein reviewed the use of MS-based materials with bactericidal properties. Due to high specific surface area and volume, tunable surface charge/pore size, stability, easy functionalization, biocompatibility and the possibility of creating hierarchical structures make MS particles excellent candidates for antimicrobial applications. Although, MS have no antimicrobial properties by itself, the functionalization and loading with different antimicrobials allow preparing a myriad of new hybrid MS materials with enhanced bactericidal properties. Antimicrobials based in small-molecules, metal-NPs or metal complexes can be adsorbed/functionalized or loaded in MS. In most cases the antibacterial efficacy of the prepared materials are significantly higher than that of free antimicrobials. Adsorbed/functionalized antimicrobials are usually not delivered and its effectivity is related with an effective raising of the local concentration of the antimicrobial due to its anchoring or adsorption on the MS surface. Moreover, MS can also serve as suitable containers for antimicrobials that are delivered in most cases by simple diffusion from the mesopores to the medium. This usually allows a sustained delivery and enhanced bactericidal properties. Moreover, MS in the forms of nanoparticles allow to design carriers able to target certain bacteria of interest. However, targeting bacteria with MS is a barely explored filed and very

few examples have been reported. Both, micro- and nano-MS have also been incorporated in composites in advanced antimicrobial applications. An alternative to simple sustained delivery is the possibility to design gated MS, in which payload release is triggered by predefined stimuli at will. The design of such gated mesoporous materials, capable of controlling on-command the release of species in the presence of a predefined stimulus, have proved very fruitful in other areas. However, despite the obvious advantage of using this approach, gated MS for antimicrobial applications have been not fully explored and new advances are envisioned in this area. A further advantage of using MS as nanocontainers is the possibility to couple MS with metal-based NPs having well-known antibiotic properties such as AgNPs and others. Most interesting MS are excellent supports to load and codeliver different antimicrobials at the same time in order to have an enhanced synergistic response. Despite the exponential development of this field, drawbacks still need to be overcome. It must be recognized that in most published works, studies on the antimicrobial activity is reported, yet there are fewer examples designed for real applications. Moreover, biocompatibility/biodegradation/toxicity behavior and degradation/clearance of MS *in vivo* and their exploitation as antibiotic delivery are still in its infancy and need to be better elucidated and more accurately assessed. Although several system (most of them based in metal NPs) have already found application in biomedical and industrial settings, the necessity to develop innovative antimicrobial formulations that cause little or no AMR mechanisms represents still an urgency for human and animal health, resulting in the unceasing research of nanomaterials that can constitute ideal antimicrobial candidates. We expect this review will help researchers working in MS and studying bacteria's resistance to antimicrobial compounds to develop new advances in this interesting, fertile and promising research area.

Acknowledgements

We thank the Spanish Government (projects MAT2015-64139-C4-1-R and AGL2015-70235-C2-2-R (MINECO/FEDER)) and the Generalitat Valenciana (project PROMETEOII/2014/047 and PROMETEO/2018/024) for support. A.B. thanks the Spanish Government for her Juan de la Cierva incorporación contract IJCI-2014-21534.

Received: ((will be filled in by the editorial staff))
Revised: ((will be filled in by the editorial staff))
Published online: ((will be filled in by the editorial staff))

References

[1] M. J. Hajipour, K. M. Fromm, A. Akbar Ashkarran, D. Jimenez de Aberasturi, I. R. de Larramendi, T. Rojo, V. Serpooshan, W. J. Parak and M. Mahmoudi, *Trends Biotechnol.*, **2012**, *30*, 499.

[2] F. von Nussbaum, M. Brands, B. Hinzen, S. Weigand and D. Häbich, *Angew. Chem. Int. Ed.*, **2006**, *45*, 5072–5129.

[3] V. Ramalingam, R. Rajaram, C. PremKumar, P. Santhanam, P. Dhinesh, S. Vinothkumar and K. Kaleshkumar, *J. Basic Microbiol.*, **2014**, *54*, 928–936.

[4] N. Beyth, Y. Houri-Haddad, A. Domb, W. Khan and R. Hazan, *Evid. Based Complement. Alternat. Med.*, **2015**, *2015*, 1–16.

[5] M. El Zowalaty, N. A. Ibrahim, M. Salama, K. Shameli, M. Usman and N. Zainuddin, *Int. J. Nanomedicine*, **2013**, 4467.

[6] W. Witte, *Infect. Genet. Evol.*, , DOI:10.1016/S1567-1348(04)00031-0.

[7] World Health Organization, Ed., *Antimicrobial resistance: global report on surveillance*, World Health Organization, Geneva, Switzerland, **2014**.

[8] Food and Agriculture Organization of the United Nations (FAO), World Organization for Animal Health (OIE) and World Health Organization (WHO), The Tripartite's Commitment Providing multi-sectoral, collaborative leadership in addressing health challenges, http://www.oie.int/fileadmin/Home/eng/Media_Center/docs/pdf/Tripartite_**2017**.pdf.

[9] C. Baker-Austin, M. S. Wright, R. Stepanauskas and J. V. McArthur, *Trends Microbiol.*, **2006**, *14*, 176–182.

[10] J. W. Costerton, G. G. Geesey and K.-J. Cheng, *Sci. Am.*, **1978**, *238*, 86–95.

[11] S. S. Branda, Å. Vik, L. Friedman and R. Kolter, *Trends Microbiol.*, **2005**, *13*, 20–26.

[12] R. Kolter and E. P. Greenberg, *Nature*, **2006**, *441*, 300–302.

[13] J. J. Harrison, R. J. Turner, L. L. R. Marques and H. Ceri, *Am. Sci.*, **2005**, *93*, 508–515.

[14] H.-C. Flemming and J. Wingender, *Nat. Rev. Microbiol.*, **2010**, *8*, 623–633.

[15] H.-C. Flemming, T. R. Neu and D. J. Wozniak, *J. Bacteriol.*, **2007**, *189*, 7945–7947.

[16] J. J. Harrison, H. Ceri and R. J. Turner, *Nat. Rev. Microbiol.*, **2007**, *5*, 928–938.

[17] G. L. Hobby, K. Meyer and E. Chaffee, *Proc. Soc. Exp. Biol. Med.*, **1942**, *50*, 281–285.

[18] J. Bigger, *The Lancet*, **1944**, *244*, 497–500.

[19] K. Lewis, *Annu. Rev. Microbiol.*, **2010**, *64*, 357–372.

[20] J. J. Harrison, *Microbiology*, **2005**, *151*, 3181–3195.

[21] M. L. Workentine, J. J. Harrison, A. M. Weljie, V. A. Tran, P. U. Stenroos, V. Tremaroli, H. J. Vogel, H. Ceri and R. J. Turner, *Environ. Microbiol.*, **2010**, *12*, 1565–1577.

[22] J. J. Harrison, R. J. Turner and H. Ceri, *BMC Microbiol.*, **2005**, *11*.

[23] D. Neut, H. C Van Der Mei, S. K Bulstra and H. J Busscher, *Acta Orthop.*, **2007**, *78*, 299–308.

[24] R. Singh, P. Ray, A. Das and M. Sharma, *J. Med. Microbiol.*, **2009**, *58*, 1067–1073.

[25] E. Piacenza, A. Presentato, E. Zonaro, J. A. Lemire, M. Demeter, G. Vallini, R. J. Turner and S. Lampis, *Microb. Biotechnol.*, **2017**, *10*, 804–818.

[26] R. M. Donlan, *Emerg. Infect. Dis.*, **2016**, *22*, 1142–1142.

[27] R. M. Donlan, *ASAIO J.*, **2000**, *46*, S47.

[28] J. T. Seil and T. J. Webster, *Int. J. Nanomedicine*, **2012**, *7*, 2767–2781.

[29] Ravishankar Rai V and Jamuna Bai A, *Nanoparticles and their potential application as antimicrobials*, A. Méndez-Vilas, FORMATEX **2011**.

[30] T. Appenzeller, *Science*, **1991**, *254*, 1300–1300.

[31] M. A. Gatoo, S. Naseem, M. Y. Arfat, A. Mahmood Dar, K. Qasim and S. Zubair, *BioMed Res. Int.*, **2014**, *2014*, 1–8.

[32] W. J. Parak, D. Gerion, T. Pellegrino, D. Zanchet, C. Micheel, S. C. Williams, R. Boudreau, M. A. L. Gros, C. A. Larabell and A. P. Alivisatos, *Nanotechnology*, **2003**, *14*, R15–R27.

[33] E. B. Anderson and T. E. Long, *Polymer*, **2010**, *51*, 2447–2454.

[34] A. Muñoz-Bonilla and M. Fernández-García, *Prog. Polym. Sci.*, **2012**, *37*, 281–339.

[35] G. Sauvet, W. Fortuniak, K. Kazmierski and J. Chojnowski, *J. Polym. Sci. Part Polym. Chem.*, **2003**, *41*, 2939–2948.

[36] D. Chung, S. E. Papadakis and K. L. Yam, *Int. J. Food Sci. Technol.*, **2003**, *5*.

[37] D.-S. Lee, J.-Y. Woo, C.-B. Ahn and J.-Y. Je, *Food Chem.*, **201**4, *148*, 97–104.

[38] J. Hiraki, *J. Antibact. Antifung. Agents*, **1995**, 349–354.

[39] L. Loomba and T. Scarabelli, *Ther. Deliv.*, **2013**, *4*, 859–873.

[40] D. F. Emerich, *Expert Opin. Biol. Ther.*, **2005**, *5*, 1–5.

[41] M. Rai, A. Yadav and A. Gade, *Biotechnol. Adv.*, **2009**, *27*, 76–83.

[42] S. Chatterjee, A. Bandyopadhyay and K. Sarkar, *J. Nanobiotechnology*, **2011**, *9*, 34.

[43] A. M. Allahverdiyev, E. S. Abamor, M. Bagirova and M. Rafailovich, *Future Microbiol.*, **2011**, *6*, 933–940.

[44] L. Esteban-Tejeda, F. Malpartida, A. Esteban-Cubillo, C. Pecharromán and J. S. Moya, *Nanotechnology*, **2009**, *20*, 505701.

[45] L. Palanikumar, S. N. Ramasamy and C. Balachandran, *IET Nanobiotechnol.*, **2014**, *8*, 111–117.

[46] T. Yanagisawa, T. Shimizu, K. Kuroda and C. Kato, *Bull. Chem. Soc. Jpn.*, **1990**, *63*, 988–992.

[47] J. S. Beck, J. C. Vartuli, W. J. Roth, M. E. Leonowicz, C. T. Kresge, K. D. Schmitt, C. T. W. Chu, D. H. Olson, E. W. Sheppard and S. B. McCullen, *J. Am. Chem. Soc.*, **1992**, *114*, 10834–10843.

[48] W. Li, J. Liu and D. Zhao, *Nat. Rev. Mater.*, **2016**, *1*, 16023.

[49] C. Argyo, V. Weiss, C. Bräuchle and T. Bein, *Chem. Mater.*, **2013**, *26*, 435–451.

[50] I. I. Slowing, J. L. Vivero-Escoto, C.-W. Wu and V. S.-Y. Lin, *Adv. Drug Deliv. Rev.*, **2008**, *60*, 1278–1288.

[51] M. Colilla, B. González and M. Vallet-Regí, *Biomater. Sci.*, **2013**, **1**, 114–134.

[52] A. Corma, *Chem. Rev.*, **1997**, *97*, 2373–2420.

[53] Y. Chen, H. Chen and J. Shi, *Adv. Mater.*, **2013**, *25*, 3144–3176.

[54] A. Llopis-Lorente, B. Lozano-Torres, A. Bernardos, R. Martínez-Máñez and F. Sancenón, *J. Mater. Chem. B*, **2017**, *5*, 3069–3083.

[55] S.-H. Wu, C.-Y. Mou and H.-P. Lin, *Chem. Soc. Rev.*, **2013**, *42*, 3862–3875.

[56] N. Hao, L. Li and F. Tang, *Int. Mater. Rev.*, **2017**, *62*, 57–77.

[57] T. Asefa and Z. Tao, *Chem. Res. Toxicol.*, **2012**, *25*, 2265–2284.

[58] J. Florek, R. Caillard and F. Kleitz, *Nanoscale*, **2017**, *9*, 15252–15277.

[59] A. Maleki, H. Kettiger, A. Schoubben, J. M. Rosenholm, V. Ambrogi and M. Hamidi, *J. Controlled Release*, **2017**, *262*, 329–347.

[60] Z. Li, J. C. Barnes, A. Bosoy, J. F. Stoddart and J. I. Zink, *Chem. Soc. Rev.*, **2012**, *41*, 2590–2605.

[61] J. M. Rosenholm, C. Sahlgren and M. Lindén, *Nanoscale*, **2010**, ***2***, 1870–1883.

[62] Y. Song, Y. Li, Q. Xu and Z. Liu, *Int. J. Nanomedicine*, **2017**, ***12***, 87.

[63] A. F. Moreira, D. R. Dias and I. J. Correia, *Microporous Mesoporous Mater.*, **2016**, *236*, 141–157.

[64] A. Baeza, M. Colilla and M. Vallet-Regí, *Expert Opin. Drug Deliv.*, **2015**, *12*, 319–337.

[65] J. Wen, K. Yang, F. Liu, H. Li, Y. Xu and S. Sun, *Chem. Soc. Rev.*, **2017**, *46*, 6024-6045.

[66] S. Niedermayer, V. Weiss, A. Herrmann, A. Schmidt, S. Datz, K. Müller, E. Wagner, T. Bein and C. Bräuchle, *Nanoscale*, **2015**, *7*, 7953–7964.

[67] K. Yang, H. Luo, M. Zeng, Y. Jiang, J. Li and X. Fu, *ACS Appl. Mater. Interfaces*, **2015**, *7*, 17399–17407.

[68] D. Lin, Q. Cheng, Q. Jiang, Y. Huang, Z. Yang, S. Han, Y. Zhao, S. Guo, Z. Liang and A. Dong, *Nanoscale*, **2013**, *5*, 4291–4301.

[69] L. Tan, M.-Y. Yang, H.-X. Wu, Z.-W. Tang, J.-Y. Xiao, C.-J. Liu and R.-X. Zhuo, *ACS Appl. Mater. Interfaces*, **2015**, *7*, 6310–6316.

[70] P. Díez, A. Sánchez, M. Gamella, P. Martínez-Ruíz, E. Aznar, C. de la Torre, J. R. Murguía, R. Martínez-Máñez, R. Villalonga and J. M. Pingarrón, *J. Am. Chem. Soc.*, **2014**, *136*, 9116–9123.

[71] T. M. Guardado-Alvarez, L. Sudha Devi, M. M. Russell, B. J. Schwartz and J. I. Zink, *J. Am. Chem. Soc.*, **2013**, *135*, 14000–14003.

[72] T. Chen, N. Yang and J. Fu, *Chem. Commun.*, **2013**, *49*, 6555–6557.

[73] X. Huang and X. Du, *ACS Appl. Mater. Interfaces*, **2014**, *6*, 20430–20436.

[74] X. Sun, Y. Zhao, V. S.-Y. Lin, I. I. Slowing and B. G. Trewyn, *J. Am. Chem. Soc.*, **2011**, *133*, 18554–18557.

[75] F. Muhammad, A. Wang, M. Guo, J. Zhao, W. Qi, G. Yingjie, J. Gu and G. Zhu, *ACS Appl. Mater. Interfaces*, **2013**, *5*, 11828–11835.

[76] S. Huang, L. Song, Z. Xiao, Y. Hu, M. Peng, J. Li, X. Zheng, B. Wu and C. Yuan, *Anal. Methods*, **2016**, *8*, 2561–2567.

[77] C. Liu, J. Zheng, L. Deng, C. Ma, J. Li, Y. Li, S. Yang, J. Yang, J. Wang and R. Yang, *ACS Appl. Mater. Interfaces*, **2015**, *7*, 11930–11938.

[78] J. Wen, K. Yang, Y. Xu, H. Li, F. Liu and S. Sun, *Sci. Rep.*, **2016**, *6*, 38931.

[79] H.-M. Meng, L. Lu, X.-H. Zhao, Z. Chen, Z. Zhao, C. Yang, X.-B. Zhang and W. Tan, *Anal. Chem.*, **2015**, *87*, 4448–4454.

[80] D. He, X. Li, X. He, K. Wang, J. Tang, X. Yang, X. He, X. Yang and Z. Zou, *J. Mater. Chem. B*, **2015**, *3*, 5588–5594.

[81] C. de la Torre, A. Agostini, L. Mondragón, M. Orzáez, F. Sancenón, R. Martínez-Máñez, M. D. Marcos, P. Amorós and E. Pérez-Payá, *Chem. Commun.*, **2014**, *50*, 3184–3186.

[82] C. de la Torre, L. Mondragón, C. Coll, F. Sancenón, M. D. Marcos, R. Martínez- Máñez, P. Amorós, E. Pérez- Payá and M. Orzáez, *Chem.- Eur. J.*, **2014**, *20*, 15309–15314.

[83] R. Bhat, À. Ribes, N. Mas, E. Aznar, F. Sancenón, M. D. Marcos, J. R. Murguía, A. Venkataraman and R. Martínez-Máñez, *Langmuir*, **2016**, *32*, 1195–1200.

[84] X.-L. Li, N. Hao, H.-Y. Chen and J.-J. Xu, *Anal. Chem.*, **2014**, *86*, 10239–10245.

[85] Y. Chang, P. Liao, H. Sheu, Y. Tseng, F. Cheng and C. Yeh, *Adv. Mater.*, **2012**, *24*, 3309–3314.

[86] S. Zhou, X. Du, F. Cui and X. Zhang, *Small*, **2014**, *10*, 980–988.

[87] I. Candel, E. Aznar, L. Mondragón, C. de la Torre, R. Martínez-Máñez, F. Sancenón, M. D. Marcos, P. Amorós, C. Guillem and E. Pérez-Payá, *Nanoscale*, **2012**, *4*, 7237–7245.

[88] A. Bernardos, L. Mondragon, E. Aznar, M. D. Marcos, R. Martínez-Máñez, F. Sancenón, J. Soto, J. M. Barat, E. Pérez-Payá and C. Guillem, *Acs Nano*, **2010**, *4*, 6353–6368.

[89] N. Hao, X. Chen, S. Jeon and M. Yan, *Adv. Healthc. Mater.*, **2015**, *4*, 2797–2801.

[90] B. Ruehle, D. L. Clemens, B.-Y. Lee, M. A. Horwitz and J. I. Zink, *J. Am. Chem. Soc.*, **2017**, *139*, 6663–6668.

[91] P. Díez, A. Sánchez, C. de la Torre, M. Gamella, P. Martínez-Ruíz, E. Aznar, R. Martinez-Manez, J. M. Pingarrón and R. Villalonga, *ACS Appl. Mater. Interfaces*, **2016**, *8*, 7657–7665.

[92] J. Liu, B. Zhang, Z. Luo, X. Ding, J. Li, L. Dai, J. Zhou, X. Zhao, J. Ye and K. Cai, *Nanoscale*, **2015**, *7*, 3614–3626.

[93] J. Zhou, N. Hao, T. De Zoyza, M. Yan and O. Ramström, *Chem. Commun.*, **2015**, *51*, 9833–9836.

[94] L. Pascual, C. Cerqueira-Coutinho, A. García-Fernández, B. de Luis, E. S. Bernardes, M. S. Albernaz, S. Missailidis, R. Martínez-Máñez, R. Santos-Oliveira and M. Orzaez, *Nanomedicine Nanotechnol. Biol. Med.*, **2017**, *13*, 2495–2505.

[95] N. K. Mal, M. Fujiwara and Y. Tanaka, *Nature*, **2003**, *421*, 350.

[96] Z. Zhao, H. Meng, N. Wang, M. J. Donovan, T. Fu, M. You, Z. Chen, X. Zhang and W. Tan, *Angew. Chem. Int. Ed.*, **2013**, *52*, 7487–7491.

[97] J. L. Paris, M. V. Cabañas, M. Manzano and M. Vallet-Regí, *ACS Nano*, **2015**, *9*, 11023–11033.

[98] A. Baeza, E. Guisasola, E. Ruiz-Hernández and M. Vallet-Regí, *Chem. Mater.*, **2012**, *24*, 517–524.

[99] V. Cauda, H. Engelke, A. Sauer, D. Arcizet, J. Rädler and T. Bein, *Nano Lett.*, **2010**, *10*, 2484–2492.

[100] E. Climent, A. Bernardos, R. Martínez-Máñez, A. Maquieira, M. D. Marcos, N. Pastor-Navarro, R. Puchades, F. Sancenón, J. Soto and P. Amorós, *J. Am. Chem. Soc.*, **2009**, *131*, 14075–14080.

[101] C. Coll, L. Mondragón, R. Martínez- Máñez, F. Sancenón, M. D. Marcos, J. Soto, P. Amorós and E. Pérez- Payá, *Angew. Chem. Int. Ed.*, **2011**, *50*, 2138–2140.

[102] E. Aznar, M. Oroval, L. Pascual, J. R. Murguía, R. Martínez-Máñez and F. Sancenón, *Chem. Rev.*, **2016**, *116*, 561–718.

[103] L. Pascual, S. E. Sayed, R. Martínez-Máñez, A. M. Costero, S. Gil, P. Gaviña and F. Sancenón, *Org. Lett.*, **2016**, *18*, 5548–5551.

[104] A. Ultimo, C. Giménez, P. Bartovsky, E. Aznar, F. Sancenón, M. D. Marcos, P. Amorós, A. R. Bernardo, R. Martínez-Máñez, A. M. Jiménez-Lara and J. R. Murguía, *Chem. - Eur. J.*, **2016**, *22*, 1582–1586.

[105] B. Lozano-Torres, L. Pascual, A. Bernardos, M. D. Marcos, J. O. Jeppesen, Y. Salinas, R. Martínez-Máñez and F. Sancenón, *Chem. Commun.*, **2017**, *53*, 3559–3562.

[106] A. Llopis-Lorente, B. Lozano-Torres, A. Bernardos, R. Martínez-Máñez and F. Sancenón, *J. Mater. Chem. B*, **2017**, *5*, 3069–3083.

[107] A. Llopis-Lorente, P. Díez, A. Sánchez, M. D. Marcos, F. Sancenón, P. Martínez-Ruiz, R. Villalonga and R. Martínez-Máñez, *Nat. Commun.*, **2017**, *8*, 15511.

[108] À. Ribes, E. Aznar, A. Bernardos, M. D. Marcos, P. Amorós, R. Martínez-Máñez and F. Sancenón, *Chem. - Eur. J.*, **2017**, *23*, 8581–8584.

[109] M. Oroval, P. Díez, E. Aznar, C. Coll, M. D. Marcos, F. Sancenón, R. Villalonga and R. Martínez-Máñez, *Chem. - Eur. J.*, **2017**, *23*, 1353–1360.

[110] C. de la Torre, L. Domínguez-Berrocal, J. R. Murguía, M. D. Marcos, R. Martínez-Máñez, J. Bravo and F. Sancenón, *Chem. - Eur. J.*, **2018**, *24*, 1890–1897.

[111] A. H. Teruel, É. Pérez-Esteve, I. González-Álvarez, M. González-Álvarez, A. M. Costero, D. Ferri, M. Parra, P. Gaviña, V. Merino, R. Martínez-Mañez and F. Sancenón, *J. Controlled Release*, **2018**, *281*, 58–69.

[112] A. García-Fernández, G. García-Laínez, M. L. Ferrándiz, E. Aznar, F. Sancenón, M. J. Alcaraz, J. R. Murguía, M. D. Marcos, R. Martínez-Máñez, A. M. Costero and M. Orzáez, *J. Controlled Release*, **2017**, *248*, 60–70.

[113] F. Sancenón, L. Pascual, M. Oroval, E. Aznar and R. Martínez-Máñez, *ChemistryOpen*, **2015**, *4*, 418–437.

[114] C. de la Torre, L. Mondragón, C. Coll, A. García-Fernández, F. Sancenón, R. Martínez-Máñez, P. Amorós, E. Pérez-Payá and M. Orzáez, *Chem. - Eur. J.*, **2015**, *21*, 15506–15510.

[115] C. de la Torre, I. Casanova, G. Acosta, C. Coll, M. J. Moreno, F. Albericio, E. Aznar, R. Mangues, M. Royo, F. Sancenón and R. Martínez-Máñez, *Adv. Funct. Mater.*, **2015**, *25*, 687–695.

[116] Y. Yang and C. Yu, *Nanomedicine Nanotechnol. Biol. Med.*, **2016**, *12*, 317–332.

[117] E. A. Azzopardi, E. L. Ferguson and D. W. Thomas, *J. Antimicrob. Chemother.*, **2012**, *68*, 257–274.

[118] D. S. Benoit and H. Koo, *Nanomedice*, **2016**, *11(8)*.

[119] T.-O. Peulen and K. J. Wilkinson, *Environ. Sci. Technol.*, **2011**, *45*, 3367–3373.

[120] G. Hidalgo, A. Burns, E. Herz, A. G. Hay, P. L. Houston, U. Wiesner and L. W. Lion, *Appl. Environ. Microbiol.*, **2009**, *75*, 7426–7435.

[121] X. Li, Y-C. Yeh, K. Giri, R. Mout, R. F. Landis, Y. S. Prakash and V. M. Rotello, *Chem. Commun.*, **2015**,*51*, 282-285

[122] A. Gupta, R. F. Landis and V. M. Rotello, *F1000Research*, **2016**, *5*, F1000.

[123] B. Duncan, X. Li, R. F. Landis, S. T. Kim, A. Gupta, L.-S. Wang, R. Ramanathan, R. Tang, J. A. Boerth and V. M. Rotello, *ACS Nano*, ***2015***, *9*, 7775–7782.

[124] J. Zhou, K. W. Jayawardana, N. Kong, Y. Ren, N. Hao, M. Yan and O. Ramström, *ACS Biomater. Sci. Eng.*, **2015**, *1*, 1250–1255.

[125] K. W. Jayawardana, H. S. N. Jayawardena, S. A. Wijesundera, T. De Zoysa, M. Sundhoro and M. Yan, *Chem. Commun.*, **2015**, *51*, 12028–12031.

[126] R. Y. Pelgrift and A. J. Friedman, *Adv. Drug Deliv. Rev.*, **2013**, *65*, 1803–1815.

[127] W. Q. Lim, S. Z. F. Phua, H. V. Xu, S. Sreejith and Y. Zhao, *Nanoscale*, **2016**, *8*, 12510–12519.

[128] Y. Wang and H. Gu, *Adv. Mater.*, **2015**, *27*, 576–585.

[129] Y. Wang, X. Ding, Y. Chen, M. Guo, Y. Zhang, X. Guo and H. Gu, *Biomaterials*, **2016**, *101*, 207–216.

[130] Z. Jiang, B. Dong, B. Chen, J. Wang, L. Xu, S. Zhang and H. Song, *Small*, **2013**, *9*, 604–612.

[131] J.-N. Liu, W.-B. Bu and J.-L. Shi, *Acc. Chem. Res.*, **2015**, *48*, 1797–1805.

[132] N. M. Idris, M. K. Gnanasammandhan, J. Zhang, P. C. Ho, R. Mahendran and Y. Zhang, *Nat. Med.*, **2012**, *18*, 1580–1585.

[133] R. Jugdaohsingh, *J. Nutr. Health Aging*, **2007**, *11*, 99.

[134] J. G. Croissant, Y. Fatieiev and N. M. Khashab, *Adv. Mater.***2017**, *29*, 1604634.

[135] P. Huang, Y. Chen, H. Lin, L. Yu, L. Zhang, L. Wang, Y. Zhu and J. Shi, *Biomaterials*, **2017**, *125*, 23–37.

[136] Y. Chen, Q. Meng, M. Wu, S. Wang, P. Xu, H. Chen, Y. Li, L. Zhang, L. Wang and J. Shi, *J. Am. Chem. Soc.*, **2014**, *136*, 16326–16334.

[137] L. Wang, M. Huo, Y. Chen and J. Shi, *Adv. Healthc. Mater.* **2017**, *6*, 1700720.

[138] X. Hao, X. Hu, C. Zhang, S. Chen, Z. Li, X. Yang, H. Liu, G. Jia, D. Liu and K. Ge, *ACS Nano*, **2015**, *9*, 9614–9625.

[139] L. Yu, Y. Chen, M. Wu, X. Cai, H. Yao, L. Zhang, H. Chen and J. Shi, *J. Am. Chem. Soc.*, **2016**, *138*, 9881–9894.

[140] V. Cauda, A. Schlossbauer and T. Bein, *Microporous Mesoporous Mater.*, **2010**, *132*, 60–71.

[141] C. Acosta, J. M. Barat, R. Martínez-Máñez, F. Sancenón, S. Llopis, N. González, S. Genovés, D. Ramón and P. Martorell, *Environ. Res.*, **2018**, *166*, 61–70.

[142] V. Cauda, C. Argyo and T. Bein, *J. Mater. Chem.*, **2010**, *20*, 8693–8699.

[143] B. Godin, J. Gu, R. E. Serda, R. Bhavane, E. Tasciotti, C. Chiappini, X. Liu, T. Tanaka, P. Decuzzi and M. Ferrari, *J. Biomed. Mater. Res. A*, **2010**, *94*, 1236–1243.

[144] D. Shen, J. Yang, X. Li, L. Zhou, R. Zhang, W. Li, L. Chen, R. Wang, F. Zhang and D. Zhao, *Nano Lett.*, **2014**, *14*, 923–932.

[145] Q. He, J. Shi, M. Zhu, Y. Chen and F. Chen, *Microporous Mesoporous Mater.*, **2010**, *131*, 314–320.

[146] G. Qi, L. Li, F. Yu and H. Wang, *ACS Appl. Mater. Interfaces*, **2013**, *5*, 10874–10881.

[147] M. Ruiz-Rico, É. Pérez-Esteve, A. Bernardos, F. Sancenón, R. Martínez-Máñez, M. D. Marcos and J. M. Barat, *Food Chem.*, **2017**, *233*, 228–236.

[148] M. Villegas, L. Garcia-Uriostegui, O. Rodríguez, I. Izquierdo-Barba, A. Salinas, G. Toriz, M. Vallet-Regí and E. Delgado, *Bioengineering*, **2017**, *4*, 80.

[149] E. Pędziwiatr-Werbicka, K. Miłowska, M. Podlas, M. Marcinkowska, M. Ferenc, Y. Brahmi, N. Katir, J.-P. Majoral, A. Felczak, A. Boruszewska, K. Lisowska, M. Bryszewska and A. El Kadib, *Chem. - Eur. J.*, **2014**, *20*, 9596–9606.

[150] M. Ferenc, N. Katir, K. Milowska, M. Bousmina, Y. Brahmi, A. Felczak, K. Lisowska, M. Bryszewska and A. El Kadib, *Microporous Mesoporous Mater.*, **2016**, *231*, 47–56.

[151] L. Li and H. Wang, *Adv. Healthc. Mater.*, **2013**, *2*, 1351–1360.

[152] L. J. Bastarrachea and J. M. Goddard, *J. Agric. Food Chem.*, **2015**, *63*, 4243–4251.

[153] J. Xu, Y. Zhang, Y. Zhao and X. Zou, *J. Phys. Chem. Solids*, **2017**, *108*, 21–24.

[154] Y. Wang, L. Li, Y. Liu, X. Ren and J. Liang, *Mater. Sci. Eng. C*, **2016,** *69*, 1075–1080.

[155] Y. Wang, Y. Liu, H. Tian, Y. Zhai, N. Pan, M. Yin, X. Ren and J. Liang, *Colloid Polym. Sci.*, **2017**, *295*, 1897–1904.

[156] Y. Wang, M. Yin, Z. Li, Y. Liu, X. Ren and T.-S. Huang, *Colloids Surf. B Biointerfaces*, **2018**, *165*, 199–206.

[157] A. Sharma, A. Dubey and R. Kurchania, *J. Porous Mater.*, **2016**, *23*, 851–855.

[158] A. Cagri Karaburun, Z. Asim Kaplancikli, N. Gundogdu-Karaburun and F. Demirci, *Lett. Drug Des. Discov.*, **2011**, *8*, 811–815.

[159] A. Sharma, G. Robin Wilson and A. Dubey, *New J. Chem.*, **2016**, *40*, 764–769.

[160] Gupta, Sarita, Verma, Purnima and Singh, Virendra, *2016*, **2016**, *55*, 362–367.

[161] J. Gehring, B. Trepka, N. Klinkenberg, H. Bronner, D. Schleheck and S. Polarz, *J. Am. Chem. Soc.*, **2016**, *138*, 3076–3084.

[162] O. Planas, R. Bresolí-Obach, J. Nos, T. Gallavardin, R. Ruiz-González, M. Agut and S. Nonell, *Molecules*, **2015**, *20*, 6284–6298.

[163] G. Zampini, O. Planas, F. Marmottini, O. Gulías, M. Agut, S. Nonell and L. Latterini, *RSC Adv.*, **2017**, *7*, 14422–14429.

[164] M. Ruiz-Rico, C. Fuentes, É. Pérez-Esteve, A. I. Jiménez-Belenguer, A. Quiles, M. D. Marcos, R. Martínez-Máñez and J. M. Barat, *Food Control*, **2015**, *56*, 77–85.

[165] B. Koneru, Y. Shi, Y.-C. Wang, S. Chavala, M. Miller, B. Holbert, M. Conson, A. Ni and A. Di Pasqua, *Molecules*, **2015**, *20*, 19690–19698.

[166] S. Sharmiladevi, A. Shanmuga Priya and M. V. Sujitha, *Int. J. Pharm. Pharm. Sci.*, **2016**, *8*, 196–201.

[167] N. Hao, K. W. Jayawardana, X. Chen and M. Yan, *ACS Appl. Mater. Interfaces*, **2015**, *7*, 1040–1045.

[168] J. Zhou, K. W. Jayawardana, N. Kong, Y. Ren, N. Hao, M. Yan and O. Ramström, *ACS Biomater. Sci. Eng.*, **2015**, *1*, 1250–1255.

[169] J. Indrigo, R. L. Hunter Jr and J. K. Actor, *Microbiology*, **2003**, *149*, 2049–2059.

[170] Samar M. Alhabardi, *Life Sci. J.*, **2016**, *13*, 31–39.

[171] N. Hao, X. Chen, K. W. Jayawardana, B. Wu, M. Sundhoro and M. Yan, *Biomater. Sci.*, **2016**, *4*, 87–91.

[172] Y. Wang, Y. A. Nor, H. Song, Y. Yang, C. Xu, M. Yu and C. Yu, *J. Mater. Chem. B*, **2016**, *4*, 2646–2653.

[173] A. C. Chan, M. Bravo Cadena, H. E. Townley, M. D. Fricker and I. P. Thompson, *J. R. Soc. Interface*, **2017**, *14*, 20160650.

[174] R. J. Mudakavi, S. Vanamali, D. Chakravortty and A. M. Raichur, *RSC Adv.*, **2017**, *7*, 7022–7032.

[175] B. G. Trewyn, C. M. Whitman and V. S.-Y. Lin, *Nano Lett.*, **2004**, *4*, 2139–2143.

[176] M. Cicuéndez, I. Izquierdo-Barba, M. T. Portolés and M. Vallet-Regí, *Eur. J. Pharm. Biopharm.*, **2013**, *84*, 115–124.

[177] X. Xia, K. Pethe, R. Kim, L. Ballell, D. Barros, J. Cechetto, H. Jeon, K. Kim and A. Garcia-Bennett, *Nanomaterials*, **2014**, *4*, 813–826.

[178] L. de Oliveira, K. Bouchmella, A. Picco, L. Capeletti, K. Gonçalves, J. H. dos Santos, J. Kobarg and M. Cardoso, *J. Braz. Chem. Soc.* **2017**, *28*, 1715–1724.

[179] R. J. Mudakavi, A. M. Raichur and D. Chakravortty, *RSC Adv*, **2014**, *4*, 61160–61166.

[180] Y. Liu, X. Liu, Y. Xiao, F. Chen and F. Xiao, *RSC Adv.*, **2017**, *7*, 31133–31141.

[181] T. S. Anirudhan, Binusreejayan and P. P. Jayan, *Des. Monomers Polym.*, **2016**, *19*, 381–393.

[182] I. Izquierdo-Barba, M. Vallet-Regí, N. Kupferschmidt, O. Terasaki, A. Schmidtchen and M. Malmsten, *Biomaterials*, **2009**, *30*, 5729–5736.

[183] A. Aguilar-Colomer, J. C. Doadrio, C. Pérez-Jorge, M. Manzano, M. Vallet-Regí and J. Esteban, *J. Antibiot. (Tokyo)*, **2017**, *70*, 259–263.

[184] P. Zhou, Y. Xia, X. Cheng, P. Wang, Y. Xie and S. Xu, *Biomaterials*, **2014**, *35*, 10033–10045.

[185] M. Colilla, M. Martínez-Carmona, S. Sánchez-Salcedo, M. L. Ruiz-González, J. M. González-Calbet and M. Vallet-Regí, *J Mater Chem B*, **2014**, *2*, 5639–5651.

[186] P. C. Balaure, B. Boarca, R. C. Popescu, D. Savu, R. Trusca, B. Ștefan Vasile, A. M. Grumezescu, A. M. Holban, A. Bolocan and E. Andronescu, *Int. J. Pharm.*, **2017**, *531*, 35–46.

[187] M. Michailidis, I. Sorzabal-Bellido, E. A. Adamidou, Y. A. Diaz-Fernandez, J. Aveyard, R. Wengier, D. Grigoriev, R. Raval, Y. Benayahu, R. A. D'Sa and D. Shchukin, *ACS Appl. Mater. Interfaces*, **2017**, *9*, 38364–38372.

[188] Z. Chang, Z. Wang, M. Lu, M. Li, L. Li, Y. Zhang, D. Shao and W. Dong, *RSC Adv.*, **2017**, *7*, 3550–3553.

[189] G. Chen, Z. Li, X. Wang, L. Xie, Q. Qi and W. Fang, *Mater. Lett.*, **2014**, *134*, 290–294.

[190] M. M. Stanton, B.-W. Park, D. Vilela, K. Bente, D. Faivre, M. Sitti and S. Sánchez, *ACS Nano*, **2017**, *11*, 9968–9978.

[191] M. Wan, J. Zhang, Q. Wang, S. Zhan, X. Chen, C. Mao, Y. Liu and J. Shen, *ACS Appl. Mater. Interfaces*, **2017**, *9*, 18609–18618.

[192] F. Wu, T. Xu, G. Zhao, S. Meng, M. Wan, B. Chi, C. Mao and J. Shen, *Langmuir*, **2017**, *33*, 5245–5252.

[193] G. Xu, X. Shen, L. Dai, Q. Ran, P. Ma and K. Cai, *Mater. Sci. Eng. C*, **2017**, *70*, 386–395.

[194] J. Yu, H. Yang, K. Li, H. Ren, J. Lei and C. Huang, *ACS Appl. Mater. Interfaces*, **2017**, *9*, 25796–25807.

[195] D. Li, W. Nie, L. Chen, Y. Miao, X. Zhang, F. Chen, B. Yu, R. Ao, B. Yu and C. He, *RSC Adv.*, **2017**, *7*, 7973–7982.

[196] S. Hashemikia, N. Hemmatinejad, E. Ahmadi and M. Montazer, *Drug Deliv.*, **2016**, *23*, 2946–2955.

[197] J. F. Zhang, R. Wu, Y. Fan, S. Liao, Y. Wang, Z. T. Wen and X. Xu, *J. Dent. Res.*, **2014**, *93*, 1283–1289.

[198] D. Rădulescu, G. Voicu, A. E. Oprea, E. Andronescu, V. Grumezescu, A. M. Holban, B. S. Vasile, A. V. Surdu, A. M. Grumezescu, G. Socol, L. Mogoantă, G. D. Mogoşanu, P. C. Balaure, R. Rădulescu and M. C. Chifiriuc, *Appl. Surf. Sci.*, **2016**, *374*, 165–171.

[199] L. M. Perez, P. Lalueza, M. Monzon, J. A. Puertolas, M. Arruebo and J. Santamaría, *Int. J. Pharm.*, **2011**, *409*, 1–8.

[200] N. Ehlert, M. Badar, A. Christel, S. J. Lohmeier, T. Luessenhop, M. Stieve, T. Lenarz, P. P. Mueller and P. Behrens, *J Mater Chem*, **2011**, *21*, 752–760.

[201] M. Cicuéndez, J. C. Doadrio, A. Hernández, M. T. Portolés, I. Izquierdo-Barba and M. Vallet-Regí, *Acta Biomater.*, **2018**, *65*, 450–461.

[202] C.J. Seneviratne, K.C.-F. Leung, C.-H. Wong, S.-F. Lee, X. Li, P.C. Leung, C.B.S. Lau, E. Wat, and L. Jin, *PLOS ONE*, **2014**, *9*, e103234.

[203] T. Tamanna, C. B. Landersdorfer, H. J. Ng, J. B. Bulitta, P. Wood, A. Yu, *Appl. Nanoscience*, **2018**, *8*, 1471–1482.

[204] N. Mas, I. Galiana, L. Mondragón, E. Aznar, E. Climent, N. Cabedo, F. Sancenón, J. R. Murguía, R. Martínez-Máñez, M. D. Marcos and P. Amorós, *Chem. - Eur. J.*, **2013**, *19*, 11167–11171.

[205] N. Velikova, N. Mas, L. Miguel-Romero, L. Polo, E. Stolte, E. Zaccaria, R. Cao, N. Taverne, J. R. Murguía, R. Martinez-Manez, A. Marina and J. Wells, *Nanomedicine Nanotechnol. Biol. Med.*, **2017**, *13*, 569–581.

[206] S. K. Alsaiari, M. A. Hammami, J. G. Croissant, H. W. Omar, P. Neelakanda, T. Yapici, K.-V. Peinemann and N. M. Khashab, *Adv. Healthc. Mater.*, **2017**, *6*, 1601135.

[207] Z. Yan, P. Shi, J. Ren and X. Qu, *Small*, **2015**, *11*, 5540–5544.

[208] F. Duan, X. Feng, Y. Jin, D. Liu, X. Yang, G. Zhou, D. Liu, Z. Li, X.-J. Liang and J. Zhang, *Biomaterials*, **2017**, *144*, 155–165.

[209] E. Yu, I. Galiana, R. Martínez-Máñez, P. Stroeve, M. D. Marcos, E. Aznar, F. Sancenón, J. R. Murguía and P. Amorós, *Colloids Surf. B Biointerfaces*, **2015**, *135*, 652–660.

[210] Y. Wu, Y. Long, Q.-L. Li, S. Han, J. Ma, Y.-W. Yang and H. Gao, *ACS Appl. Mater. Interfaces*, **2015**, *7*, 17255–17263.

[211] Q. Li, Y. Wu, H. Lu, X. Wu, S. Chen, N. Song, Y.-W. Yang and H. Gao, *ACS Appl. Mater. Interfaces*, **2017**, *9*, 10180–10189.

[212] B.-Y. Lee, Z. Li, D. L. Clemens, B. J. Dillon, A. A. Hwang, J. I. Zink and M. A. Horwitz, *Small*, **2016**, *12*, 3690–3702.

[213] B. González, M. Colilla, J. Díez, D. Pedraza, M. Guembe, I. Izquierdo-Barba, M. Vallet-Regí, *Acta Biomater.* **2018**, *68*, 261-271.

[214] H. H. Lara, N. V. Ayala-Núñez, L. del C. Ixtepan Turrent and C. Rodríguez Padilla, *World J. Microbiol. Biotechnol.*, **2010**, *26*, 615–621.

[215] A. R. Shahverdi, A. Fakhimi, H. R. Shahverdi and S. Minaian, *Nanomedicine Nanotechnol. Biol. Med.*, **2007**, *3*, 168–171.

[216] S. Sarkar, A. D. Jana, S. K. Samanta and G. Mostafa, *Polyhedron*, **2007**, *26*, 4419–4426.

[217] S. Shrivastava, T. Bera, A. Roy, G. Singh, P. Ramachandrarao and D. Dash, *Nanotechnology*, **2007**, *18*, 225103.

[218] G. Ren, D. Hu, E. W. C. Cheng, M. A. Vargas-Reus, P. Reip and R. P. Allaker, *Int. J. Antimicrob. Agents*, **2009**, *33*, 587–590.

[219] E. Martinezflores, J. Negrete and G. Torresvillasenor, *Mater. Des.*, **2003**, *24*, 281–286.

[220] Magiorakos A.- P., Srinivasan A., Carey R. B., Carmeli Y., Falagas M. E., Giske C. G., Harbarth S., Hindler J. F., Kahlmeter G., Olsson- Liljequist B., Paterson D. L., Rice L. B., Stelling J., Struelens M. J., Vatopoulos A., Weber J. T. and Monnet D. L., *Clin. Microbiol. Infect.*, **2011**, *18*, 268–281.0

[221] Y. Matsumura, K. Yoshikata, S. Kunisaki and T. Tsuchido, *Appl. Environ. Microbiol.*, **2003**, *69*, 4278–4281.

[222] Silver Simon, *FEMS Microbiol. Rev.*, **2006**, *27*, 341–353.

[223] J. P. Ruparelia, A. K. Chatterjee, S. P. Duttagupta and S. Mukherji, *Acta Biomater.*, **2008**, *4*, 707–716.

[224] J. R. Morones, J. L. Elechiguerra, A. Camacho, K. Holt, J. B. Kouri, J. T. Ramírez and M. J. Yacaman, *Nanotechnology*, **2005**, *16*, 2346–2353.

[225] Shuguang Wang, R. Lawson, P. C. Ray and Hongtao Yu, *Toxicol. Ind. Health*, **2011**, *27*, 547–554.

[226] C. E. Santo, N. Taudte, D. H. Nies and G. Grass, *Appl. Environ. Microbiol.*, **2008**, *74*, 977–986.

[227] C. Nathan and A. Cunningham-Bussel, *Nat. Rev. Immunol.*, **2013**, *13*, 349–361.

[228] S. J. Soenen, P. Rivera-Gil, J.-M. Montenegro, W. J. Parak, S. C. De Smedt and K. Braeckmans, *Nano Today*, **2011**, *6*, 446–465.

[229] X. Pan, J. E. Redding, P. A. Wiley, L. Wen, J. S. McConnell and B. Zhang, *Chemosphere*, **2010**, *79*, 113–116.

[230] A. A. Ashkarran, M. Ghavami, H. Aghaverdi, P. Stroeve and M. Mahmoudi, *Chem. Res. Toxicol.*, **2012**, 1231–1242.

[231] J. Fang, D. Y. Lyon, M. R. Wiesner, J. Dong and Alvarez, *Environ. Sci. Amp Technol.*, **2007**, *41*, 2636–2642.

[232] A. Simon-Deckers, S. Loo, M. Mayne-L'hermite, N. Herlin-Boime, N. Menguy, C. Reynaud, B. Gouget and M. Carrière, *Environ. Sci. Technol.*, **2009**, *43*, 8423–8429.

[233] Y.-W. Baek and Y.-J. An, *Sci. Total Environ.*, **2011**, *409*, 1603–1608.

[234] Y. Tian, J. Qi, W. Zhang, Q. Cai and X. Jiang, *ACS Appl. Mater. Interfaces*, **2014**, *6*, 12038–12045.

[235] R.-S. Huang, B.-F. Hou, H.-T. Li, X.-C. Fu and C.-G. Xie, *RSC Adv.*, **2015**, *5*, 61184–61190.

[236] R.-H. Dong, Y.-X. Jia, C.-C. Qin, L. Zhan, X. Yan, L. Cui, Y. Zhou, X. Jiang and Y.-Z. Long, *Nanoscale*, **2016**, *8*, 3482–3488.

[237] P. Xu, J. Liang, X. Cao, J. Tang, J. Gao, L. Wang, W. Shao, Q. Gao and Z. Teng, *J. Colloid Interface Sci.*, **2016**, *474*, 114–118.

[238] Q. Shen, J. Wang, H. Yang, X. Ding, Z. Luo, H. Wang, C. Pan, J. Sheng and D. Cheng, *J. Non-Cryst. Solids*, **2014**, *391*, 112–116.

[239] X. Wan, L. Zhuang, B. She, Y. Deng, D. Chen and J. Tang, *Mater. Sci. Eng. C*, **2016**, *65*, 323–330.

[240] Y. Song, H. Jiang, B. Wang, Y. Kong and J. Chen, *ACS Appl. Mater. Interfaces*, **2018**, *10*, 1792–1801.

[241] M. Liong, B. France, K. A. Bradley and J. I. Zink, *Adv. Mater.*, **2009**, *21*, 1684–1689.

[242] L. H. Dong, T. Liu, L. Zhang and Y. S. Yin, *Adv. Mater. Res.*, **2011**, *236–238*, 1775–1778.

[243] T. Liu, Y. Dong, T. He, N. Guo and F. Zhang, *Surf. Eng.*, **2014**, *30*, 6–10.

[244] B. Yin, T. Liu, L. H. Dong, L. Zhang and Y. S. Yin, *Adv. Mater. Res.*, **2012**, *463–464*, 1479–1483.

[245] H. Yang, Y. Liu, Q. Shen, L. Chen, W. You, X. Wang and J. Sheng, *J. Mater. Chem.*, **2012**, *22*, 24132.

[246] H. Yang, W. You, Q. Shen, X. Wang, J. Sheng, D. Cheng, X. Cao and C. Wu, *RSC Adv*, **2014**, *4*, 2793–2796.

[247] S. Pandey and J. Ramontja, *Int. J. Biol. Macromol.*, **2016**, *93*, 712–723.

[248] C. Ma, Q. Wei, B. Cao, X. Cheng, J. Tian, H. Pu, A. Yusufu and L. Cao, *PLOS ONE*, **2017**, *12*, e0172499.

[249] Z. Ma, H. Ji, Y. Teng, G. Dong, D. Tan, M. Guan, J. Zhou, J. Xie, J. Qiu and M. Zhang, *J. Mater. Chem.*, **2011**, *21*, 9595.

[250] B. Naik, V. Desai, M. Kowshik, V. S. Prasad, G. F. Fernando and N. N. Ghosh, *Particuology*, **2011**, *9*, 243–247.

[251] Y. Gao, Q. Dong, S. Lan, Q. Cai, O. Simalou, S. Zhang, G. Gao, H. Chokto and A. Dong, *ACS Appl. Mater. Interfaces*, **2015**, *7*, 10022–10033.

[252] D. Carmona, P. Lalueza, F. Balas, M. Arruebo and J. Santamaría, *Microporous Mesoporous Mater.*, **2012**, *161*, 84–90.

[253] Z. Chang, Z. Wang, M. Lu, D. Shao, J. Yue, D. Yang, M. Li and W. Dong, *Colloids Surf. B Biointerfaces*, **2017**, *157*, 199–206.

[254] M. Lu, Q. Wang, Z. Chang, Z. Wang, X. Zheng, D. Shao, W. Dong and Y. Zhou, *Int. J. Nanomedicine*, **2017**, *12*, 3577–3589.

[255] A. Saad, E. Cabet, A. Lilienbaum, S. Hamadi, M. Abderrabba and M. M. Chehimi, *J. Taiwan Inst. Chem. Eng.*, **2017**, *80*, 1022–1030.

[256] Y. Wang, X. Ding, Y. Chen, M. Guo, Y. Zhang, X. Guo and H. Gu, *Biomaterials*, **2016**, *101*, 207–216.

[257] Z. Song, Y. Ma, G. Xia, Y. Wang, W. Kapadia, Z. Sun, W. Wu, H. Gu, W. Cui and X. Huang, *J. Mater. Chem. B*, **2017**, *5*, 7632–7643.

[258] Y. Kuthati, R. K. Kankala, P. Busa, S.-X. Lin, J.-P. Deng, C.-Y. Mou and C.-H. Lee, *J. Photochem. Photobiol. B*, **2017**, *169*, 124–133.

[259] Yoshimura M., Namura S., Akamatsu H. and Horio T., *Br. J. Dermatol.*, **2008**, *135*, 528–532.

[260] T. Matsunaga, R. Tomoda, T. Nakajima and H. Wake, *FEMS Microbiol. Lett.*, **1985**, *29*, 211–214.

[261] B. Kim, D. Kim, D. Cho and S. Cho, *Chemosphere*, **2003**, *52*, 277–281.

[262] C. Chawengkijwanich and Y. Hayata, *Int. J. Food Microbiol.*, **2008**, *123*, 288–292.

[263] A. Majdalawieh, M. C. Kanan, O. El-Kadri and S. M. Kanan, *J. Nanosci. Nanotechnol.*, **2014**, *14*, 4757–4780.

[264] R. S. Norman, J. W. Stone, A. Gole, C. J. Murphy and T. L. Sabo-Attwood, *Nano Lett.*, **2008**, 302–306.

[265] A. N. Brown, K. Smith, T. A. Samuels, J. Lu, S. O. Obare and M. E. Scott, *Appl. Environ. Microbiol.*, **2012**, *78*, 2768–2774.

[266] Chamundeeswari Munusamy, Sobhana S. S. Liji, Jacob Justin P., Kumar M. Ganesh, Devi M. Pandima, Sastry Thotapalli P. and Mandal Asit B., *Biotechnol. Appl. Biochem.*, **2010**, *55*, 29–35.

[267] Y. Zhao, Y. Tian, Y. Cui, W. Liu, W. Ma and X. Jiang, *J. Am. Chem. Soc.*, **2010**, *132*, 12349–12356.

[268] R. Brayner, R. Ferrari-Iliou, N. Brivois, S. Djediat, M. F. Benedetti and F. Fiévet, *Nano Lett.*, **2006**, *6*, 866–870.

[269] M. Heinlaan, A. Ivask, I. Blinova, H.-C. Dubourguier and A. Kahru, *Chemosphere*, **2008**, *71*, 1308–1316.

[270] N. G. Chorianopoulos, D. S. Tsoukleris, E. Z. Panagou, P. Falaras and G.-J. E. Nychas, *Food Microbiol.*, **2011**, *28*, 164–170.

[271] R. Y. Pelgrift and A. J. Friedman, *Adv. Drug Deliv. Rev.*, **2013**, *65*, 1803–1815.

[272] P.-C. Maness, S. Smolinski, D. M. Blake, Z. Huang, E. J. Wolfrum and W. A. Jacoby, *Appl. Environ. Microbiol.*, **1999**, *65*, 4094–4098.

[273] B. Díez, N. Roldán, A. Martín, A. Sotto, J. A. Perdigón-Melón, J. Arsuaga and R. Rosal, *J. Membr. Sci.*, **2017**, *526*, 252–263.

[274] R. Zarzuela, M. Carbú, M. L. A. Gil, J. M. Cantoral and M. J. Mosquera, *Mater. Des.*, **2017**, *114*, 364–372.

[275] Y. Tao, E. Ju, J. Ren and X. Qu, *Adv. Mater.*, **2015**, *27*, 1097–1104.

[276] K. Cendrowski, *J. Nanomedicine Nanotechnol.*, **2013**, *4* (6).

[277] K. Cendrowski, M. Peruzynska, A. Markowska-Szczupak, X. Chen, A. Wajda, J. Lapczuk, M. Kurzawski, R. J. Kalenczuk, M. Drozdzik and E. Mijowska, *Biomed. Microdevices*, **2014**, *16*, 449–458.

[278] R. Rakhshaei and H. Namazi, *Mater. Sci. Eng. C*, **2017**, *73*, 456–464.

[279] J.-L. Hu, Q.-H. Yang, H. Lin, Y.-P. Ye, Q. He, J.-N. Zhang and H.-S. Qian, *Nanoscale*, **2013**, *5*, 6327.

[280] J. Gehring, D. Schleheck, B. Trepka, S. Polarz, *ACS Appl. Mater. Interfaces* **2015**, *7*, 1021–1029.

[281] C. Dai, Y. Yuan, C. Liu, J. Wei, H. Hong, X. Li and X. Pan, *Biomaterials*, 2009, **30**, 5364–5375.

[282] C. Wang, H. Hong, Z. Lin, Y. Yuan, C. Liu, X. Ma and X. Cao, *RSC Adv.*, **2015**, *5*, 104289–104298.

[283] D. Şen Karaman, S. Sarwar, D. Desai, E. M. Björk, M. Odén, P. Chakrabarti, J. M. Rosenholm and S. Chakraborti, *J. Mater. Chem. B*, **2016**, *4*, 3292–3304.

[284] S.-H. Min, J.-H. Yang, J. Y. Kim and Y.-U. Kwon, *Microporous Mesoporous Mater.*, **2010**, *128*, 19–25.

[285] S. Pourshahrestani, E. Zeimaran, N. Adib Kadri, N. Gargiulo, S. Samuel, S. V. Naveen, T. Kamarul and M. R. Towler, *J. Mater. Chem. B*, **2016**, *4*, 71–86.

[286] Y. Song, H. Jiang, H. Bi, G. Zhong, J. Chen, Y. Wu and W. Wei, *ACS Omega*, **2018**, *3* (1), 973–981.

[287] S. Ghosh and V. Vandana, *Mater. Res. Bull.*, **2017**, *88*, 291–300.

[288] Y. Kuthati, R. K. Kankala, S.-X. Lin, C.-F. Weng and C.-H. Lee, *Mol. Pharm.*, **2015**, *12*, 2289–2304.

[289] C.-C. Chen, H.-H. Wu, H.-Y. Huang, C.-W. Liu and Y.-N. Chen, *Int. J. Environ. Res. Public. Health*, **2016**, *13*, 99.

[290] X. Li, W. Zuo, M. Luo, Z. Shi, Z. Cui and S. Zhu, *Chem. Res. Chin. Univ.*, **2013**, *29*, 1214–1218.

[291] S. Rostamnia, E. Doustkhah, S. Estakhri and Z. Karimi, *Phys. E Low-Dimens. Syst. Nanostructures*, **2016**, *76*, 146–150.

[292] L. Laskowski, M. Laskowska, K. Fijalkowski, H. Piech, J. Jelonkiewicz, M. Jaskulak, A. Gnatowski and M. Dulski, *J. Nanomater.*, **2017**, 1–12.

[293] D. Díaz-García, P. Ardiles, S. Prashar, A. Rodríguez-Diéguez, P. Páez, and S. Gómez-Ruiz, *Pharmaceutics*, **2019**, *11 (1)*, 30.

[294] L. Tahmasbi, T. Sedaghat, H. Motamedi, M. Kooti. *J. Solid State Chem.* **2018**, *258*, 517–525.

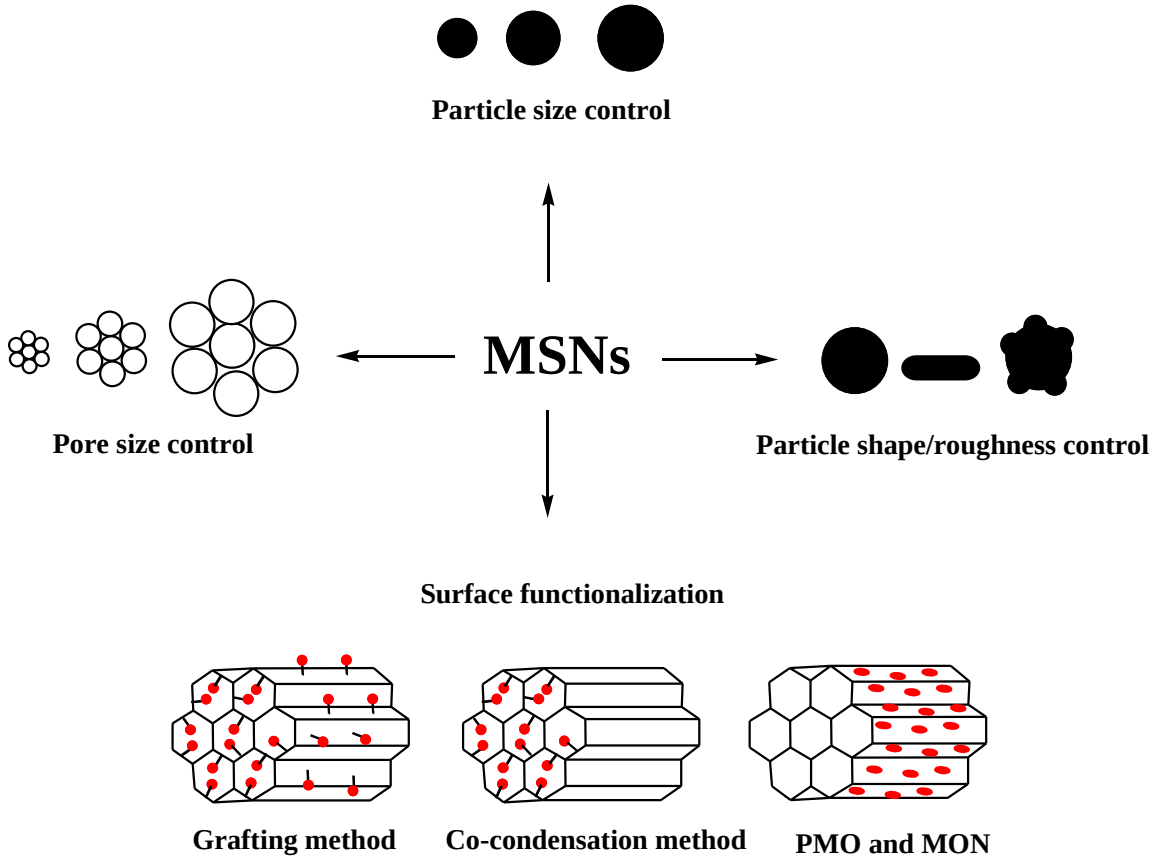

Figure 1. Tunable properties of Mesoporous Silica Nanostructures (MSNs).

Scheme 1. Multifunctionality of Mesoporous Silica Nanostructures (MSNs).

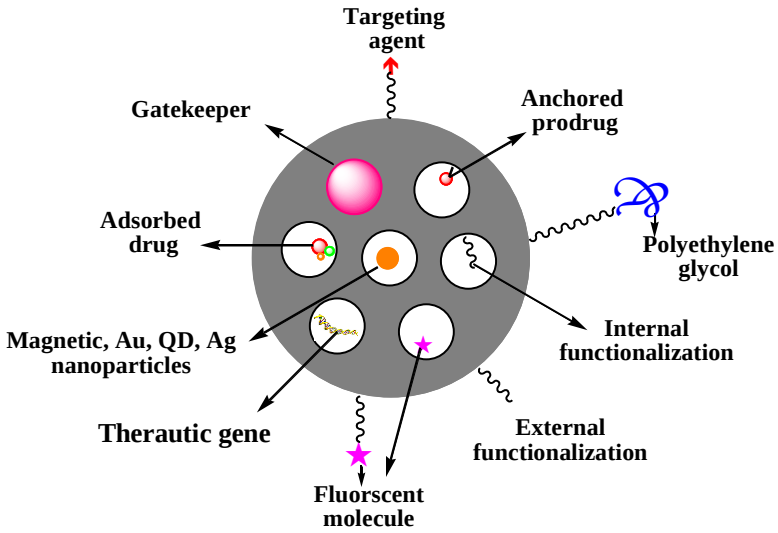

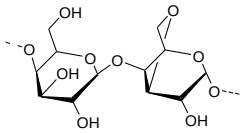
agarose

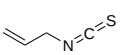
allyl isothiocyanate

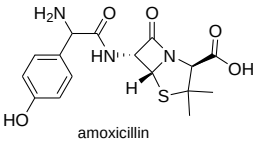
amoxicillin

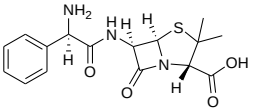
ampicillin

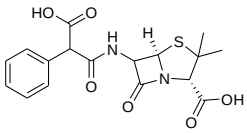
carbenicillin

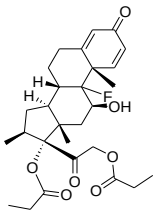
betamethasone

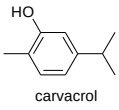
carvacrol

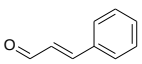
cinnamaldehyde

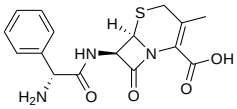
cephalexin

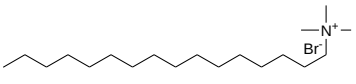
cetyltrimethylammonium bromide

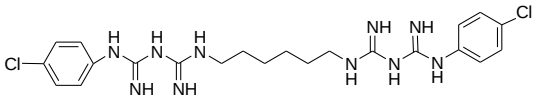
chlorhexidine

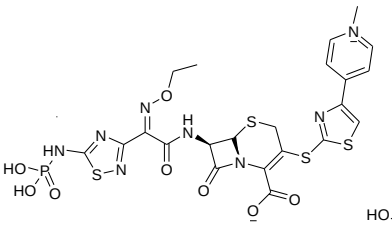
ceftaroline fosamil

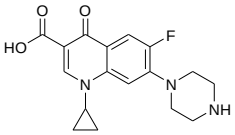
ciprofloxacin

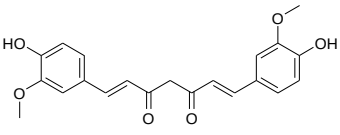
curcumin

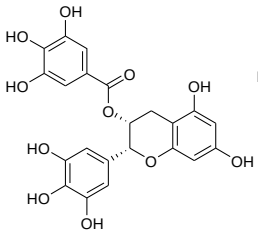
epigallocatechin gallate

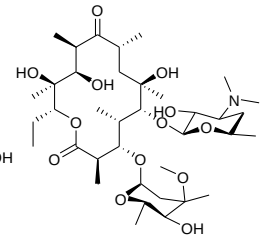
erythromycin

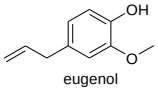

eugenol

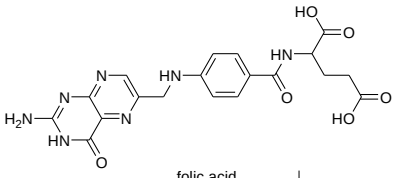

folic acid

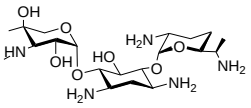

gentamicin

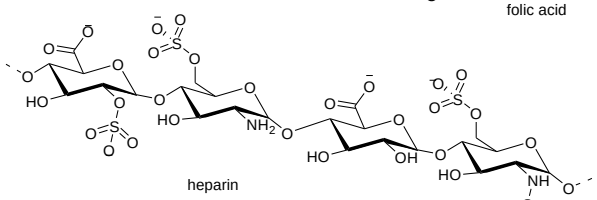

heparin

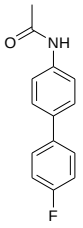

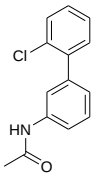

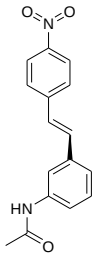

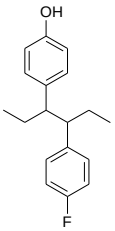

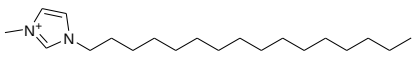

Br⁻

1-hexadecyl-3-methylimidazolium bromide

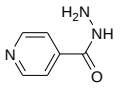

isoniazid

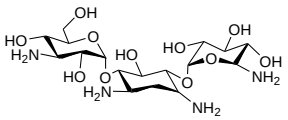

kanamycin A

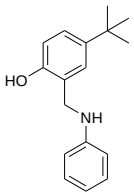

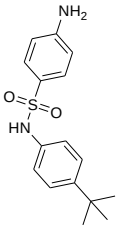

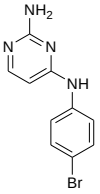

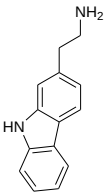

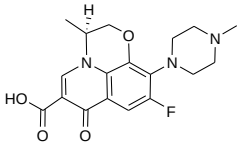

levofloxacin

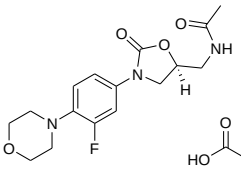

linezolid

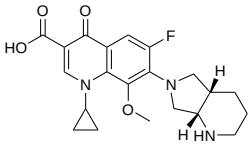

moxifloxacin

Histidine kinase autophosphorylation inhibitors (HKAIs)

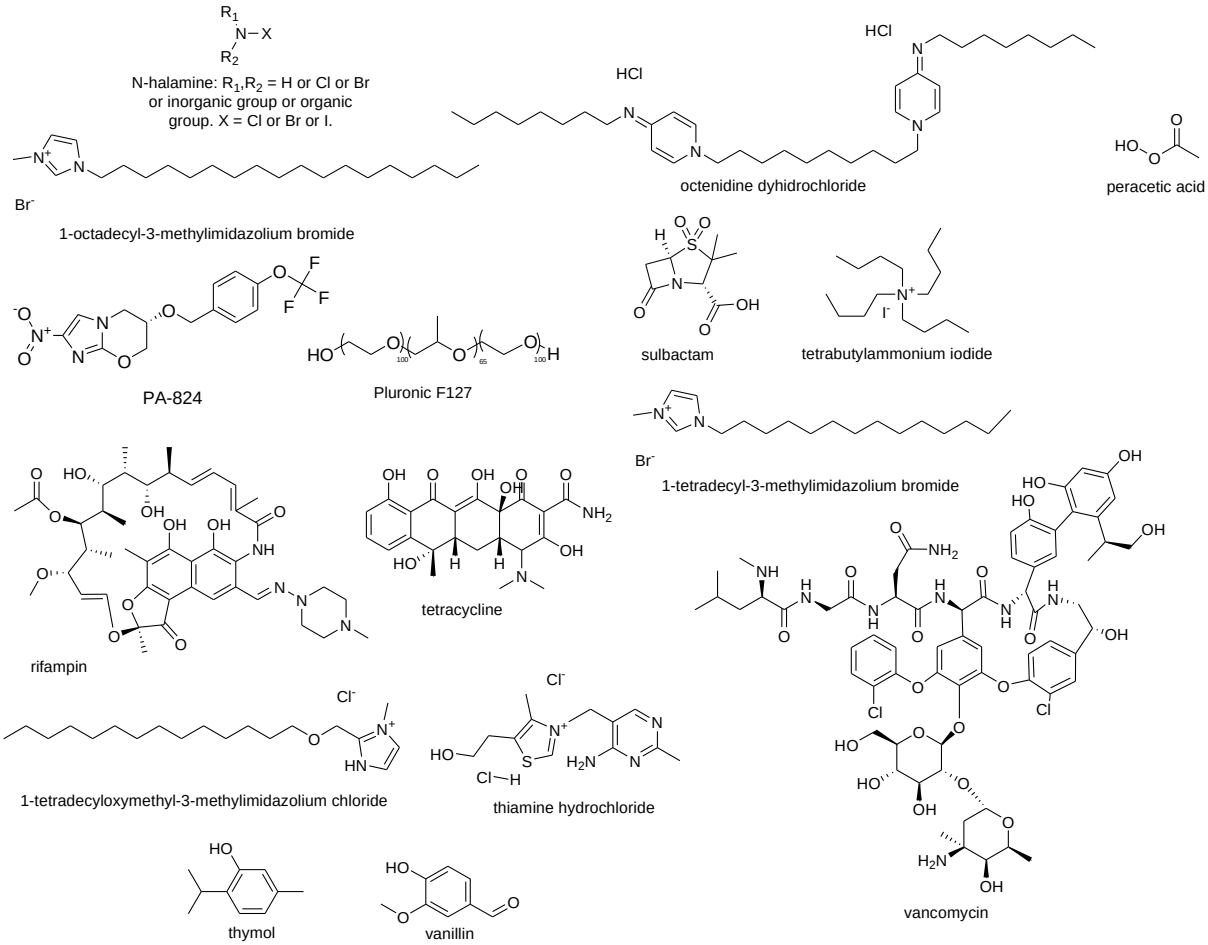

Chart 1. Chemical structures of the cargos loaded into the inorganic supports used in the preparation of antibacterial materials.

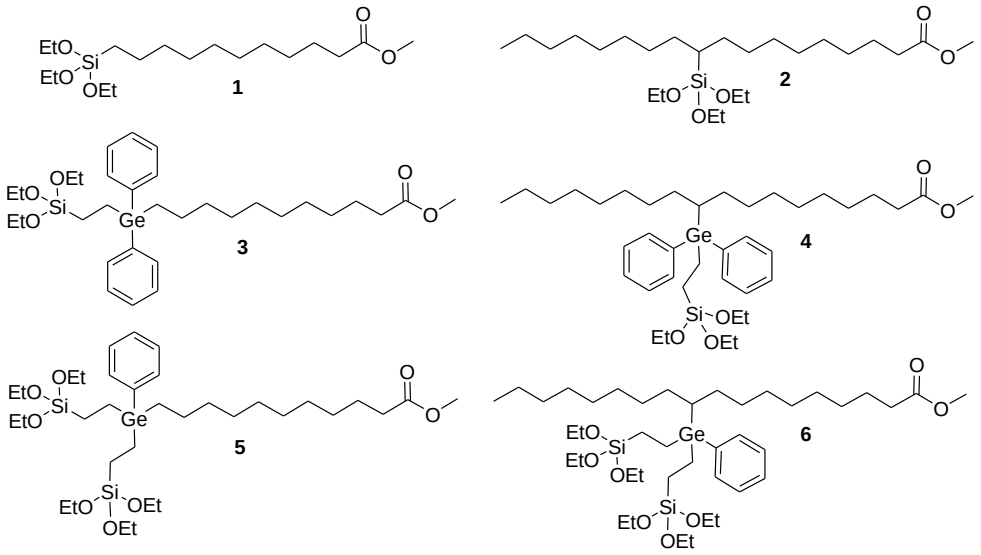

Figure 2. Silylated natural fatty acids used to functionalize SBA-15 and to prepare PMOs with antibacterial activity.

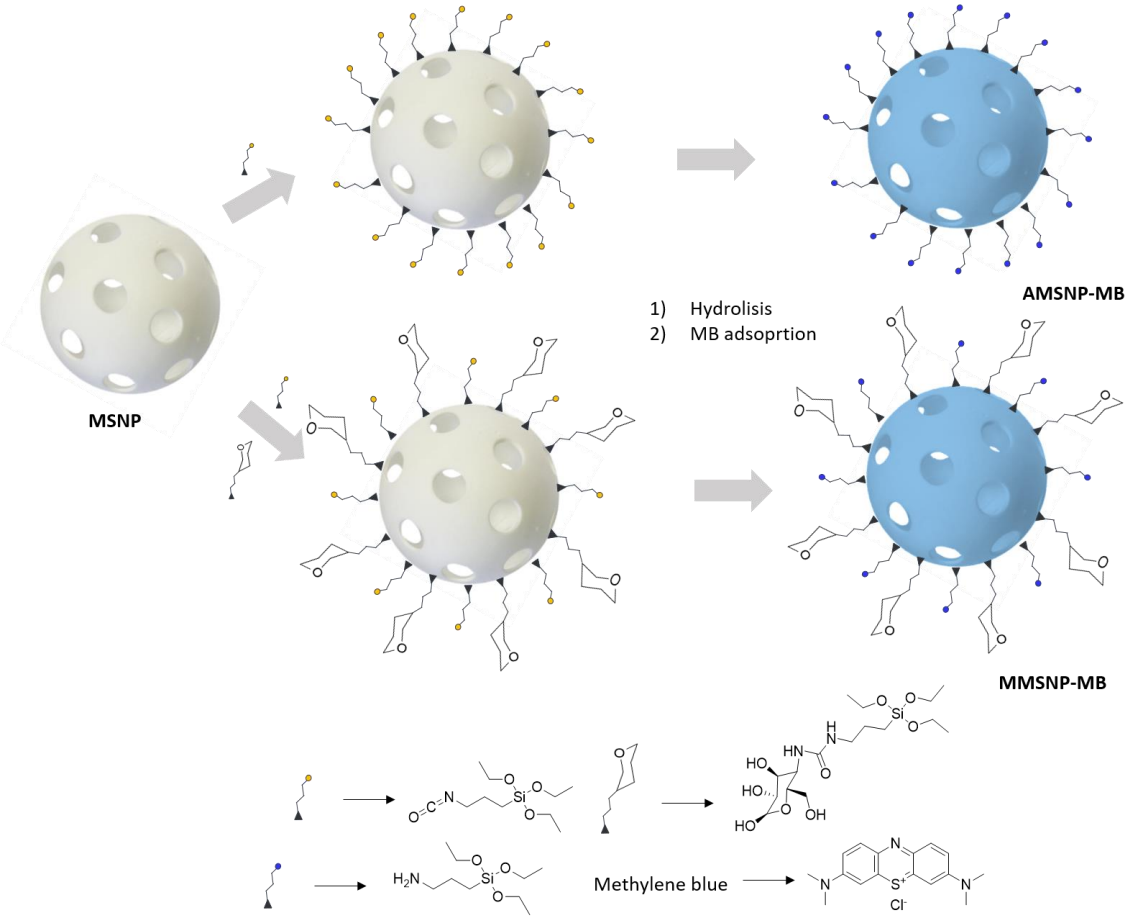

Figure 3. MSNs loaded with methylene blue and coated with aminopropyl or with mannose moieties with antibacterial photodynamic activity.

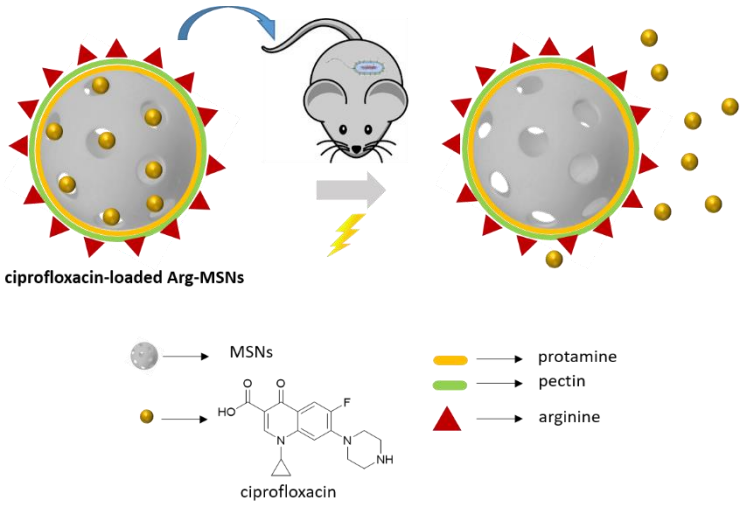

Figure 4. MSNs loaded with ciprofloxacin and functionalized with arginine for targeting and treatment of intracellular *Salmonella*.

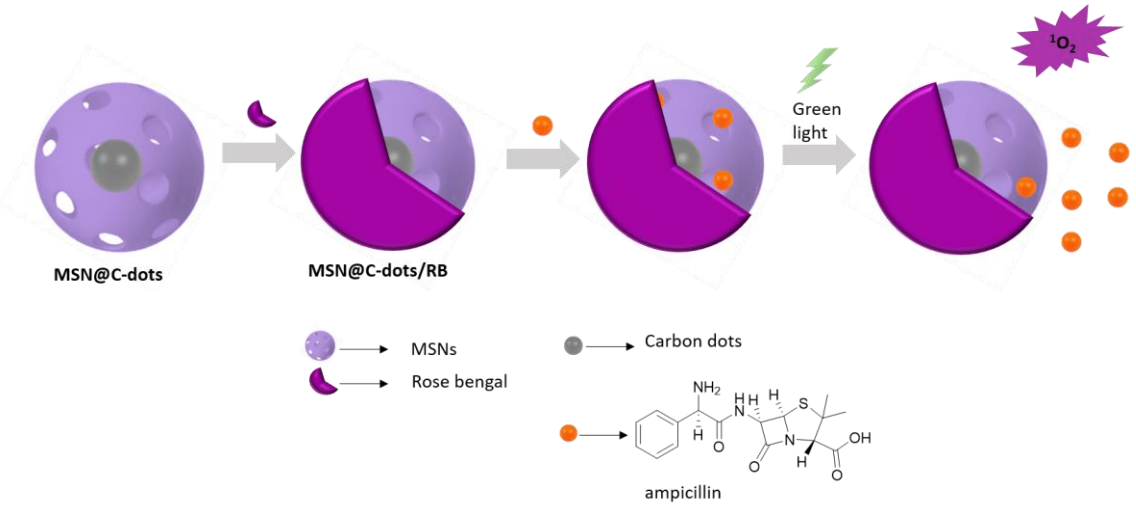

Figure 5. Multifunctional nanoplatform based on MSNs and containing C-dots, Rose Bengal and drugs for an efficient inhibition of bacterial growth.

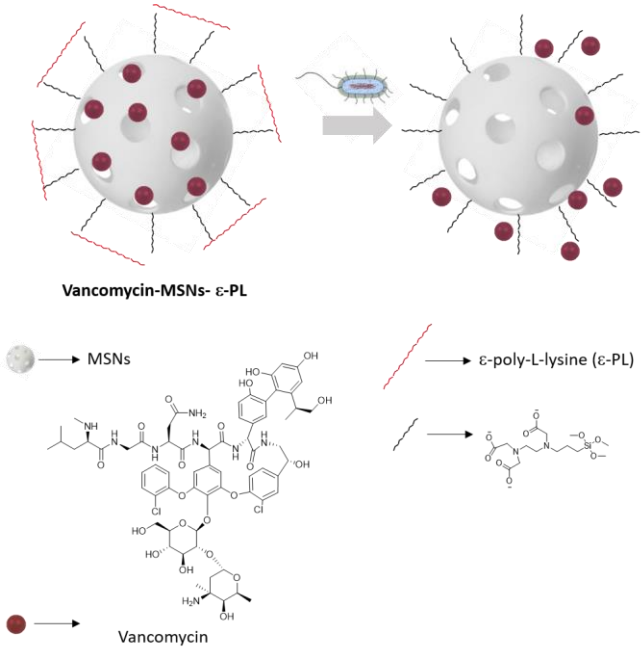

Figure 6. MSNs loaded with vancomycin and capped with ε-poly-L-lysine that were used as antimicrobial agent against *E. coli*, *S. typhi* and *E. carotovora*.

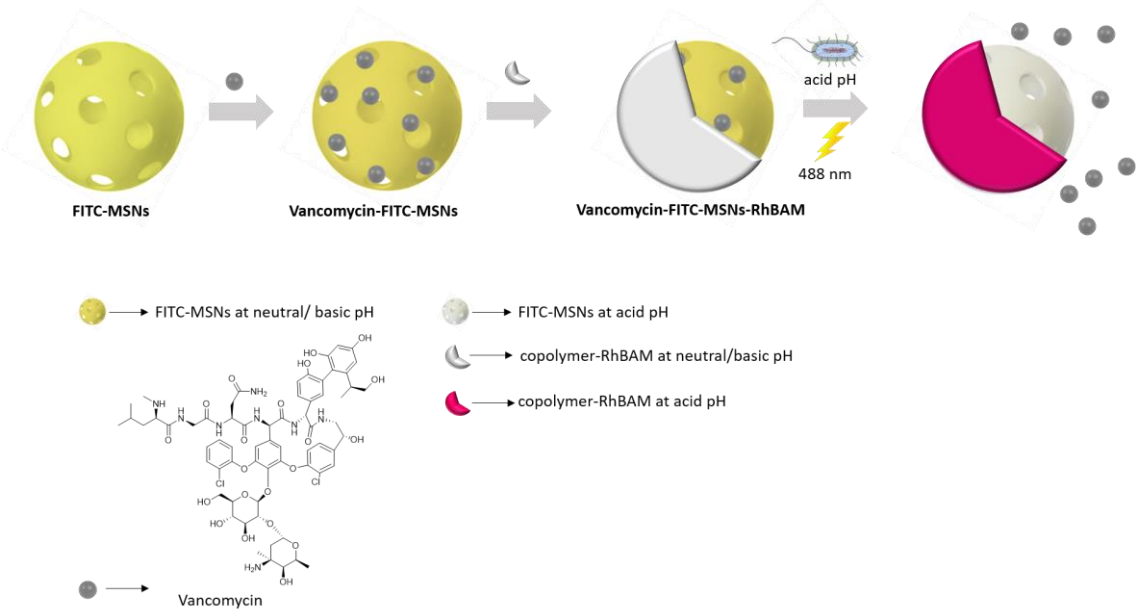

Figure 7. MSNs derivatized with fluorescein, loaded with vancomycin and capped with a pH-sensitive hydrogel for the efficient killing of *E. coli*.

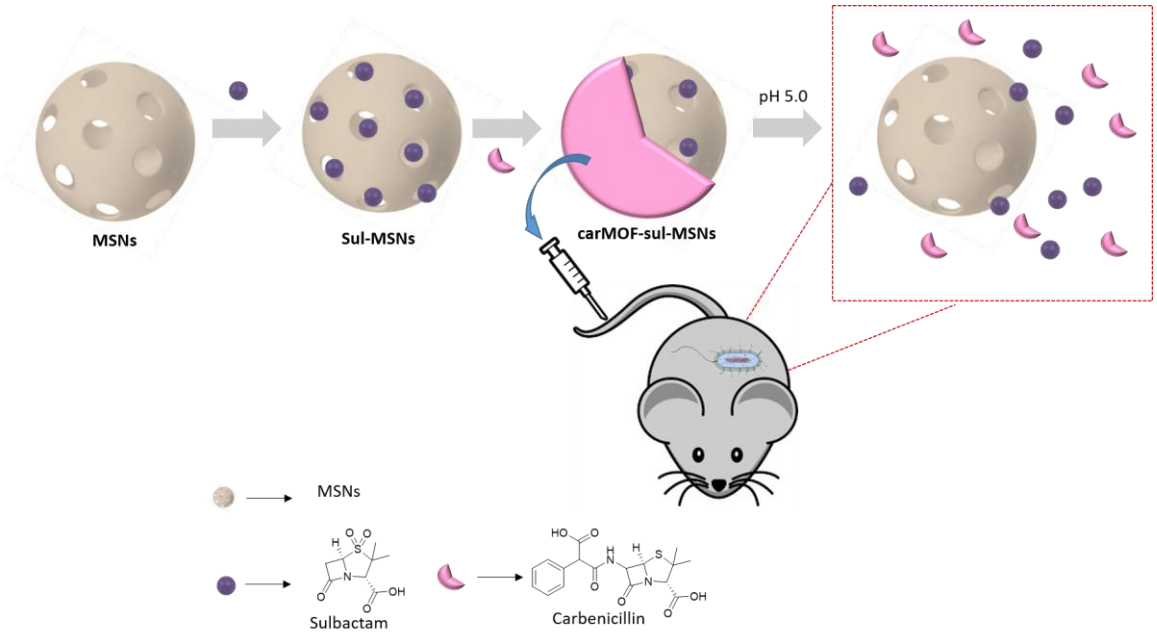

Figure 8. MSNs loaded with sulbactam and coated with a metal-organic framework used for the efficient inhibition of methicillin-resistant *S. aureus*.

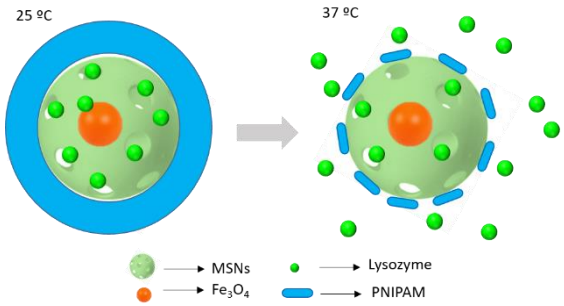

Figure 9. Silica nanoparticles coated with a thermosensitive polymer for the efficient delivery of lysozyme.

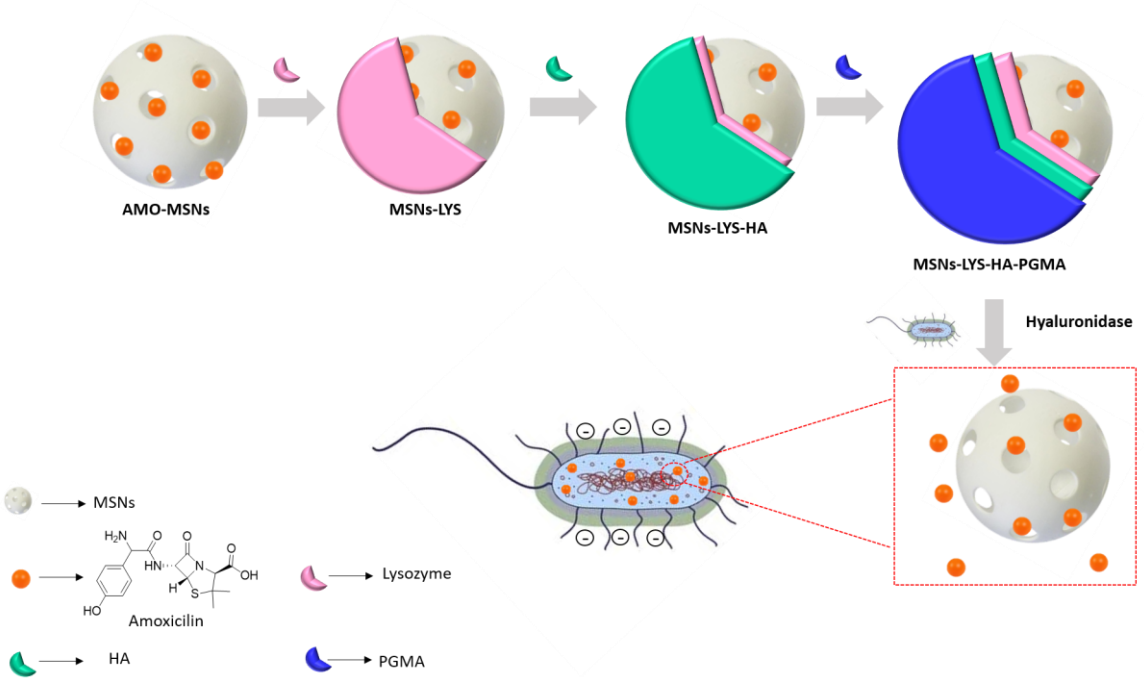

Figure 10. Schematic representation of the layer-by-layer synthesis of self-assembled nanoparticles loaded with amoxicillin for efficient bacterial elimination.

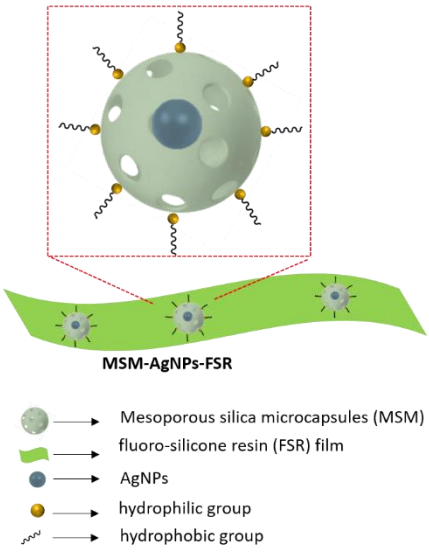

Figure 11. Fluoro-silicone resin film with MS microcapsules containing AgNPs embedded with antibacterial activity.

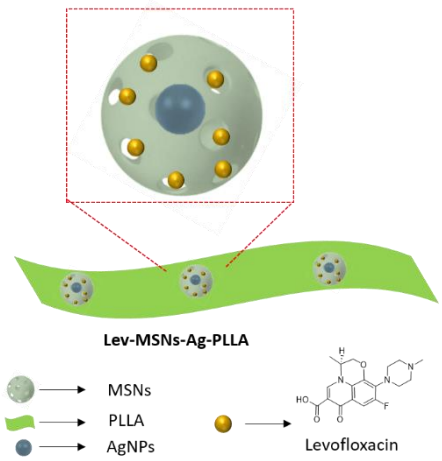

Figure 12. Antibacterial electros pun fibres containing AgNPs coated with a mesoporous shell loaded with levofloxacin.

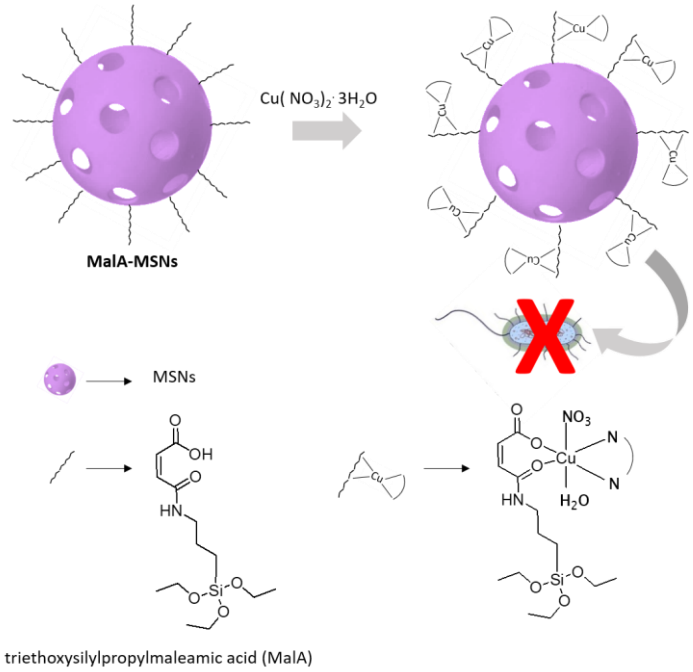

Figure 13. Schematic representation of the synthesis of MS NPs containing a maleamato ligand and the subsequent coordination of copper (II) ions.

Table 1. Summary of MS-based particles with bactericidal properties.

Antibiotic	**MS-Composition**	**SizePCPs** Size/surface modification	**Targeted microorganism**	**MIC Values**	**Ref.**
Agarose, heparin	MSNs films	aminopropyl moieties functionalized/ antimicrobial agent loaded	*S. aureus*, *E. coli*	ND	[192]

AgNPs	MCM-41	antimicrobial agent loaded/ silver nanoparticles functionalized	*S. aureus*, *E. coli*	320, 80 μg mL^{-1}	[234]
AgNPs	Mesoporous silica microspheres	130 nm/ aminopropyl moieties functionalized/ silver nanoparticles functionalized	*S. aureus*, *E. coli*	0.156, 0.313 mg mL^{-1}	[235]
AgNPs	MSNs	aminopropyl moieties functionalized/ silver nanoparticles functionalized/poly-ε-caprolactone nanofibrous membranes	*S. aureus*, *E. coli*	ND	[236]
AgNPs	HMSNs	poly(styrene-co-methyl methacrylate-co-methacrylic acid) hollow-structure template/ *n*-butylamine functionalized/ silver nanoparticles functionalized	*S. aureus*, *E. coli*	ND	[237]
AgNPs	Hollow MSPs (HMSPs)	AgNPs loaded	*E. coli*	ND	[238]
AgNPs	MSNs	mercaptopropyl moieties functionalized/ AgNPs loaded	*S. aureus*, *E. coli*	73.10, 36.55 mg L^{-1}	[239]
AgNPs	SBA-15	dopamine was adsorbed/ silver nanoparticles functionalized	*S. aureus*, *E. coli*	ND	[240]
AgNPs	Mesoporous silica shell	Ag nanocrystals less than 20 nm/ PEI coated/ silver nanoparticles functionalized	*E. coli*, *B. anthracis*	100 μg mL^{-1}	[241]
AgNPs	MSNs	10 nm AgNPs/ 50 nm MNSs/ silver nanoparticles functionalized	*V. natriegens*	10 μg mL^{-1}	[242]
AgNPs	MSNs	10 nm AgNPs/ 50 nm MNSs/ silver nanoparticles functionalized/AgNPS-MSNs embedded in an organosiloxane polymer and deposited in aluminum films	*V. natriegens*	ND	[243]
AgNPs	MSNs	10 nm AgNPs/ 50 nm MNSs/ silver nanoparticles	*V. natriegens*	ND	[244]

		functionalized/AgNPs-MSNs embedded in an organosiloxane polymer and deposited in aluminum films			
AgNPs	MSPs	silver absorbed into sulfonated polystyrene beads/ AgNPs loaded	*E. coli*	ND	[245]
AgNPs	MSPs	loading MSPs-AgNPs on a fluoro-silicone resin film/ AgNPs loaded	*E. coli*	ND	[246]
AgNPs	MSPs	embedded sodium alginate-coated AgNPs	*S. aureus*, *S. epidermis*, *B. cereus*, *B. subtilis*, *E. faecalis*, *E. coacae*, *E. coli*, *K. oxytoca*, *K. pneumonia*, *P. mirabilis*, *P. vulgaris*, *P. aeruginosa*, *E. aerogenes*	55-250, $\mu g\ mL^{-1}$	[247]
AgNPs	MSNs	silver nanoparticles functionalized/ peptide platelet-derived growth factor BB loaded	*E. coli*, *S. aureus*, *P. aeruginosa*, *Bacteroides fragilis*, *Candida sporogenes*	ND	[248]
AgNPs, ibuprofen	Mesoporous SiO_2 fibers	silver nanoparticles functionalized	*E. coli*	ND	[249]
AgNPs	SBA-15	silver nanoparticles functionalized or core shell formed	*E. coli*	ND	[250]
AgNPs	MSNs	CdTe quantum dots loaded/ aminopropyl moietis functionalized/ silver nanoparticles functionalized	*S. aureus*, *E. coli*	ND	[251]
AgNPs, peracetic acid	SBA-15	antimicrobial agent loaded/ silver nanoparticles loaded	*S. aureus*	110, 70 $\mu g\ mL^{-1}$	[252]
AgNPs, CTAB	MSNs	CTAB inside the pores/ aminopropyl moieties grafted/ silver nanoparticles functionalized	*S. aureus*, *E. coli*	20, 10 $\mu g\ mL^{-1}$	[253]

AgNPs, chlorhexidine	MSNs	aminopropyl moieties functionalized/ pH-responsive release/ silver nanoparticles functionalized	*S. aureus*, *E. coli*	25, 12.5 μg mL^{-1}	[254]
AgNPs	SBA-15	aminopropyl moieties functionalized/ Polypyrrole (PPy)-Ag-mesoporous silica particles	*E. coli*	200-300 μg mL^{-1}	[255]
AgNPs, levofloxacin	MSNs	levofloxacin loaded/ silver nanoparticles functionalized	*E. coli*, *K. pneumoniae*	ND	[256]
AgNPs, levofloxacin	MSNs	levofloxacin loaded/ silver nanoparticles functionalized/ solid incorporated onto electrospun nanofibers of poly-L-lactide	*S. aureus*	28, 12 mg mL^{-1}	[257]
AgNPs, Cu ions, curcumin	Cu-MSNs	aminopropyl moieties functionalized/ light-responsive bacterial effect/ silver nanoparticles functionalized	*E. coli*	ND	[258]
AgNPs, CuO	SBA-15	aminopropyl moieties functionalized/ silver nanoparticles or cupper ions functionalized	*S. aureus*, *E. coli*	ND	[273]
AgNPs	PMOs	PMOs contained thiol and sulfonyl moieties/ inhibit bacterial biofilms	*P. aeruginosa*	0.5-0.25 mg mL^{-1}	[280]
AuNPs	MSNs	aminopropyl moieties and carboxylic groups functionalized/ gold nanoparticles functionalized	*S. aureus*, *E. coli*, *B. subtilis*	ND	[275]
Bismuth oxychloride	KIT-6	KIT-6 prepared under hydrothermal conditions/ photocatalytic ability/ metal ions contained	*S. aureus*, *E. faecalis*, *E. coli*, *P. aeruginosa*	32, 40 μg mL^{-1}	[286]
CdS	SiO_2 nanospheres	300 nm /antimicrobial agent functionalized	*E. coli*	50 μg L^{-1}	[279]
Chlorhexidine	MSNs	antimicrobial agent loaded/ inhibit bacterial biofilms	*S. mutans*, *S. sobrinus*, *F. nucleatum*, *A.actinomycetemc*	100, 200, 100, 100, 200 μg mL^{-1}	[202]

			omitans, *E. faecalis*		
Copper ions	Silica-based nanocomposites	metal ions contained	*S. cerevisiae*	ND	[274]
Copper ions	SBA-15	metal ions loaded or functionalized	*E. coli*	ND	[292]
Copper ions	MSNs	maleamato ligand functionalized and coordinaed with copper (II) ions	*S. aureus*, *E. coli*	4.1, 10.4 μg mL	[293]
Copper ions, niquel ions, gentamicine	MSNs	condensation of 2-hydroxy-3-methoxybenzaldehyde and amine-functionalized MSNs/ copper and nickel complexes anchored/ carrier for gentamicin	*B. subtilis*, *S. aureus*, *E. coli*, *P. aeruginosa*	ND	[294]
Gallium ions	Mesoporous bioactive glasses	metal ions contained	*S. aureus*, *E. coli*	ND	[285]
Gentamicin	MSNs	antimicrobial agent loaded/ polyehtyleneimine and polystyrene sulfonate-polyallylaminecoated/ inhibit bacterial biofilms	*S. aureus*, *S. pneumoniae*	ND	[203]
Histidine kinase autophosphorylation inhibitors	MCM-41	ε-poly-L-lysine capped-MSNs/ bacteria-responsive gated MSNs/ antimicrobial agent loaded	*E. coli*, *S. marcescens*	ND	[205]
Isoniazid	Hollow MSNs (HMSNs)	amine-functionalized/ antimicrobial agent loaded	*M. smegmatis*	640, 320 μg mL^{-1}	[167]
Isoniazid	MSNs	functionalized with α,α-trehalose through azide-mediated surface photoligation/ antimicrobial agent loaded	*M. smegmatis*	3−4, 4.5−5 mg mL^{-1}	[168]
Levofloxacin	Mesoporous matrices	impregnation (IP) and surfactant-assisted drug loading, also denoted as one-pot (OP)/ antimicrobial agent loaded	*E. coli*	ND	[176]

Levofloxacin	Mesostructured SiO_2–CaO–P_2O_5 glass	pH sensitive gated MSNs/ hydroxyapatite nanoparticles/ antimicrobial agent loaded	*S. auerus*	ND	[201]
Levofloxacin	MSNs	antibiotic agent loaded/ external surface decorated with polycationic dendrimers/pH controlled realease	*E. coli*	5 μg mL^{-1}	[213]
Linezolid	MCM-48	440 nm/ antibiotic adsorption loaded	*S. aureus*	ND	[199]
Lysine	MCM-41	antimicrobial agent functionalized	*S. aureus*, *E. coli*	ND	[148]
Lysozyme	MSNs	antimicrobial agent functionalized	*E. coli*	75 μg mL^{-1}	[151]
Lysozyme	small-sized and large-pore dendritic MSNs	antimicrobial agent loaded	*E. coli*	500 μg mL^{-1}	[172]
Lysozyme, kanamycin	MSNs	kanamycin loaded-aminopropyl moieties functionalized/ lysozyme- gold nanoparticles functionalized/ medical device	*E. coli*, *B. safensis*	ND	[202]
Lysozyme	Fe_3O_4MSNs	poly(N-isopropylacrylamide) coated MSNs/ thermoresponsive gated MSNs/ antimicrobial agent loaded	*Bacillus cereus*, *Micrococcus luteus*	ND	[209]
Methylene blue	MSNs	antimicrobial agent functionalized	*E. coli*, *P. aeruginosa*	ND	[162]
Moxifloxacin	MSNs	functionalized with disulfide snap-tops/ β-CD capped/ redox-triggered gated MSNs/ antimicrobial agent loaded	*F. tularensis*	6.25–400 ng mL^{-1}	[212]
N-halamine	MSNs	antimicrobial agent functionalized	*S. aureus*, *E. coli*	ND	[153]
N-halamine	SBA-15	antimicrobial agent functionalized	*S. aureus*, *E. coli*	ND	[154]

N-halamine	SBA-15	antimicrobial agent functionalized	*S. aureus*, *E. coli*	ND	[155]
N-halamine	SBA-15	antimicrobial agent functionalized	*S. aureus*, *E. coli*	ND	[156]
Octenidine dyhidrochloride	MSNs	MSNs coated titanium disks/ antimicrobial agent loaded	*S. aureus*, *E. coli*	ND	[193]
PA-824, moxifloxacin	Mesoporous silica particles (MSPs)	antimicrobial agent loaded	*M. tuberculosis*	3.33, 1.11 $\mu g\ mL^{-1}$	[177]
Parmetol S15	MCM-48	400 nm/ functionalized in the external surface with dimethyloctadecyl[3-(triethoxysilyl)propyl]ammonium chloride and dimethyltetradecyl[3-(triethoxysilyl)propyl]ammonium chloride/ antibiotic loaded	*S. aureus*, *E.coli*	ND	[187]
Protoporphyrin IX (PpIX)	Compact silica nanoparticles, MSNs, stellate-MSNs, larger pore-MSNs	antimicrobial agent functionalized	*S. aureus*	ND	[163]
Rose Bengal/ ampicillin	C-dots MSNs	photodynamic synergetic therapy/ Rose Bengal-MSN@C-dots/ light responsive gated MSNs/ antimicrobial agent loaded and functionalized	*E. coli*	100 $\mu g\ mL^{-1}$	[180]
Rose Bengal, S-nitrosothiol	MSNs	antimicrobial agent functionalized	*P. aeruginosa*	ND	[161]
rhBMP-2	SBA-15	macroporous scaffolds of zein, SBA-15, and hydroxypropyltrimethyl ammonium chloride chitosan/ antimicrobial agent loaded	*S. aureus*, *E. coli*	ND	[184]
Silver ions	Calcium-doped mesoporous silica spheres	metal ions loaded	*S. aureus*, *E. coli*	ND	[281]
Silver ions	Calcium-doped mesoporous silica spheres	amino-functionalized/ metal ions functionalized	*E. coli*	ND	[282]

Silver ions, kanamycin	spherical, small rods and larger rods MSNs	chitosan coated/ metal ions functionalized/ antimicrobial agent loaded	*S. aureus*, *E. coli*, *V. cholerae*	200 μg mL^{-1}	[283]
Silver ions	MSNs	amino-functionalized/ silver nanoparticles formed	*S. aureus*, *E. coli*	110, 70 μg mL^{-1}	[287]
Silver ions	MSNs	butylaldehyde and indole-3-acetic acid moieties functionalized/ pH-responsive silver release/ silver nanoparticles functionalized	*S. aureus*, *E. coli*, *B. subtilis*, *S. epidermis*	120, 30 μg mL^{-1}	[288]
Silver ions	SBA-15	aminopropyl and ethylenediaminetretraacetic acid moietis functionalized/ metal ions functionalized	*S. aureus*, *E. coli*	30 μg mL^{-1}	[289]
Silver ions	MSPs	thiol-functionalized/ metal ions loaded	*Candida albicans*, *S. mutans*	ND	[290]
Silver ions	SBA-15	silver nanoparticles functionalized/ polypropylene polymer composite	*E. coli*, *B. anthracis*	ND	[284]
Silver ions	SBA-15	silver nanoparticles functionalized at pH 9	*E. coli*	ND	[291]
Silylated natural fatty acids	SBA-15	antimicrobial agent functionalized	*S. aureus*, *E. coli*, *S. epidermis*, *P. vulgaris*, *P. aeruginosa*	0.01-20 μg mL^{-1}	[149]
Tetracycline	MSNs	antimicrobial agent loaded	*E. coli*	ND	[165]
Tetracycline	MSNs	antimicrobial agent loaded	*S. aureus*, *E. coli*	ND	[166]
Tetracycline, ZnO	MCM-41	carboxymethyl cellulose hydrogel-MCM-41-ZnO/ antimicrobial agent loaded	*S. aureus*, *E. coli*	ND	[278]
1-tetradecyl-3-methylimidazolium bromide (C_{14}MIMBr), 1-hexadecyl-3-methylimidazolium bromide (C_{16}MIMBr), 1-octadecyl-3-methylimidazolium	spheres, ellipsoids, rods, and tubes MSNs	antimicrobial agent loaded	*E. coli*	ND	[175]

bromide (C_{18}MIMBr), and 1-tetradecyloxymethyl-3-methylimidazolium chloride (C_{14}OCMIMCl))					
TiO_2	MSNs	antimicrobial agent functionalized	*E. coli*	ND	[276]
TiO_2	Mesoporous silica nanotubes	antimicrobial agent functionalized	*E. coli*	ND	[277]
Vancomycin	Mesoporous silica nanoparticles (MSNs)	antibiotic functionalized	*S. aureus*, *E. coli*	200 μg mL^{-1}	[146]
Vancomycin/ rifampin	SBA-15	antimicrobial agent loaded	*S. aureus*, *S. epidermis*	ND	[183]
Vancomycin	MCM-41	ε-poly-L-lysine capped-MSNs/ bacteria-responsive gated MSNs/ antimicrobial agent loaded	*E. coli*, *Salmonella typhi*, *Erwinia carotovora*	2.89 μg mL^{-1}, 16.7 mg mL^{-1}	[204]
Vancomycin	MSNs	poly (N-isopropyl acrylamide-co-acrylic acid) copolymerized with rhodamine B-capped MSNs/ acid-responsive gated MSNs/ antimicrobial agent loaded	*E. coli*	280 μg mL^{-1}	[207]
Vinyl carbazole	SBA-15	antimicrobial agent functionalized	*S. aureus*, *S. mutans*, *E. coli*, *S. typhi*.	350, 200, 320, 640 μg mL^{-1}	[158]
Vinyl imidazole	SBA-15	antimicrobial agent functionalized	*S. aureus*, *S. mutans*, *E. coli*, *S. typhi*.	320-500 μg mL^{-1}	[159]
Zinforo	MCM-48	100 nm/ matrix-assisted pulsed laser evapora-tion (MAPLE)-deposited coatings or thin films/ antimicrobial agent loaded	*E. coli*	ND	[198]

Aziz Maleki received his Ph.D. degree in organic chemistry from the Institute for Advanced Studies in Basic Sciences (IASBS), Zanjan, Iran. He then worked as a postdoctoral fellow in Zanjan University of Medical Sciences (ZUMS). At present, he is currently an assistant professor at Department of Pharmaceutical Nanotechnology, ZUMS, Zanjan, Iran. His research interests focus on the fabrication and characterization of novel mesoporous and 2D materials for catalytic and biomedical applications.

Raymond J. Turner joined the University of Calgary, Canada in 1998 in the Department of Biological Sciences and is presently a Professor of Biochemistry and Microbiology. His PhD is in Biophysical Chemistry and postdoctoral fellowships in area of antimicrobial resistance and bioenergetics. He has held the post of Associate Department Head. He has received excellence in research and excellence in graduate student supervision awards. Present research interests include: metal(loid) toxicity/resistance mechanisms towards bacteria, the microbiology of nanomaterials, and Biofilm physiology. He has contributed over 250 publications and holds 8 patents/licences.

Ramón Martínez-Máñez received his Ph.D. in Chemistry from the University of Valencia in 1986 and was a postdoctoral fellow at Cambridge University, UK. He is a full professor at the Polytechnic University of Valencia. Presently, he is the director of the IDM Research Institute at the Polytechnic University of Valencia. He is the co-author of more than 300 research publications and nine patents. His current research interest involves developing new sensing methods for different chemicals of interest, including explosives and chemical warfare agents. He is also involved in designing gated hybrid materials for delivery applications.

Drug delivery systems to combat bacterial infections based on mesoporous silica nanoparticles are described.

Bactericidal nanoparticles

Andrea Bernardos, Elena Piacenza, Félix Sancenón, Hamidi Mehrdad, Aziz Maleki,* Raymond J. Turner* and Ramón Martínez-Máñez*

Mesoporous Silica-Based materials with Bactericidal Properties